Expression and immunogenicity of HBV surface antigens following *in vitro* and *in vivo* gene delivery using recombinant adenoviruses

Keila Dias Neves

A dissertation submitted to the Faculty of Health Sciences, University of the Witwatersrand, Johannesburg, in fulfilment of the requirements for the degree of

Master of Science in Medicine

Johannesburg, 2024

Declaration

I, Keila Dias Neves, declare that this dissertation is my own work. It is being submitted to the Faculty of Health Sciences at the University of the Witwatersrand, Johannesburg in fulfilment of a Master of Science in Medicine. This dissertation has not been submitted before for any degree or examination at this or any other university.

05 June 2024 .....

Date

.....

Signature

Dedication

"My faith rests not in what I am, or shall be, or feel, or know,
but in what Christ is, in what He has done, and in what He is doing for me."
Charles Spurgeon

To Christ, I owe it all.

"Then I saw another angel flying in the midst of heaven, having the everlasting gospel to preach to those who dwell on the earth – to every nation, tribe, tongue and people – saying with a loud voice, "Fear God and give glory to Him for the hour of His judgement has come; and worship Him who made heaven and earth, the sea and springs of water.""
Revelation 14:6-7

Publications and Conference Presentations

1. Farhad, T., Neves, K., Arbuthnot, P. and Maepa, M.B., 2022. Adenoviral Vectors: Potential as Anti-HBV Vaccines and Therapeutics. *Genes*, *13*(11), p.1941.
2. Neves, K., Arbuthnot, P. and Maepa, M.B., 2022. Poster entitled *Production of recombinant adenoviruses encoding the HBV large and small surface antigens using the AdEasy system* presented at the Medical Biosciences Research Thrust (MBRT) 2022 Research Symposium, University of the Witwatersrand, Johannesburg, South Africa.
3. Neves, K., Arbuthnot, P. and Maepa, M.B., 2023. Poster entitled *Induction of immunity against HBV following a single dose injection of HBV surface antigen-expressing adenoviral vector in mice* presented at the 30th Annual Meeting of the European Society of Gene and Cell Therapy (ESGCT), Brussels, Belgium.
4. Neves, K., Arbuthnot, P. and Maepa, M.B., 2023. Poster entitled *Expression and immunogenicity of hepatitis B virus (HBV) large and small surface antigens following in vitro and in vivo gene delivery using recombinant adenoviruses* presented at the IUIS 18th International Congress of Immunology, Cape Town, South Africa.
5. Neves, K., Arbuthnot, P. and Maepa, M.B., 2023. Poster entitled *Hepatitis B virus (HBV) surface antigens delivered in vitro and in vivo using recombinant adenoviruses for immunisation against HBV infection* presented at the Medical Biosciences Research Thrust (MBRT) 2023 Research Symposium, University of the Witwatersrand, Johannesburg, South Africa.
6. Jacobs, R., Dogbey, M.D., Mnyandu, N., Neves, K., Barth, S., Arbuthnot, P. and Maepa, M.B., 2023. AAV Immunotoxicity: Implications in Anti-HBV Gene Therapy. *Microorganisms*, *11*(12), p.2985.

Abstract

Hepatitis B virus (HBV) infection poses a global health problem affecting almost 300 million people. Immunisation remains one of the most effective methods of HBV prevention. The HBV surface antigen (HBsAg) is one of the primary clinical markers for acute or chronic HBV infection. It is an important component of anti-HBV vaccines because of its presence on the viral envelope and interaction with neutralising antibodies (NAbs). Current vaccines against HBV, which deliver only the HBV small surface antigen (SHBsAg) as a purified peptide in a 3-dose regimen, are often less effective in people over the age of 40 years and in immunocompromised individuals. Additionally, these vaccines are limited to mostly humoral immunity. Recent widespread use of viruses as vectors for vaccine delivery has propelled use of adenoviruses (Ads) to the front line of vaccine research. Adenoviral vectors (AdVs) are attractive candidates for anti-HBV vaccine design because of their ability to induce both cell-mediated and humoral immune responses. Therefore, this study was conducted to assess the efficiency of AdVs in the delivery of HBV SHBsAg or large surface antigen (LHBsAg) and induction of HBV specific immune responses. Recombinant AdVs encoding either the LHBsAg (Ad5-LHBsAg), SHBsAg (Ad5-SHBsAg) or *Firefly luciferase* (FLuc) reporter (Ad5-FLuc) were produced. Infection of Human Embryonic Kidney 293T (HEK293T) cells with Ad5-SHBsAg showed dose-dependent expression of SHBsAg in both supernatant and lysate samples. However, as expected, significantly higher expression of LHBsAg was seen in lysates from cells infected with Ad5-LHBsAg when compared to supernatant samples, because the LHBsAg peptide is not naturally secreted. Intramuscular injection of Ad5-FLuc to Balb/c mice showed significant expression of FLuc at days 1 and 3 after injection with Ad5-FLuc, with expression decreasing by day 7, as expected. Analysis of cellular immunity showed HBV-specific IFN-γ responses in mice vaccinated with Ad5-SHBsAg, Ad5-LHBsAg and EUVAX-B control. Additionally, anti-HBsAg antibodies were detected in mice vaccinated with Ad5-SHBsAg and EUVAX-B. This study shows that AdVs are promising candidates for novel anti-HBV vaccine design and may circumvent current challenges of available anti-HBV vaccines by inducing more robust immune responses while decreasing the doses required for immunisation. This research bodes well for future work in the development of vaccine regimens involving other AdVs against a variety of infectious diseases.

Acknowledgements

I would like to express my deepest gratitude to my supervisor Professor Betty Maepa, who patiently guided and supported me as I worked on this project. Her wisdom and expertise have been an integral part of this research, and I am forever grateful for her willingness to answer my millions and millions of questions.

I would also like to thank my co-supervisor Professor Patrick Arbuthnot for not only the insight and advice that he has always pleasantly and patiently provided regarding this project, but also for establishing a research unit where young scientists like me can discover their love for scientific research.

Research is very often about collaboration, so I would like to thank the members of the Wits/SAMRC Antiviral Gene Therapy Research Unit who have played a role in getting me to this point. I am grateful for the help and support that I have received, but even more so for the friends that I have made.

I would like to thank the Poliomyelitis Research Foundation (PRF) and the Wits Faculty Research Committee (FRC) for the funding that I have received to complete my MSc.

To all my dearest family and friends from all around the world who have encouraged me and prayed for me, I am deeply grateful. Thank you for listening to me talk and talk … and talk science.

Lastly, I would like to especially thank my parents, Leila and Emanuel Neves, who have been my best friends and my biggest fans since the day I was born. Thank you for teaching me from a very young age that God will always take care of me. Words alone will never be enough to express my gratitude for how their encouragement and prayers have carried me through life's ups and downs. My prayer is that God will repay them thousands of times over for what they have done for me.

Table of Contents

Declaration i

Dedication ii

Publications and Conference Presentations iii

Abstract iv

Acknowledgements v

Table of Contents vi

List of Figures xi

List of Tables xii

List of Abbreviations xiii

Chapter 1 1

1 Introduction 1

1.1 Hepatitis B 1

1.1.1 Hepatitis B virus 1

1.1.2 Anti-HBV immunity 3

1.1.2.1 Innate immunity 3

1.1.2.2 Adaptive immunity 4

1.2 Preventative measures and treatments of HBV infection 4

1.2.1 Antiviral therapies 4

1.2.2 Vaccination against HBV 5

1.3 Alternative vaccination strategies 6

1.4 Adenoviruses 7

1.4.1 Adenoviruses as gene delivery vectors 10

1.4.2 Adenoviruses as vaccine vectors 13

1.4.2.1 Ebola virus 13

1.4.2.2 Human Immunodeficiency Virus (HIV) 14

1.4.2.3 Influenza virus 14

1.5 The impact of COVID-19 on vaccine design 15

1.5.1 Sputnik V 15
1.5.2 Oxford-AstraZeneca ChAdOx1 16
1.5.3 Janssen Ad26.COV2.S 16
1.6 The potential of AdV-based anti-HBV vaccines 17
1.7 Study Aim 18
1.8 Study Objectives 18
Chapter 2 19
2 Materials and Methods 19
2.1 Construction of shuttle plasmids bearing *LHBsAg*, *SHBsAg* or *FLuc* genes 19
2.1.1 Isolation of *LHBsAg*, *SHBsAg* and *FLuc* genes from carrier plasmids 19
2.1.2 Ligation of *LHBsAg*, *SHBsAg* and *FLuc* genes into pShuttle-CMV backbone 20
2.2 Construction of Adenoviral genome plasmids expressing *LHBsAg*, *SHBsAg* and *FLuc* 21
2.2.1 Screening of recombinants with *Pac*I and *Eco*RV 21
2.3 Adenoviral vector production 22
2.4 Adenoviral amplification 23
2.5 Quantification of passage 0 and passage 1 AdV infectious units 23
2.5.1 Quantification of passage 0 and passage 1 AdV infectious units using GFP reporter AdV 23
2.5.2 Quantification of passage 1 AdV infectious units using immunostaining 24
2.6 Large-scale recombinant AdV production, harvest, and purification 24
2.6.1 AdV purification using CsCl gradient ultracentrifugation 25
2.7 Quantification of viral particle equivalents of CsCl purified AdVs 26
2.8 *In-vitro* AdV functionality tests 27
2.8.1 Infection of HEK293T cells with recombinant AdVs 27
2.8.2 Enzyme-linked immunosorbent assay (ELISA) for detection of HBV antigens produced by AdVs 27
2.8.3 Luciferase assay 27

2.9 *In vivo* AdV functionality tests 28
2.9.1 Intramuscular injection and bleeding 28
2.9.2 Bioluminescence imaging 29
2.9.3 Termination procedures 29
2.9.3.1 Splenocyte processing and stimulation 29
2.9.4 Flow cytometry analysis of cellular immune responses 30
2.9.5 HBsAg antibody ELISA 31
2.10 Statistical analyses 32
Chapter 3 33
3 Results 33
3.1 Successful ligation of *LHBsAg*, *SHBsAg* and *FLuc* genes into pShuttle-CMV backbone 33
3.2 Production of recombinant AdV genome plasmids carrying *LHBsAg*, *SHBsAg* and *FLuc* genes 36
3.3 Recombinant AdV production and amplification 37
3.3.1 Large-scale AdV production (P2) and purification 40
3.4 Transgene expression *in vitro* 42
3.4.1 *In vitro LHBsAg* and *SHBsAg* expression from Ad5-LHBsAg and Ad5-SHBsAg 42
3.4.2 *In vitro* FLuc expression from Ad5-FLuc 44
3.5 Transgene expression and induction of HBV-specific immunity in mice 44
3.5.1 *In vivo* FLuc expression 44
3.5.2 *In vivo* HBV-specific cytokine responses 47
3.5.3 *In vivo* HBsAb responses 49
Chapter 4 50
4 Discussion 50
4.1 Successful construction of recombinant pAd5 DNA 50
4.2 Ad5 production and amplification 52
4.3 Efficient *in vitro* transgene expression from recombinant AdVs 52

4.4 *In vivo* transgene expression and immunogenicity 53

Conclusions and Future work 55

References 56

5 Appendix A – General protocols and recipes 66

5.1 Bacterial work 66

5.1.1 Growth media 66

5.1.1.1 Luria-Bertani (LB) medium 66

5.1.1.2 Luria-Bertani (LB) agar 66

5.1.1.3 Antibiotics (Ampicillin and Kanamycin) 66

5.1.2 Bacterial transformation 66

5.1.2.1 $CaCl_2$ transformation buffer 66

5.1.2.2 Preparation of competent bacteria 66

5.1.3 Heat shock transformation of competent *E. coli* 67

5.2 Plasmid and DNA preparations 67

5.2.1 Buffer preparations 67

5.2.1.1 Resuspension buffer (buffer P1) 67

5.2.1.2 Lysis buffer (buffer P2) 67

5.2.1.3 Neutralisation buffer (buffer P3) 67

5.2.1.4 Wash buffer (buffer QC) 68

5.2.1.5 Equilibration buffer (buffer QBT) 68

5.2.1.6 Elution buffer (buffer QF) 68

5.2.2 Large-scale plasmid isolation 68

5.2.3 Small-scale plasmid isolation 69

5.3 Plasmid DNA manipulations 69

5.3.1 PCR amplification 69

5.3.2 Plasmid linearisation 70

5.3.3 Ligation reactions 70

5.3.4 Restriction digestion 70

5.4 Plasmid DNA extraction and agarose gel analysis 70

5.4.1 Agarose gel electrophoresis 70

5.4.2 Gel extraction 71

5.5 Tissue culturing 71
5.5.1 Cell culture media and reagents 71
5.5.1.1 High glucose Dulbecco's modified Eagles medium (DMEM) (5L) 71
5.5.1.2 Saline-Ethylenediaminetetraacetic acid (EDTA) 71
5.5.2 Cell culture procedures 72
5.5.2.1 Cell resuscitation from freezer stocks 72
5.5.2.2 Cell detachment and seeding 72
5.5.2.3 Cell storage in LN_2 72
5.6 AdV production, amplification, and purification 73
5.6.1 CsCl gradient 73
5.6.2 10 mM Tris-HCl 73
5.6.3 40% sucrose 73
5.6.4 AdV quantification 73
5.6.4.1 Immunostaining 73
5.7 ELISA 73
5.7.1 ELISA wash buffer 73
5.8 *In vivo* procedures 74
5.9 Complete study design 75
6 Supplementary Data 77
6.1 General DNA and plasmid information 77
6.1.1 Plasmids used in this study 77
6.1.2 Maps of plasmids used in this study 78
6.1.3 Plasmids constructed in this study 80
6.1.4 Maps of shuttle plasmids constructed in this study 81
6.1.5 Maps of pAdEasy plasmids constructed in this study 82
6.1.6 AdVs produced in this study 83
6.2 *In vivo* FLuc expression 84

List of Figures

Figure 1.1: HBV particle and genome structure. 2
Figure 1.2: Adenovirus structural biology. 8
Figure 1.3: Adenoviral replication cycle. 10
Figure 1.4: Three classes of adenoviral vectors. 12
Figure 3.1: Amplification of *SHBsAg* and *FLuc* genes out of carrier plasmids. 34
Figure 3.2: Restriction enzyme analysis of shuttle plasmid clones. 35
Figure 3.3: Screening of recombinant AdV DNA 37
Figure 3.4: Transfection efficiency using pAd5-GFP reporter. 38
Figure 3.5: Ad5-GFP infection at P1. 39
Figure 3.6: CPE at day of harvest of P1 40
Figure 3.7: CPE at day of harvest of P2 41
Figure 3.8: AdV purification using CsCl gradient ultracentrifugation. 42
Figure 3.9: *In vitro* LHBsAg and SHBsAg expression. 43
Figure 3.10: *In vitro* FLuc expression. 44
Figure 3.11: *In vivo* bioluminescence imaging. 46
Figure 3.12: *In vivo* HBV-specific cytokine responses. 48
Figure 3.13: *In vivo* antibody levels after vaccination of mice. 49
Figure 5.1: *In vivo* timeline. 74
Figure 5.2: Recombinant AdV production. 76
Figure 6.1: Transgene carrier plasmid maps. 78
Figure 6.2: Plasmids used for viral production and quantification. 79
Figure 6.3: pShuttle-CMV clones constructed in this study. 81
Figure 6.4: Recombinant AdV plasmids constructed in this study. 82
Figure 6.5: *In vivo* bioluminescence imaging. 84

List of Tables

Table 2.1: Primers used for PCR amplification of *SHBsAg* and *FLuc* sequences out of carrier plasmids 19
Table 2.2: Primer sequences for *LHBsAg*, *SHBsAg* and *FLuc* transgene sequencing 20
Table 2.3: Derivation of Area counted in fields/well 24
Table 2.4: HVF and HVR primers used for qPCR quantification of AdVs (Palmer and Ng, 2003) 26
Table 2.5: qPCR cycling conditions.....27
Table 3.1: Viral quantification after AdV production and amplification 40
Table 3.2: Final average AdV yields after quantification using qPCR 42
Table 5.1: Cycling conditions for PCR amplification of *SHBsAg* and *FLuc* sequences.....70
Table 5.2: Volumes for cell culture procedures.....72
Table 6.1: Description and source of plasmids used in this study 77
Table 6.2: Description of plasmids constructed in this study 80
Table 6.3: Recombinant AdVs produced in this study.....83

List of Abbreviations

Abs – antibodies

Ad2 – adenovirus serotype 2

Ad26 – adenovirus serotype 26

$Ad26^-$ – Ad26 seronegative

$Ad26^+$ – Ad26 seropositive

Ad4 – adenovirus serotype 4

Ad5 – adenovirus serotype 5

Ad5-FLuc – adenovirus encoding Firefly luciferase

Ad5-LHBsAg – adenovirus encoding HBV large surface antigen

Ad5-SHBsAg – adenovirus encoding HBV small surface antigen

Ad7 – adenovirus serotype 7

Ads – adenoviruses

AdVs – adenoviral vectors

APCs – antigen-presenting cells

AREC – Wits Animal Research Ethics Committee

BSA – Bovine Serum Albumin

CAR – coxsackie adenovirus receptor

cccDNA – covalently closed circular DNA

CMV – cytomegalovirus

CPE – cytopathic effects

CSC – Cell Stimulation Cocktail

CTLs – cytotoxic T lymphocytes

DAB – 1 x 3,3-Diaminobenzidine

DMEM – Dulbecco's modified Eagle's medium

DMSO – dimethyl sulfoxide

DNA – deoxyribonucleic acid

E. coli – Escherichia Coil

EDTA – ethylenediaminetetraacetic acid

ELISA – Enzyme-linked immunosorbent assay

ER – endoplasmic reticulum

FBS – Fetal Bovine Serum

FLuc – *Firefly luciferase*

GFP – Green Fluorescent Protein

HA – Hemagglutinin

HBcAg – HBV core antigen

HBeAg – HBV envelope antigen

HBsAg – HBV surface antigen

HBV – Hepatitis B virus

HCC – Hepatocellular carcinoma

HEK293T – Human Embryonic Kidney 293T cells

HIV – Human Immunodeficiency Virus

HRP – horseradish peroxidase

HVF – Helper virus forward primer

HVR – Helper virus reverse primer

IFNs – Interferons

Ifus – infectious units

IgG – immunoglobulin G

IL – Interleukin

ITRs – inverted terminal repeats

LARII – Luciferase Assay Reagent II

LB – Luria-Bertani medium

LHBsAg – HBV large surface antigen

MCS – multiple cloning site

MHBsAg – HBV middle surface antigen

MHCI – Major Histocompatibility Complex I

MHCII – Major Histocompatibility Complex II

MOI – multiplicity of infection

MOPS – 3-(N-morpholino) propane-1-sulfonic acid

mRNA – messenger ribonucleic acid

NAbs – neutralising antibodies

NAs – nucleoside/nucleotide analogues

NK – Natural Killer cells

NRTIs – nucleoside/nucleotide reverse transcriptase inhibitors

NTCP – sodium-taurocholate co-transporting polypeptide

ORFs – open reading frames

PBS – Phosphate Buffered Saline

PCR – Polymerase Chain Reaction

PEG – polyethylene glycol

PLB – Passive Lysis Buffer

PRRs – Pattern Recognition Receptors

qPCR – quantitative real-time polymerase chain reaction

rc-DNA – relaxed circular DNA

RLU – Relative Light Units

RNA – ribonucleic acid

RPMI – Roswell Park Memorial Institute medium

SARS-CoV-2 – severe acute respiratory syndrome coronavirus 2

SDS – sodium dodecyl sulphate

SEM – Standard Error of the Mean

SHBsAg – HBV small surface antigen

SVP – subviral particles

TAE – Tris-acetate-EDTA

TFH – T follicular helper cells

Th1 – T helper 1

Th2 – T helper 2

TNF – Tumour Necrosis Factor

Tregs – regulatory T cells

WHO – World Health Organisation

WRAF – Wits Research Animal Facility

Chapter 1

Introduction

1.1 Hepatitis B

Hepatitis B virus (HBV) is the causative agent of hepatitis B. According to the World Health Organisation (WHO), 254 million people were living with HBV, with ~1.1 million new infections annually, making it a serious global health concern. More than 95% of those who are infected with HBV during adulthood present with a self-limited or acute infection that can be cleared by the immune system (Lavanchy, 2005). However, in endemic regions such as Sub-Saharan Africa and Asia-Pacific, children are the most at-risk of life-threatening HBV infection. Perinatal transmission from mother to child or horizontal transmission to children from other infected family members, often leads to chronic HBV and may cause other complications such as liver cirrhosis and hepatocellular carcinoma (HCC) (Chuang, Tsai and Ou, 2022; Iannacone and Guidotti, 2022). Additionally, chronic HBV infection poses an economic burden, with increasing costs proportional to the severity of the disease (Lavanchy, 2005). By the year 2030, the WHO aims to eliminate the threat of viral hepatitis, encouraging countries to lower the incidence and mortality by 90% and 65% respectively (Ginzberg, Wong and Gish, 2018). However, HBV's resistance to existing drugs and co-infection with Human Immunodeficiency Virus (HIV), poverty, stigma and lack of education surrounding the disease, and limited access to diagnostic tests hinder disease elimination efforts (McNaughton *et al.*, 2019).

1.1.1 Hepatitis B virus

HBV is an enveloped virus belonging to the *Hepadnaviridae* family, consisting of an icosahedral capsid surrounding a 3.2 kb partially double-stranded relaxed circular DNA (rc-DNA) genome (Figure 1.1). Upon binding of the virus to the host sodium-taurocholate co-transporting polypeptide (NTCP) and subsequent entry into the hepatocyte, the viral envelope is removed (Farhad *et al.*, 2022). Thereafter, the rc-DNA is transported to the nuclear pores by nucleocapsids, which, upon arrival at the nuclear pore, disintegrate and release the rc-DNA into the nucleus (Schreiner and Nassal, 2017). Inside the hepatocyte nucleus, viral polymerase converts the rc-DNA into covalently closed circular DNA (cccDNA), a form of DNA that is extremely stable (Farhad *et al.*, 2022). This cccDNA remains in the hepatocyte nucleus as a

minichromosome, providing the instructions for RNA polymerase II-mediated synthesis of viral transcripts and contributing to viral persistence (McNaughton *et al.*, 2019; Schreiner and Nassal, 2017). This relatively small genome is made of four overlapping open reading frames (ORFs), namely P, preS/S (HBsAg), preC/C (HBcAg) and X, encoding polymerase, surface, precore/core and X proteins respectively (Figure 1.1) (Tsukuda and Watashi, 2020).

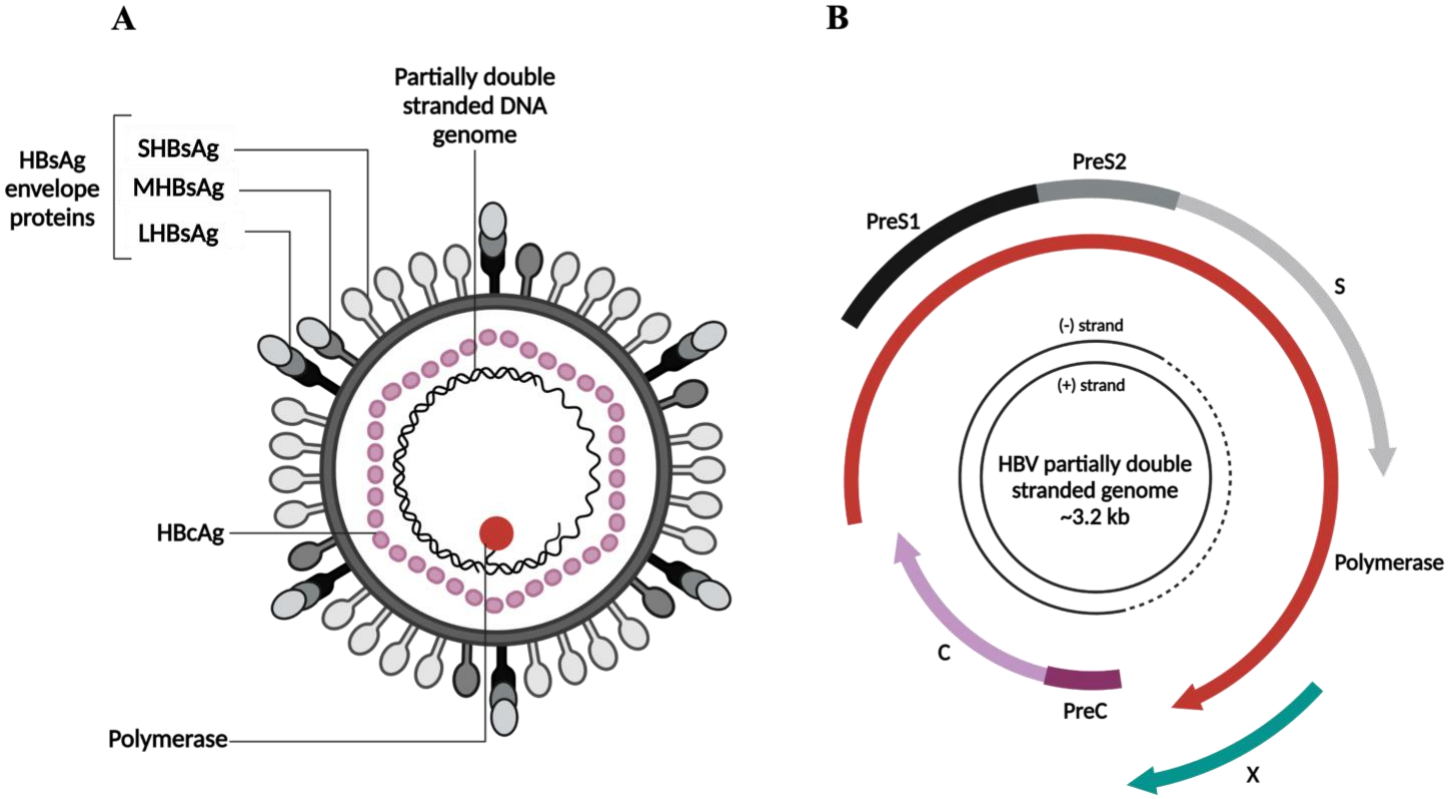

Figure 1.1: HBV particle and genome structure.

A. HBV particle consisting of a partially double-stranded genome enclosed by an icosahedral capsid and an envelope displaying the HBsAg large (LHBsAg), middle (MHBsAg) and small (SHBsAg) envelope proteins. **B.** The 3.2 kb, partially double stranded circular HBV genome consisting of four open reading frames (ORFs), which together encode precore/core (PreC), polymerase, and X proteins, as well as the surface/envelope proteins, within which three separate start codons allow for synthesis of the large, middle, and small surface proteins (Figure created with Biorender).

Diagnosis of acute or chronic HBV requires serology testing, which depends on the presence of viral biomarkers, such as HBsAg (Ott *et al.*, 2012). Chronic HBV infection can be specifically described as the persistent presence of HBsAg in the serum for at least six months (Pattyn *et al.*, 2021). The preS/S open reading frame of the HBV genome encodes three different envelope proteins, namely, large (LHBsAg), middle (MHBsAg) and small (SHBsAg)

(Figure 1.1) (Pollicino *et al.*, 2012). These structurally similar proteins are synthesised from three different start codons within the same open reading frame (i.e., *pre*S1, *pre*S2, and *S* respectively) (Figure 1.1) (Pollicino *et al.*, 2012). Together, these proteins represent HBsAg, which is synthesised in the endoplasmic reticulum (ER) and can sometimes be present in the serum at higher levels than necessary for virion assembly (Churin, Roderfeld and Roeb, 2015). These excess surface proteins bud from the ER/Golgi complex as subviral particles (SVP), which, through a mechanism known as "viral apoptotic-like mimicry," can contribute to immune tolerance (Churin, Roderfeld and Roeb, 2015; Vanlandschoot and Leroux-Roels, 2003).

1.1.2 Anti-HBV immunity

1.1.2.1 Innate immunity

HBV can replicate within the hepatocytes without causing direct cell damage (Tan, Koh and Bertoletti, 2015). HBV DNA and antigens only become detectable approximately five weeks after initial infection, whereafter the virus infects most hepatocytes (Fong *et al.*, 1994). This initial lag is believed to be the result of immune evasion by the virus as opposed to viral clearance by the immune system (Busca and Kumar, 2014). During infection, HBV may reduce the response of circulating neutrophils (Hu *et al.*, 2019). This results in the accumulation of neutrophils in the liver, causing hepatic tissue damage (Adugna, 2023). The host immune responses, while fighting off infection in an attempt to control the virus, contribute to liver inflammation and damage (Tan, Koh and Bertoletti, 2015). Innate immunity represents a non-specific first line of defence that is elicited by the recognition of HBV structures by pattern-recognition receptors (PRRs) (Busca and Kumar, 2014). The defensive barriers of innate immunity can be anatomic, physiologic, endocytic and phagocytic, and inflammatory (Marshall *et al.*, 2018). Innate immune responses, during the early stages of HBV infection, are activated by viral nucleic acids, viral proteins, tissue damage, and subsequent activation of antiviral cytokines (i.e., IFN-α) and natural killer (NK) cells to delay initial viral spread (Tan, Koh and Bertoletti, 2015). NK cells are the main effector population of the innate immune system, causing infected cells to die by cytokine and chemokine release (Chen *et al.*, 2005). NK cells, however, can also contribute to adaptive immunity by interacting with T and B lymphocytes, and antigen-presenting cells (APCs) (Chen *et al.*, 2005).

1.1.2.2 Adaptive immunity

Innate immune responses are critical for the activation of adaptive immunity. Adaptive immunity involves antigen-specific responses and immunological memory, which allows for more efficient immune responses upon future exposure to the antigen (Marshall *et al.*, 2018). Long-term immunity to HBV infection depends on the presence of anti-HBsAg neutralising antibodies in the serum (Pattyn *et al.*, 2021). Despite the importance of innate immunity, the ultimate outcome of viral infection is based on the presence, number and strength of HBV-specific T (i.e., helper or cytotoxic) and B cells (Bertoletti and Ferrari, 2016). The cytokines produced by CD4 T cells contribute to the development of CD8 cytotoxic T lymphocytes (CTLs), which destroy infected hepatocytes, thereby clearing HBV infection (Chisari, 1997). Cellular immunity to HBV involves Major Histocompatibility Complex class I (MHCI)-restricted $CD8^+$ cytotoxic T cells, which eliminate HBV infected cells either by inducing programmed cell death of hepatocytes, or cytotoxic T lymphocyte-induced non-cytopathologic intracellular inactivation of HBV (Chisari, Isogawa and Wieland., 2010; Chisari, 1997). The release of interferon (IFN) and tumour necrosis factor (TNF) cytokines by $CD8^+$ T cells contribute to HBV inactivation in target cells (Adugna, 2023). These T helper 1 (Th1) cytokines, along with Interleukin-2 (IL-2) contribute to cell-mediated immunity (Stoop *et al.*, 2005). Additionally, Major Histocompatibility Complex class II (MHCII)-restricted $CD4^+$ helper T cells contribute to antibody production against HBV viral envelope antigens (Busca and Kumar, 2014). In patients with chronic hepatitis B, increased levels of circulating $CD4^+CD25^+$ regulatory T cells (Tregs) may influence viral persistence and can suppress effective antiviral immune responses (Peng *et al.*, 2008). Studies into anti-HBV adaptive immunity have predominantly focussed on the T cell responses, however, B cells also mediate the effects of viral infection through antigen presentation, antibody secretion and immune regulation (Cai and Yin, 2020). IL-21, produced by T follicular helper (TFH) cells, a subset of T helper cells that regulate humoral immune responses, contributes to B cell development into antibody-forming cells (Xing, Xu and Yu, 2013).

1.2 Preventative measures and treatments of HBV infection

1.2.1 Antiviral therapies

Available antiviral medications can suppress viral replication and delay disease progression, thus lowering the incidence of HBV associated diseases and decreasing mortality (Hutin *et al.*, 2018; Yoo *et al.*, 2018). The most commonly available antiviral treatments include

nucleoside/nucleotide reverse transcriptase inhibitors (NRTIs), also known as nucleoside/nucleotide analogues (NAs), and IFNs. While the former interferes with viral reproduction by acting as false substrates for reverse transcriptase, thereby prematurely terminating the elongation of viral DNA, the latter inhibits viral entry into hepatocytes, increases immune responses to the virus, and can partially degrade cccDNA and epigenetically supress its transcription (Xia and Liang, 2019). Current therapeutic goals of HBV, specifically chronic HBV, include loss of HBsAg, anti-HB seroconversion, and inactivation of cccDNA (Xia and Protzer, 2017; Xia and Liang, 2019). While available antivirals play a crucial role in controlling viral infection, there are several limitations, and complete virological cure is rarely achieved. Because the cccDNA can persist for decades due to its long half-life, NRTIs/NAs require life-long administration because of the limited effects on the cccDNA and can often become ineffective due to viral resistance (Xia and Liang, 2019). Additionally, IFNs (particularly IFN-α), while able to elicit immunomodulatory and direct antiviral effects, are often difficult to tolerate, and the response rate is limited to 5%-20% (Xia and Protzer, 2017).

1.2.2 Vaccination against HBV

Global vaccination of new-borns against HBV remains the most vital strategy in preventing chronic HBV infection and HBV-related mortality (Wong *et al.*, 2022). Recombivax HB® was licensed in the United States in 1986, followed by Engerix-B in 1989. These vaccines are both still available in paediatric and adult formulations and are administered as a 3-dose series on a 0, 1- and 6-month schedule. Currently available HBV vaccines make use of recombinant technology to produce SHBsAg in yeast cells. The harvested and purified SHBsAg is administered as a protein-based vaccine and stimulates a humoral immune response. A study performed by Wong *et al* on vaccinated individuals born between 1988-2002 and unvaccinated individuals born between 1970-1987, reported a decrease in chronic HBV infection from 14.3% to 6.7% in subjects born in 1970 and 1988, respectively. They concluded that universal HBV vaccination notably decreased incidences of chronic HBV infection and therefore, may also play a role in decreasing HCC and other hepatic events (Wong *et al.*, 2022). While these protein-based vaccines are widely used for immunization against HBV, there are still several limitations. Firstly, these vaccines are less effective in recipients over the age of 40 years, as well as in immunocompromised individuals, which may be concerning in places like Sub-Saharan Africa where infections such as HIV and HBV have a high co-infection rate. Secondly, protein-based vaccines are limited to humoral immunity, and while humoral immunity is often

sufficient in immunising against invading pathogens, a more robust immune response may be generated if both a cell-mediated and humoral immune response is produced after vaccination. Lastly, most current HBV vaccines require a 3-dose regimen, which may also be an issue in low-income countries where the socioeconomic environment prevents access to appropriate and consistent healthcare. Therefore, research into alternative vaccination and immunisation methods is essential to address these issues.

1.3 Alternative vaccination strategies

Vaccination represents one of the most important and effective medical interventions ever developed. Traditionally, vaccines have been produced by isolating and attenuating or inactivating the infectious agent before administration to the human immune system (Grimm and Ackerman, 2013). While these vaccines have effectively targeted pathogens with low antigen variability (i.e., polio, measles, mumps, and rubella), in some instances, these methods are associated with adverse effects, including inflammatory, allergic, and autoimmune responses (Heidary *et al.*, 2022). Additionally, the emergence of pathogens with the ability to change rapidly with more complex immune evasion strategies have called for more advanced vaccines (Grimm and Ackerman, 2013).

Subunit vaccines have been prominent and effective candidates for vaccine design, delivering only the microbial components required to produce appropriate immune responses (Moyle and Toth, 2013). Subunit vaccines possess many desirable qualities, including their increased safety and lot-to-lot consistency, as well as the ability to stimulate potent immune responses (Moyle and Toth, 2013). They are, however, weaker than traditional vaccines, and require the incorporation of adjuvants with potent immunostimulatory effects (Pulendran and Ahmed, 2011). Vaccines should ideally be safe, display long-term stability, and provide life-long protection after only a single dose (Moyle and Toth, 2013). However, subunit vaccines often require multiple doses. Next-generation vaccine technologies, including nucleic acids, viral vectors and artificial antigen presenting cells have been investigated as candidates for vaccine design (Jacob-Dolan and Barouch, 2022).

Next-generation vaccines are characterised by an enhanced ability to block infection and transmission, improved durability, and enhanced breadth of protection to variants. Additionally, the primary advantage of these vaccine platforms is that they are highly and

relatively easily adaptable because they can be developed based on sequence information alone (van Riel and de Wit, 2020). Production of artificial antigen presenting cells loaded with peptides that would otherwise be provided or produced by vaccination is achieved by transducing immortalised cells with lentiviruses to mimic antigen presenting cells (van Riel and de Wit, 2020). However, this approach is poorly explored. Nucleic acid-based vaccines consist of either synthetic DNA or mRNA constructs encoding the antigens of interest. Administration of DNA and mRNA vaccines require a carrier molecule for efficient uptake (i.e., lipid nanoparticle) and entry into cells (van Riel and de Wit, 2020). In addition to nucleic acid-based and antigen presenting vaccines, viral vector-based platforms are also attractive for next-generation vaccine design. Since the development of the first SV40 viral vector expressing a foreign gene, other viruses have been used as vaccine vectors (Travieso *et al.*, 2022). Some of these include lentiviruses, poxviruses, herpesviruses, and vesicle stomatitis virus. These vectors are either replication competent or replication defective and express the antigens of interest to induce immune responses (Travieso *et al.*, 2022). Specifically, the use of adenoviral vectors (AdVs) as vaccine vectors has been appealing to scientists and researchers for many years (Farhad *et al.*, 2022).

1.4 Adenoviruses

Adenoviruses (Ads) are nonenveloped viruses that form part of the *mastadenoviridae* genera under the *Adenoviridae* family. Ads consists of a double stranded DNA genome that is present within a protein core that is surrounded by an icosahedral protein shell (Figure 1.2). On the surface of the Ad capsid are three exposed proteins, namely hexon, fibre and penton (Figure 1.2). Approximately 70 human serotypes have been discovered, with the widely studied serotype 2 (Ad2) and serotype 5 (Ad5) causing upper respiratory infections (Chang, 2021). The linear duplex DNA genome encodes ~35 proteins that are either expressed “early” (i.e., before initiation of viral DNA replication) or “late” (i.e., following initiation of DNA replication). These “early” and “late” genes clearly divide the Ad infection cycle into two phases. The “early” phase controls viral entry into the host cell and viral genome entry into the host cell nucleus. The “late” phase controls gene expression related to production and assembly of Ad capsid proteins. An Ad-infected cell produces about one million copies of viral DNA within 40 hours, making Ad DNA replication a very efficient process (Hoeben and Uil, 2013).

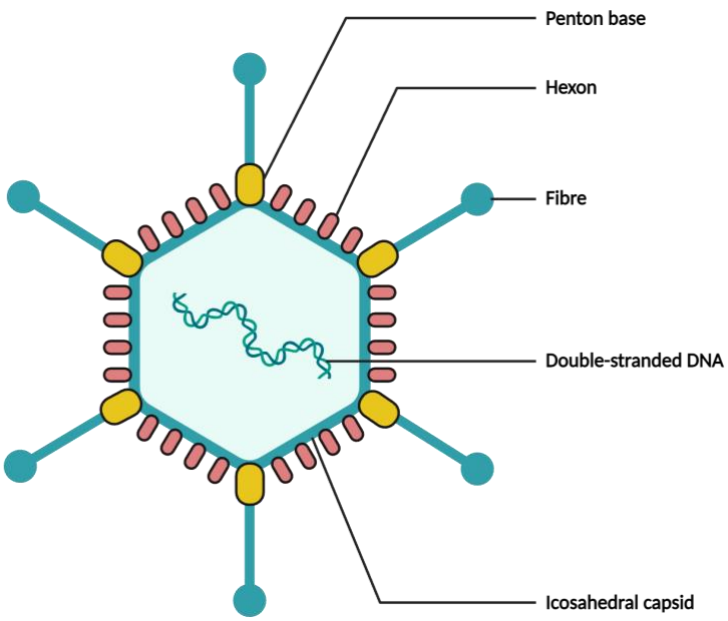

Figure 1.2: Adenovirus structural biology.

Adenoviruses are double-stranded DNA viruses with an icosahedral capsid consisting of fibre, hexon and penton proteins, which mediate viral binding and entry into host cells (Figure created with Biorender).

Adenovirus infection occurs via receptor-mediated endocytosis (Figure 1.3). Generally, endocytosis is facilitated by primary interactions between Ad fibre proteins and the coxsackie-adenovirus receptor (CAR), however, some serotypes bind elsewhere, including CD46 (Gaggar, Shayakhmetov and Lieber, 2003) and sialic acid residues (Arnberg *et al.*, 2000). After primary binding, a secondary interaction occurs between the penton base on the viral surface and integrins on the target cell surface (Leen *et al.*, 2006). Following internalisation and uncoating, Ad particles travel to the nucleus where they translocate the viral genome through nuclear pores, allowing for viral gene expression (Leen *et al.*, 2006) (Figure 2.1. B). Ultimately, viral assembly and escape is achieved by viral DNA replication and the production of Ad structural polypeptides (Leen *et al.*, 2006). The Ad genome is made up of four "early" genes (E1-E4), and five "late" genes (L1-L5) flanked by inverted terminal repeats (ITRs) (Figure 1.4). The packaging signal is located immediately after the left ITR (Figure 1.4). At the beginning of viral replication, expression of the E1 gene produces proteins that regulate expression of the other viral genes (Abudoureyimu *et al.*, 2019). These "early" genes also encode proteins involved in DNA replication, immunomodulation, cell lysis and protein stability (Jennings and Parks, 2023). The subsequent activation of "late" genes, which are

alternatively spliced and play a role in viral DNA packaging, is accompanied by reduced expression of "early" genes (Jennings and Parks, 2023; Fessler and Young, 1998)

One of the major obstacles involving the use of Ads as vectors, particularly for gene therapy, is that the host immune system contains effective mechanisms of viral detection and subsequent activation of inflammatory or cytotoxic responses (Hendrickx *et al.*, 2014). Immunity to Ads begins with activation of a systemic pro-inflammatory state by releasing IL-6, TNF-α and IL-1β pro-inflammatory cytokines (Mistchenko *et al.*, 1994; Atasheva and Shayakhmetov, 2016). Infected macrophages release cytokines and chemokines that recruit other cytotoxic immune cells to eliminate virus-infected cells (Atasheva and Shayakhmetov, 2016). The release of type I IFNs by Ad-infected cells signals the expression of effector antiviral genes in surrounding non-infected cells (Atasheva and Shayakhmetov, 2016). In the weeks following Ad infection or exposure, the adaptive immune system produces high-affinity anti-Ad IgG antibodies.

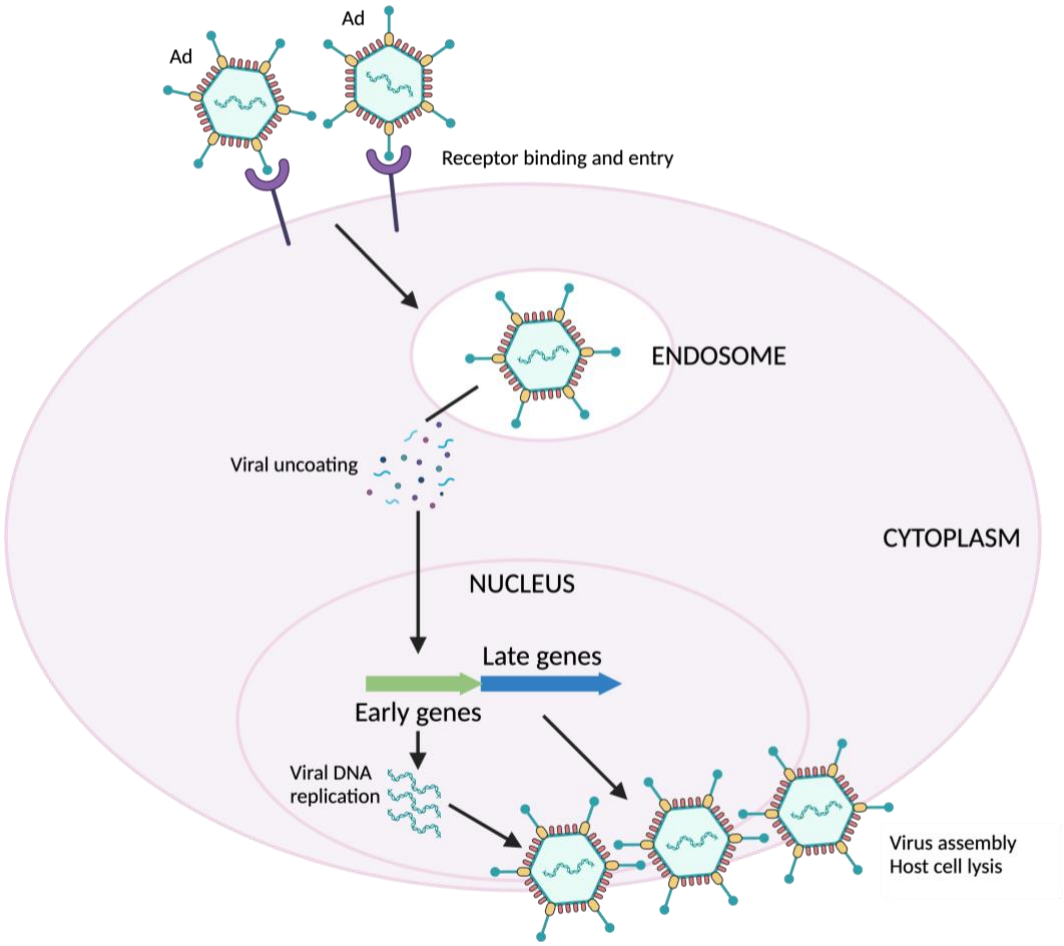

Figure 1.3: Adenoviral replication cycle.

Adenoviral replication cycle is characterised by receptor binding and endocytosis. Ad viral particles are transported to the nucleus after uncoating, where expression of early and late Ad genes leads to viral DNA replication, structural polypeptide production, and finally, Ad assembly and viral exit by host cell lysis (Figure created with Biorender and adapted from Leen *et al.*, 2006).

1.4.1 Adenoviruses as gene delivery vectors

Ads are a common tool for the transfer of foreign genetic material into mammalian cells because their biology is well studied. They can infect both dividing and non-dividing cells, induce strong expression of transgenes, and can be easily produced and purified at a large scale (Mendonça *et al.*, 2021; Danthinne, 1999). Three classes of AdVs exist, namely, first, second and third generation AdVs. All non-replicative AdVs have the E1 region of the genome deleted. First-generation AdVs may have the E3 region deleted in addition to E1, increasing the transgene capacity to ~8 kb (Figure 1.4 B) (Abudoureyimu *et al.*, 2019). First-generation AdVs

have often been used in vaccine development to deliver target antigens to cells and induce immunity against a host of infections (Farhad *et al.*, 2022). Second-generation AdVs have the E2 and E4 regions deleted in addition to E1 and E3, increasing the transgene capacity to ~12 kb (Chang, 2021) (Figure 1.4 C). Lastly, third-generation or gutless AdVs have all Ad genes deleted, leaving only the non-coding ITRs and the packaging signal (Araújo *et al.*, 2022). This increases the transgene carrying capacity to ~36 kb. The lack of Ad protein expression reduces vector immunogenicity and prolongs transgene expression, making them attractive candidates for gene therapy (Farhad *et al.*, 2022) (Figure 1.4 D).

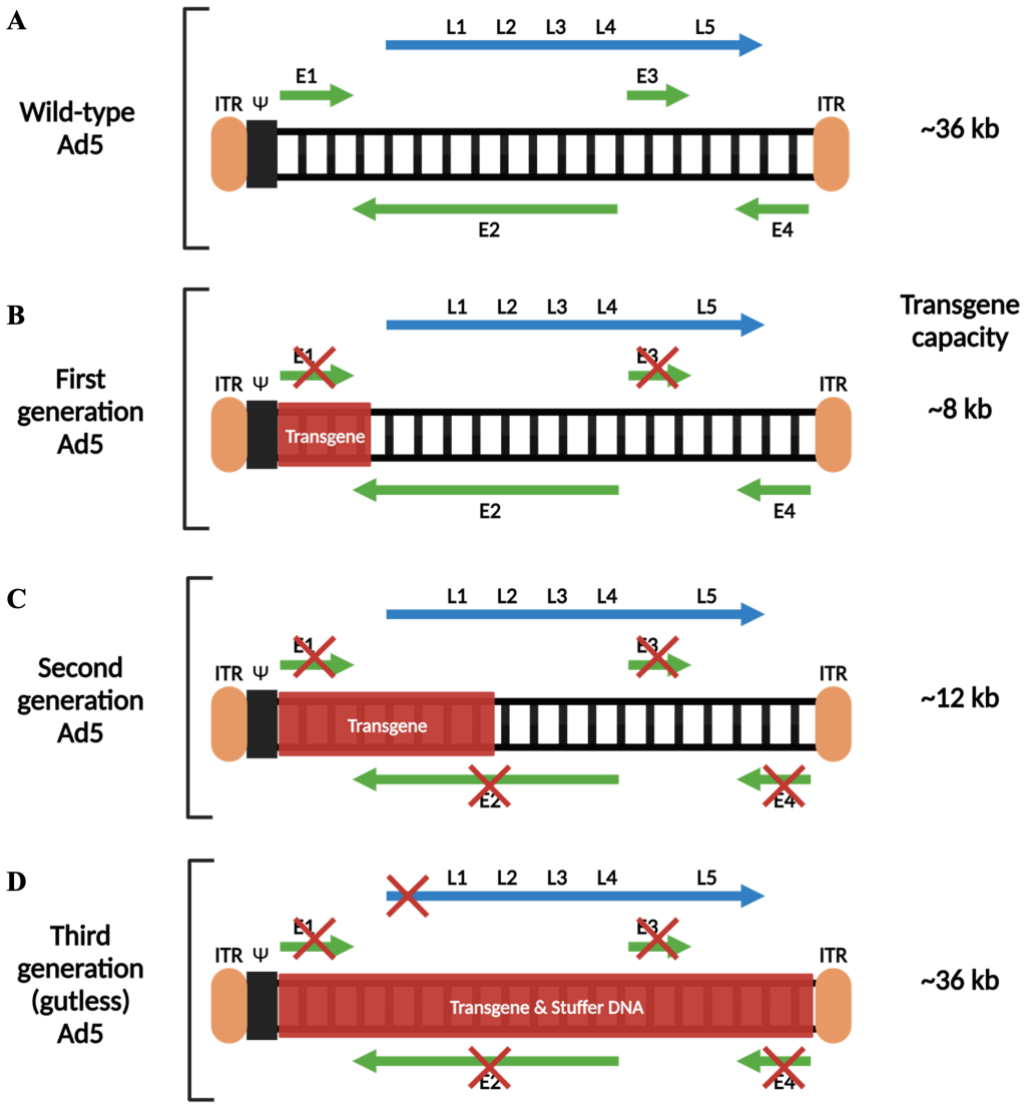

Figure 1.4: Three classes of adenoviral vectors.

A. Wildtype Ad5 genome showing the early (E) and late (L) genes, inverted terminal repeats (ITRs) and the packaging signal (Ψ). **B.** First-generation AdVs have both E1 and E3 regions deleted and a carrying capacity of ~8 kb. **C.** Second-generation AdVs, like first-generation AdVs have the E1 and E3 regions deleted. These AdVs also have an increased carrying capacity of ~12 kb due to the deletion of the E2 and E4 regions. **D.** Third-generation AdVs, also known as gutless AdVs have all the Ad genes removed to accommodate ~36 kb transgenes. A stuffer sequence is used to adjust the genome size closer to 36 kb (Figure created with Biorender and adapted from Chang, 2021).

1.4.2 Adenoviruses as vaccine vectors

While most therapeutic applications do not benefit from the AdVs ability to induce both an innate and adaptive immune response, this characteristic is useful for vaccine design (Tatsis and Ertl, 2004; Coughlan, Kremer and Shayakhmetov, 2022). Innate immune responses differ from adaptive immune responses in that they are produced during early infection and do not induce immunological memory (Farhad *et al.*, 2022). Contrastingly, the activation of B and T cell differentiation by the adaptive immune system result in the subsequent production of immunological memory (Shirley *et al.*, 2020). Other characteristics that make AdVs appealing for use as vaccine vectors include the reduced risk of genotoxicity, strong target antigen expression and relatively easy scalability to meet vaccine demand (Bangari and Mittal, 2006; Kremer, 2020; Mendonça *et al.*, 2021). Although the information on the use of AdVs in anti-HBV vaccines is limited, these viruses have been used as vaccine vectors for the immunisation against other pathogens (Farhad *et al.*, 2022).

1.4.2.1 Ebola virus

The Ebola virus was first discovered in 1976 and has since then caused various outbreaks in Africa. Ebola virus infection is extremely severe, characterised by haemorrhagic fever and an average death rate of ~50%. Because very few anti-Ebola therapies have been developed, research into anti-Ebola vaccines has been well supported. A common vaccine regimen against Ebola infection includes administration of the Ad26.ZEBOV vaccine, a recombinant Ad26 vaccine, followed by the MVA-BN-Filo vaccine, a modified vaccinia Ankara vaccine. During Ebola virus outbreaks, healthcare and frontline workers are at extremely high risk of contracting and spreading the virus (Larivière *et al.*, 2023). In a study conducted by Larivière *et al*, the safety and immunogenicity of a heterologous 2-dose Ad26.ZEBOV, MVA-BN-Filo vaccine regimen was assessed in frontliners and healthcare providers of the Democratic Republic of the Congo. Before vaccination, the baseline mean anti-EBOV IgG concentration among participants was 54.8 EU/ml, increasing to 274.3 EU/ml after the first dose, and 4166.3 EU/ml after the second dose (Larivière *et al.*, 2023). After a single Ad26.ZEBOV dose, 62.9% of participants were considered responders, and 95.2% were considered responders after the full vaccine regimen (Larivière *et al.*, 2023). Several studies have been conducted throughout Africa and Europe where this vaccine regimen was safe, well-tolerated and immunogenic (Man-Lik Choi *et al.*, 2023; Anywaine *et al.*, 2022 Pollard *et al.*, 2021).

1.4.2.2 Human Immunodeficiency Virus (HIV)

To date, there are no effective vaccines against HIV infection, however, the use of AdVs as potential vaccine candidates has been pursued (Sakurai, Tachibana and Mizuguchi, 2022). In a double-blind, randomised, placebo-controlled clinical trial conducted by Baden *et al*, systemic and mucosal immune responses induced by an E1/E3-deleted recombinant Ad26 vaccine expressing a modified gp140 HIV-1 clade A Env glycoprotein were assessed in baseline Ad26-seronegative ($Ad26^-$) and Ad26-seropositive ($Ad26^+$) healthy participants. The results showed that a single intramuscular dose of Ad26EnvA produced peripheral and mucosal EnvA-specific IgG antibodies in both $Ad26^-$ and $Ad26^+$ participants (Baden *et al.*, 2015). Additionally, analysis of peripheral and mucosal EnvA-specific IFN-γ T cell responses showed detectable $CD8^+$ and $CD4^+$ responses in both $Ad26^-$ and $Ad26^+$ participants (Baden *et al.*, 2015). One challenge for HIV-1 vaccine development, however, is eliciting broader immune responses to circulating HIV-1 strains (Barouch *et al.*, 2018). Barouch and colleagues conducted a study published in 2018 to assess the safety and immunogenicity of vaccine regimes involving an initial dose of Ad26 expressing mosaic Env/Gag/Pol antigens and a booster dose with Ad26 or MVA expressing these antigens with or without aluminium adjuvanted clade C Env gp140 protein. All vaccine regimens forming part of the study were well tolerated, with the mosaic Ad26 prime/Ad26+gp140 boost vaccine showing the most immunogenicity in humans and eliciting Env-specific T cell, antibody and antibody-dependent phagocytosis responses (Barouch *et al.*, 2018).

1.4.2.3 Influenza virus

While conventional vaccines against influenza virus infection have focussed on the use of live attenuated, inactivated, or split viruses, these vaccines, however, have a relatively low efficiency and a narrow range of coverage (Sakurai, Tachibana and Mizuguchi, 2022). Because of this, and because influenza infection is a public health concern, other vaccination strategies are being investigated, including recombinant AdVs expressing influenza proteins. When the effects of an Ad5-based avian H5N1 vaccine, specifically encoding hemagglutinin (HA) isolated from the 2003-2005 Vietnam outbreak, were tested by Gao *et al.*, the results showed that vaccination conferred protection against viral challenge and induced both cellular and humoral immunity in mice (Gao *et al.*, 2006). Additionally, because H5N1 is commonly spread by poultry, including domestic chickens, the efficacy of this Ad5-based vaccine was tested on these birds (Gao *et al.*, 2006). After subcutaneous immunisation and boosting upon viral

challenge, all immunised birds were found to be protected against viral infection (Gao *et al.*, 2006).

1.5 The impact of COVID-19 on vaccine design

The recent pandemic caused by severe acute respiratory syndrome coronavirus 2 (SARS-CoV-2) was first declared by the WHO as a global public health emergency in January of 2020. Attempting to prevent the spread of the virus, governments around the world implemented measures including quarantine, social distancing and isolation of patients who presented with symptoms of SARS-CoV-2 infection (Jafari *et al.*, 2022). Given the urgency of the situation and the lack of effective licensed treatment, vaccination was the best approach to disease control (Jafari *et al.*, 2022). Since then, the global demand for rapid and effective vaccine production has intensified. COVID-19 vaccine development has highlighted the impact of scientific advances (Jafari *et al.*, 2022). This has prompted investment into next-generation vaccine platforms. Some of the more widely recognised vaccines based on AdV technology include, the Russian-developed Sputnik V Ad-based vaccine, the Oxford-AstraZeneca ChAdOx-1 vaccine, and the Janssen Ad26.COV2.S vaccine.

1.5.1 Sputnik V

Developed by the Gamaleya Research Institute of Epidemiology and Microbiology is Russia, Sputnik V or Gam-COVID-Vac was the first registered vaccine against COVID-19 based on a combination human adenovirus vector platform. This vaccine regimen involves intramuscular administration of recombinant Ad26 and Ad5, which both carry the full-length gene for SARS-CoV-2 S glycoprotein, in a 21-day interval. Phase I/II clinical trials, completed in August, 2020 demonstrated cellular and humoral immune responses in participants and a good safety profile, with no serious adverse effects detected (Logunov *et al.*, 2020). Thereafter, a randomised, double-blind, placebo-controlled, multicentre, phase III trial was performed at 25 hospitals and polyclinics in Moscow, Russia to assess the efficacy, immunogenicity, and safety of Sputnik V against SARS-CoV-2-induced COVID-19 infection in adults (Logunov *et al.*, 2021). In this particular vaccine regimen, Ad26-S was administered as the first dose and Ad5-S as the second dose. The full dosage was 1×10^{11} viral particles in 0.5 ml per dose for intramuscular injection. The placebo was made up of vaccine buffer without recombinant AdVs and administered at an equal volume as the vaccine and via the same injection route. The results of this phase 3 vaccination trial showed a 91.6% efficacy against COVID-19 infection, with only 0.3% of

participants reporting serious adverse effects unrelated, however, to the vaccine. Additionally, the vaccine induced robust cellular and humoral immune responses in participants of all age groups (Logunov *et al.*, 2021, p. 3).

1.5.2 Oxford-AstraZeneca ChAdOx1

To avoid pre-existing immunity to human adenovirus serotypes, the ChAdOx1 nCoV-19 vaccine was developed using the simian adenovirus vector, ChAdOx1, encoding the full-length SARS-CoV-2 spike protein. In a phase I/II, single-blind, randomised, controlled clinical trial, both cellular and humoral immune responses were obtained after a single dose (5×10^{10} viral particles) of ChAdOx1 nCoV-19, with no serious adverse events relating to vaccination reported (Folegatti *et al.*, 2020). Additionally, the safety and efficacy of the ChAdOx1 nCoV-19 vaccine was tested by Voysey *et al* in four randomised controlled trials in Brazil, South Africa, and the United Kingdom. In this study, one group of vaccinated participants were given two doses of 5×10^{10} viral particles (standard dose), while a subset of the participants in the United Kingdom trial were given half of the standard dose as a first dose and the standard dose as a second dose. Administration of two standard doses, or a low dose followed by a standard dose showed 62.1% and 90.0% efficacy, respectively. Results showed that vaccine efficacy was 62.1% in participants who received two standard doses, and 90.0% in those who received a low dose followed by the standard dose, resulting in an overall vaccine efficacy of 70.4% across both groups (Voysey *et al.*, 2021). Only three adverse events were considered possibly related to the vaccine (Voysey *et al.*, 2021).

1.5.3 Janssen Ad26.COV2.S

The Janssen COVID-19 vaccine was developed by Janssen Vaccines in the Netherlands and Janssen Pharmaceuticals, a subsidiary of the American company, Johnson & Johnson. The vaccine was developed as a recombinant replication-incompetent human Ad26 vector encoding the full-length SARS-CoV-2 spike protein. In a multicentre, placebo-controlled, phase I/IIa trial, healthy adults received the Ad26.COV2.S vaccine or placebo in a single or double-dose regimen (i.e., low dose of 5×10^{10} viral particles per ml and a high dose of 1×10^{11} viral particles per ml) (Sadoff, Le Gars, *et al.*, 2021). Twenty-nine days following the first dose, NAbs were detected against wild-type virus. Further development of this vaccine candidate was supported by the immunogenicity and safety profiles of Ad26.COV2.S (Sadoff, Le Gars, *et al.*, 2021). Additionally, in an international, randomised, double-blind, placebo-controlled,

phase III trial, randomly selected participants were given either a single dose of Ad26.COV2.S at 5×10^{10} viral particles or a placebo. Administration of a single-dose of Ad26.COV2.S was protective against symptomatic and asymptomatic COVID-19 infection. Additionally, vaccination proved effective against severe disease, including hospitalisation and death (Sadoff, Gray, *et al.*, 2021). The success of Ad-based vaccines for SARS-CoV-2 bodes well for the research and implementation of Ad-based vaccines for immunisation against other pathogens in the future, including hepatitis B (Farhad *et al.*, 2022).

1.6 The potential of AdV-based anti-HBV vaccines

While AdV-based vaccine research has made meaningful contributions to immunisation against various infectious diseases, including SARS-CoV-2, it is important to note that there is a significant gap in the application of AdVs to vaccination against HBV (Farhad *et al.*, 2022), with only few studies conducted using AdVs as vaccine mechanisms in chimpanzees and dogs in the late 1980s and mid-1990s. In a study published in 1989 by Lubeck *et al*, the immunogenicity and efficacy of sequential oral immunisation with Ad7 and Ad4-based vaccines encoding HBsAg was evaluated in four chimpanzees with low neutralising antibody profiles for both Ad7 and Ad4. The study found that anti-HBsAg responses were induced in 2/4 chimpanzees (Lubeck *et al.*, 1989). Another study published in 1994 by Chengalvala *et al* evaluated immunogenicity in dogs following vaccination with Ad4 or Ad7 recombinant AdVs encoding HBsAg. Transtracheal immunisation with either Ad4ΔE3H or Ad7ΔE3H showed dose-dependent anti-HBsAg antibody responses as early as 14 days after vaccination (Chengalvala *et al.*, 1994). Boosting with heterotypic viruses (i.e., either Ad7ΔE3H or Ad4ΔE3H respectively) 12 weeks following the first vaccine showed elevated and persistent anti-HBsAg levels in animals that presented with significant primary anti-HBsAg responses (Chengalvala *et al.*, 1994). The use of AdVs has also been applied to anti-HBV immunotherapeutics and therapeutic vaccines, whereby recombinant AdVs encoding genes for various HBV proteins are administered after HBV infection to stimulate the immune system to produce an antiviral response (Martin *et al.*, 2015; Chinnakannan *et al.*, 2020). This study has been conducted to address the gap in AdV-based anti-HBV vaccine research.

1.7 Study Aim

This study aims to investigate the expression and immunogenicity of the HBV large (LHBsAg) and small (SHBsAg) surface antigens following *in vitro* and *in vivo* gene delivery using recombinant adenoviruses.

1.8 Study Objectives

I. To construct recombinant adenoviral DNA encoding the LHBsAg, SHBsAg and FLuc using the AdEasy system.
II. To produce, amplify and purify recombinant adenoviruses by transfecting Human Embryonic 293T (HEK293T) cells with recombinant DNA produced.
III. To assess transgene expression from AdVs in cultured HEK293T cells.
IV. To determine transduction following intramuscular injection of AdVs in Balb/c mice.
V. To evaluate induction of HBV-specific T cell responses in mice vaccinated with AdVs.
VI. To determine HBV-specific antibody production in mice vaccinated with AdVs.

Chapter 2

Materials and Methods

2.1 Construction of shuttle plasmids bearing *LHBsAg*, *SHBsAg* or *FLuc* genes

2.1.1 Isolation of *LHBsAg*, *SHBsAg* and *FLuc* genes from carrier plasmids

To isolate the LHBsAg-encoding DNA, 60 µg of the pUC-57-LHBs plasmid carrying the *LHBsAg* sequence (Supplementary Data – Table 6.1 & Figure 6.1 A) was digested with *Acc*65I and *Hind*III. The digested DNA was run on a 1% agarose gel and the LHBsAg fragment was extracted using the QIAGEN QIAquick Gel Extraction Kit (Qiagen, MD, USA) according to manufacturer's instructions (Appendix A – Section 5.4.2). DNA concentration was measured using the NanoPhotometer® Spectrophotometer (Implen Inc., CA, USA).

To isolate *SHBsAg* and *FLuc*, the fragments were PCR-amplified out of carrier plasmids, pUC-57-MCS-polyA-SHBs and PGL4.50[luc2/CMV/Hygro] respectively (Supplementary Data – Table 6.1 & Figure 6.1 B & C) using forward and reverse primers containing *Acc*65I and *Hind*III restriction sites respectively (Table 2.1). PCR amplicons were digested with *Acc*65I and *Hind*III in a double digest reaction and purified using the QIAGEN QIAquick Gel Extraction Kit (Qiagen, MD, USA) according to manufacturer's instructions (Appendix A – Section 5.4.2). PCR cycling conditions are outlined in Appendix A – Table 5.1.

Table 2.1: Primers used for PCR amplification of *SHBsAg* and *FLuc* sequences out of carrier plasmids

Primer name	Primer sequence	Description
SHBsAg Forward	5'-GCCTAG**GGTACC**ATG GAGAATATTACTTC-3'	Forward primer to amplify *SHBsAg* sequence with *Acc*65I restriction site indicated in red
SHBsAg Reverse	5'-TAGCC**AAGCTT**TCA AATGTAGACCCAC-3'	Reverse primer to amplify *SHBsAg* sequence with *Hind*III restriction site indicated in blue
FLuc Forward	5'-GCCTAG**GGTACC**AT GGAAGATGCCAAA-3'	Forward primer to amplify *FLuc* sequence with *Acc*65I restriction site indicated in red

FLuc Reverse	5'-TAGCC**AAGCTT**TT ACACGGCGATCTTG-3'	Reverse primer to amplify *FLuc* sequence with *Hind*III restriction site indicated in blue

2.1.2 Ligation of *LHBsAg*, *SHBsAg* and *FLuc* genes into pShuttle-CMV backbone

The pShuttle-CMV backbone bearing homology arms to the AdV genome (Supplementary Data – Table 6.1 & Figure 6.2 A) was prepared for ligation by enzymatic digestion with *Acc*65I and *Hind*III. Digested backbone was run on a 1% agarose gel and the backbone fragment (i.e., 7442 bp) was extracted using the QIAGEN QIAquick Gel Extraction Kit (Qiagen, MD, USA) according to manufacturer's instructions (Appendix A – Section 5.4.2). DNA concentration was measured using the NanoPhotometer® Spectrophotometer (Implen Inc., CA, USA).

For ligation of *LHBsAg*, *SHBsAg* and *FLuc* genes into the pShuttle-CMV backbone, ligation was performed according to the NEB T4 DNA ligase ligation protocol (New England Biolabs, MA, USA). The reactions were set up according to the procedure in Appendix A – Section 5.3.3. Ligation reactions were then used to transform chemically competent *E. coli* (Appendix A – Section 5.1.3). A no-insert control was set up alongside each ligation reaction.

Clones were screened by enzymatic digestion. Clones encoding LHBsAg (Supplementary Data – Table 6.2 & Figure 6.3 A) were screened with *Acc*65I and *Hind*III in a double digest reaction and *Apa*LI in a single digest reaction (Appendix A – Section 5.3.4). Clones encoding SHBsAg and FLuc (Supplementary Data – Table 6.2 & Figure 6.3 B & C) were both screened with *Acc*65I and *Hind*III in a double digest reaction and in an additional double digest reaction with *Eco*32I and *BgL*II, and *Apa*LI and *Sca*I respectively (Appendix A – Section 5.3.4).

Sequencing of cloned *LHBsAg*, *SHBsAg* and *FLuc* transgenes was performed by Inqaba Biotechnical Laboratories (Pty) Ltd. Primers used for sequencing are outlined in Table 2.2.

Table 2.2: Primer sequences for *LHBsAg*, *SHBsAg* and *FLuc* transgene sequencing

Sequence	Forward Primer	Reverse Primer
LHBsAg	5'-CGCAAATGGG CGGTAGGCGTG-3'	5'-CCACCCTTAA CCACGCCCAG-3'
SHBsAg	5'-CGCAAATGGG CGGTAGGCGTG-3'	5'-GTTCAGGGGGA GGTGTGGGAGG-3'
FLuc	5'-CGCAAATGGG CGGTAGGCGTG-3'	5'-GTTCAGGGGGA GGTGTGGGAGG-3'

2.2 Construction of Adenoviral genome plasmids expressing *LHBsAg*, *SHBsAg* and *FLuc*

In preparation for co-transformation, shuttle plasmid clones encoding LHBsAg, SHBsAg and FLuc (Supplementary Data – Table 6.2 & Figure 6.3) were linearised with *Eco*RI (Appendix A – Section 5.3.2).

One microgram of the linearised clone DNA, mixed in a maximum of 4 µl dH_2O was added to 100 ng pAdEasy-1 DNA, an adenoviral genome sequence bearing plasmid (Supplementary Data – Table 6.1 & Figure 6.2 B), mixed in a maximum of 1 µl dH_2O. The complete mixture was added to 20 µl electrocompetent BJ5183 *E. coli* (Agilent, CA, USA) and transferred to a 2 mm prechilled electroporation cuvette, taking care to avoid introducing bubbles. Electroporation was performed at 2000 V, 200 Ω and 23 µF. One millilitre prewarmed SOC/LB medium (New England Biolabs, MA, USA) was immediately added the cuvette and the mixture was transferred to a clean tube. After sealing the tube with parafilm, the mixture was incubated at 37°C with shaking for 1 hour. About 600 µl, 300 µl/200 µl and 100 µl of electroporated mixture was separately plated on agar plates supplemented with kanamycin and incubated at 37°C for 48 hours. Several of the smallest colonies were picked from the plates and cultured before small scale plasmid DNA isolation (Appendix A – Section 5.2.3) and agarose gel electrophoresis (Appendix A – Section 5.4.1). To avoid further recombination events, high molecular weight recombinant DNA from several clones was separately transformed into DH5α/10-β *E. coli* and plated on agar plates before small scale plasmid DNA isolation (Appendix A – Section 5.2.3).

2.2.1 Screening of recombinants with *Pac*I and *Eco*RV

Recombinant AdV DNA from DH5α/10-β *E. coli* was digested with *Pac*I and of the positive recombinants that showed a banding pattern of ~30 kb and ~4.5 kb, one was selected for large scale plasmid isolation (Appendix A – Section 5.2.2) and confirmation by restriction analysis with *Pac*I. Recombinant DNA encoding green fluorescent protein (GFP), which was previously produced using the pAdTrack-CMV shuttle plasmid (Supplementary Data – Table 6.1 & Figure 6.2 C), was also digested alongside the recombinants encoding LHBsAg, SHBsAg and FLuc. To further confirm integrity, all recombinants were digested with *Eco*RV. Screening digest reactions with *Pac*I and *Eco*RV were set up as described in Appendix A – Section 5.3.4 and

digested recombinant DNA samples were run on a 1% agarose gel (Appendix A – Section 5.4.1).

2.3 Adenoviral vector production

In preparation for transfection, 12 µg of recombinant AdV DNA (Supplementary Data – Table 6.2 & Figure 6.4) was digested with *Pac*I to remove the bacterial sequences (Appendix A – Section 5.3.4). About 1 µg of the digested DNA was analysed by agarose gel electrophoresis (Appendix A – Section 5.4.1) to confirm complete digestion. HEK293T cells were grown to 90-100% confluency in a 75 cm^2 cell culture flask. The cells were then seeded in 25 cm^2 flasks at 15% confluency (Appendix A – Section 5.5.2.2). Cells were left to grow overnight at 37°C and 5% CO_2. Transfection was performed with 10 µg *Pac*I digested recombinant AdV DNA using Lipofectamine™ 3000 reagent according to manufacturer's instructions (Invitrogen, Thermo Fisher Scientific, MA, USA). For each AdV DNA sample, transfection mixtures were prepared by adding together ~10 µg AdV DNA, 10 µl p3000 and Opti-MEM to a final volume of 250 µl. Lipofectamine mix was prepared by mixing 15 µl Lipofectamine™ 3000 with 235 µl Opti-MEM for a final volume of 250 µl. Thereafter, 250 µl Lipofectamine mix was added to 250 µl transfection mix and incubated at room temperature for 15 minutes. After incubation, 500 µl Lipofectamine transfection mixture was added to cells and the cells were incubated at 37°C and 5% CO_2. Transfection with pAd5-GFP recombinant DNA was performed in parallel and used as a reporter to assess transfection efficiency. Note that transfections were not all performed on the same day, but rather when plasmid DNA was ready. Cells transfected with pAd5-LHBsAg, pAd5-SHBsAg and pAd5-FLuc (Supplementary Data – Figure 6.4), however, lacked the presence of reporter genes that are visible with fluorescent microscopy, and were instead monitored for CPE (e.g., cell rounding, clumping, lifting from the surface of the flask).

Spent medium was replaced 24 hours after transfection to remove lipofectamine to prevent cell toxicity and death. Thereafter, half of the spent medium was replaced only when medium colour turned yellow. Cells were monitored for cytopathic effects (CPE) (i.e., rounding, clumping, detaching from flask) and collected in spent medium once ~100% CPE was observed. Collected cells were supplemented with 10% sucrose (Appendix A – Section 5.6.3) and lysed by 3 × freeze-thaw cycles at -80°C followed by a 37°C water bath to release recombinant AdVs. The virus in the lysate was considered Passage 0 (P0) AdV.

2.4 Adenoviral amplification

HEK293T cells were grown to 90-100% confluency in a 75 cm^2 cell culture flask. HEK293T cells were then seeded at 10% confluency in 75 cm^2 flasks (Appendix A – Section 5.5.2.2). The protocol for cell seeding was used based on confluency and not exact cell numbers. Confluency is dependent on the surface of the flask that is covered by cells and varies with different cell lines. For viral production, amplification and large-scale production, exact cell counts were not needed for transfection/infection. AdVs were harvested from P0 and used for subsequent infection of HEK293T cells. Cells were infected with P0 AdV on the same day at a multiplicity of infection (MOI) of ~0.1. Infected cells were incubated at 37°C and 5% CO_2 for 5-7 days with replacement of half of the spent medium only when medium turned yellow. Cells were monitored for CPE and collected in spent medium once ~100% CPE was observed. Collected cells were supplemented with 10% sucrose (Appendix A – Section 5.6.3) and lysed by 3 × freeze-thaw cycles at -80°C followed by a 37°C water bath to release recombinant AdVs. The virus in the lysate was considered Passage 1 (P1) AdV.

2.5 Quantification of passage 0 and passage 1 AdV infectious units

2.5.1 Quantification of passage 0 and passage 1 AdV infectious units using GFP reporter AdV

To easily assess production and amplification success, GFP expressing AdV (Ad5-GFP) was produced using a previously constructed plasmid AdV plasmid encoding GFP and amplified in parallel with all AdV productions and amplifications. To quantify infectious units (ifus), HEK293T cells were seeded in a 24-well cell culture plate at 50-60% confluency (Appendix A – Section 5.5.2.2). Cells were infected on the same day in duplicate with serial dilutions (i.e., undiluted, 10×, 100× and 1000×) of P0 or P1 Ad5-GFP. Infected cells were incubated at 37°C and 5% CO_2 for 48 hours. Cells emitting green light under fluorescent microscopy were counted. Fields/well values were obtained from Table 2.3 and the following formula was used to determine ifu/ml:

$$number\ of\ ifu/ml: \frac{(infected\ cells\ per\ field) \times (fields\ per\ well)}{volume\ of\ virus\ (ml) \times dilution\ factor}$$

Table 2.3: Derivation of Area counted in fields/well

Objective Lenses	Fields/wells		
	12 well plate area = 3.8 cm^2	24 well plate area = 2.0 cm^2	96 well plate area = 0.32 cm^2
4×	19	10	1.6
5×	30	16	2.6
10×	150	79	12.6
20×	594	313	50

2.5.2 Quantification of passage 1 AdV infectious units using immunostaining

HEK293T cells were seeded in a 24-well cell culture plate at 50% confluency (Appendix A – Section 5.5.2.2). Cells were infected on the same day in duplicate with serial dilutions (i.e., undiluted, 10×, 100× and 1000×) of either P1 Ad5-LHBsAg, P1 Ad5-SHBsAg or P1 Ad5-FLuc. Infected cells were incubated at 37°C and 5% CO_2 for 48 hours. After 48 hours, the spent medium was removed, and the cells were left to air dry for 5 minutes. Cells were fixed to the plate with 300 µl ice-cold methanol (100%) and incubated at -20°C for 20 minutes. Methanol was removed and cells were washed twice with 300 µl 1 × phosphate buffered saline (PBS). Five drops of blocking buffer (3 drops of serum mixed in 1 × PBS) was added to each well and incubated at room temperature for 20 minutes. Blocking buffer was removed and cells were washed once with 1 × PBS. Cells were permeabilised with 300 µl permeabilisation solution (Appendix A – Section 5.6.4.1) for 5 minutes at room temperature. Permeabilization solution was removed, and cells were washed once with 1 × PBS. Three hundred microliters of Ad hexon specific primary antibody (1000 × dilution) (Takara Bio Inc., SHG, JP) was added to each well and incubated at room temperature for 1 hour. The primary antibody was removed, and cells were washed with 1 × PBS before adding 300 µl of horseradish peroxidase (HRP)-conjugated secondary antibody (1000 × dilution) (Takara Bio Inc., SHG, JP) and incubating at room temperature for 30 minutes. The secondary antibody was removed, and cells were washed once with 1 × PBS. To stain the cells, 300 µl of 1 × 3,3'-Diaminobenzidine (DAB) substrate was added to each well and the stain was left to develop for 30 minutes. Stained cells were counted under a light microscope and ifu/ml calculated as described above.

2.6 Large-scale recombinant AdV production, harvest, and purification

HEK293T cells were grown to 90-100% confluency in 175 cm^2 cell culture flasks. Cells were then seeded at 10% confluency (Appendix A – Section 5.5.2.2) in 20 × 175 cm^2 flasks. Cells were infected with P1 Ad5-LHBsAg, Ad5-SHBsAg, or Ad5-FLuc at an MOI of ~0.1. Infected

cells were incubated at 37°C and 5% CO_2 for 7-8 days with half spent medium replacement when medium turned yellow. Cells were monitored for CPE and collected in spent medium once ~100% CPE was observed. Cells were pelleted by centrifugation at ~100 × g for 5 minutes at room temperature. After discarding the supernatant, cells were resuspended in ~10 ml 100 mM Tris-HCL and supplemented with 10% sucrose (Appendix A – Section 5.6.3). Cells were stored at -80°C until viral purification.

2.6.1 AdV purification using CsCl gradient ultracentrifugation

HEK293T cells harvested from AdV large scale production were lysed with 2 ml 5% sodium deoxycholate and incubated at room temperature for 30 minutes, mixing ~ every 5 minutes. Three hundred and forty microliters of 1 M $MgCl_2$ and 1 µl benzonase/5 ml (Thermo Fischer Scientific, MA, USA) was added to the lysate and incubated at 37°C for 1 hour, mixing ~ every 10 minutes. To remove cell debris, cell lysate was then centrifuged at ~3000 × g for 30 minutes. A cesium chloride (CsCl) gradient was set up in Ultra-Clear™ centrifuge tubes (Beckman Coulter Life Sciences, IN, USA). The gradient was prepared by overlaying 2 ml of 1.35 g/ml CsCl solution with 3 ml of 1.25 g/ml CsCl solution (Appendix A – Section 5.6.1) in two separate tubes. The AdV-containing supernatant was then carefully added dropwise to the gradient in each tube to form the top layer. The tubes were centrifuged at ~155 036 × g in the Optima™ L-80 XP ultracentrifuge (Beckman Coulter Life Sciences, IN, USA) for 1 hour at 4°C. The AdV bands (present towards the bottom of each tube) were extracted, placed together into a clean Ultra-Clear™ centrifuge tube and overlaid with 1.35 g/ml CsCl solution (Appendix A – Section 5.6.1). The tubes were centrifuged at ~79 100 × g in the Optima™ L-80 XP ultracentrifuge (Beckman Coulter Life Sciences, IN, USA) for 24 hours at 4°C. After 24 hours, the AdV band (present towards the top of the tube) was extracted using a 22-gauge needle and transferred to a Slide-A-Lyzer dialysis cassette (Thermo Fischer Scientific, MA, USA) pre-soaked in 10 mM Tris-HCL dialysis buffer (Appendix A – Section 5.6.2). The dialysis buffer was changed after 3 hours, and the cassette was left to dialyse overnight at 4°C. The dialysis buffer was changed twice more every 3 hours and the purified AdVs were extracted from the dialysis cassette using a 22-gauge needle. The purified AdV solution was supplemented with 10% glycerol, aliquoted into 50 µl, 100 µl and 200 µl aliquots and stored at -80°C.

2.7 Quantification of viral particle equivalents of CsCl purified AdVs

AdV DNA (Supplementary Data – Table 6.2 & Figure 6.4) was extracted from 50 µl purified virus using the QIAamp DNA Blood Mini Kit (Qiagen, MD, USA) according to manufacturer's instructions. Briefly, the volume of purified virus was made up to 200 µl with 1 × PBS. Twenty microliters proteinase K and 200 µl buffer AL were added to the tube and incubated at 56°C for 10 minutes. To the solution, 200 µl of 100% ethanol was added and the sample was placed in a QIAamp mini spin column (Qiagen, MD, USA). The sample was centrifuged at ~5900 × g for 1 minute and the liquid waste in the collection tube was discarded. The spin column was placed back into the collection tube and 500 µl wash buffer 1 was added. The tube was centrifuged at ~5900 × g for 1 minute and the liquid waste in the collection tube was discarded. The spin column was placed back into the collection tube and 500 µl wash buffer 2 was added. The tube was centrifuged at ~16 100 × g for 1 minute and the liquid waste in the collection tube was discarded. The spin column was transferred back into the collection tube and centrifuged at ~16 100 × g for 1 minute to remove any residual wash buffer. The spin column was then transferred to a clean tube and AdV DNA was eluted in 200 µl dH_2O.

Standards for qPCR were set up by preparing serial dilutions (10^1 – 10^9) of the pNG150D Ad plasmid (Supplementary Data – Table 6.1 & Figure 6.2 D) bearing AdV target sequences (donated by Philip Ng, Houston Baylor College of Medicine). qPCR reactions were set up with 10 µl SYBR green (Roche, BS, CH), 5 µl sample (i.e., standards, extracted AdV DNA or dH_2O), 3 µl dH_2O, 1 µl of AdV specific HVF forward primer and 1 µl of AdV specific HVR reverse primer per reaction. Primers and qPCR cycling conditions have been outlined in Tables 2.4 and 2.5, respectively.

Table 2.4: HVF and HVR primers used for qPCR quantification of AdVs (Palmer and Ng, 2003)

Primer name	Primer sequence
HV Forward (HVF)	5'-TGGGCGTGGTGCCTAAAA-'3
HV Reverse (HVR)	5'-GCCTGCCCCTGGCAAT-'3

Table 2.5: qPCR cycling conditions

Step	Temperature	Duration	Cycles
Initial denaturation	95°C	2 minutes	1
Denaturation	98°C	30 seconds	30
Annealing	60°C	15 seconds	
Extension	72 C	30 sec – 2 mins	
Final Extension	72°C	5 mins – 10 mins	1
Cooling	4°C	∞	1

2.8 *In-vitro* AdV functionality tests

2.8.1 Infection of HEK293T cells with recombinant AdVs

HEK293T cells from a 75 cm^2 flask at 100% confluency were seeded in 3 separate 24-well cell culture plates at 50% confluency. HEK293T cells in each plate were infected in quadruplicate with either Ad5-LHBsAg, Ad5-SHBsAg or Ad5-FLuc at MOIs of 1, 10, 100 and 1000. Infected cells were incubated at 37°C and 5% CO_2 for 48 hours.

2.8.2 Enzyme-linked immunosorbent assay (ELISA) for detection of HBV antigens produced by AdVs

Supernatants and cell lysates from cells infected with Ad5-LHBsAg, Ad5-SHBsAg and Ad5-FLuc were harvested after 48 hours. An ELISA was performed using the Monolisa™ HBsAg ULTRA kit (Bio-Rad Laboratories Inc., CA, USA) according to the manufacturer's instructions. Briefly, the contents of the kit were left to equilibrate to room temperature before adding 100 µl of each sample, both supernatants and lysates, to wells pre-coated with mouse monoclonal anti-HBsAg antibodies. To each sample, 50 µl of conjugate solution was added and mixed. The plate was covered with adhesive film and incubated at 37°C for 1 hour 30 minutes. The plate was washed 5 times with washing solution using an APW-200 microplate washer (Allsheng Instruments Co., HA, CN) and 100 µl freshly prepared development solution was added to each well and incubated at room temperature in the dark for 30 minutes. After development, 100 µl stopping solution was added to each well, mixed and the optical density was read at 490 nm and 655 nm using the Multiskan SkyHigh Microplate Spectrophotometer (Thermo Fischer Scientific, MA, USA).

2.8.3 Luciferase assay

Supernatant and cell lysate samples from cells infected with Ad5-FLuc were harvested 48 hours after infection. Cells were lysed by removing cell culture media and incubating for 15 minutes

in 100 µl 1 × Passive Lysis Buffer (PLB) (Promega Corporation, WI, USA) with shaking. After incubation, 10 µl cell lysate was added to a white 96-well plate and mixed with 50 µl Luciferase Assay Reagent II (LARII). FLuc levels were measured in relative light units (RLU) using the GloMax® Discover Microplate Reader (Promega Corporation, WI, USA).

2.9 *In vivo* AdV functionality tests

In vivo experimental procedures were approved by the Wits Animal Research Ethics Committee [AREC; ethical clearance number 2022/09/03/c] and were performed under the supervision of the staff at the Wits Research Animal Facility (WRAF). Thirty female Balb/c mice (sourced from the National Institute for Communicable Diseases of South Africa), ~16 – 22 grams, were randomly assigned into 5 groups of 3 in two separate batches and underwent 1 week of habituation. All 6 mice were used for quantification of bioluminescence, however, for *in vivo* cytokine and antibody response tests, 5 mice were used due to the necessary exclusion of one mouse for each group.

2.9.1 Intramuscular injection and bleeding

Randomly assigned mice were injected with AdVs or commercial HBV vaccine (EUVAX-B) as follows:

I. 1×10^9 vpe Ad5-LHBsAg per mouse
II. 1×10^9 vpe Ad5-SHBsAg per mouse
III. 1×10^9 vpe Ad5-FLuc per mouse
IV. 0.8 µg EUVAX-B (20 µg/ml) per mouse
V. 50 µl saline per mouse

At day 0, all 15 mice were anaesthetised by inhalation with isoflurane and blood samples were taken by retro-orbital puncture. Immediately after bleeding, each group of 3 mice was injected intramuscularly (inner left thigh) with 50 µl of either 1×10^9 vpe AdV or 0.8 µg EUVAX-B or saline (Appendix A – Figure 5.1). After injection, blood samples were collected by retro-orbital puncture at days 7, 14, 21, 28 and 35 (Appendix A – Figure 5.1). After each retro-orbital bleed, blood samples were collected in Eppendorf tubes and placed at ~4-8°C for 1 hour 30 minutes and then centrifuged at ~6000 × g for 10-30 minutes. Approximately between 10 µl and 100 µl of serum was harvested and stored in autoclaved Eppendorf tubes at -80°C.

2.9.2 Bioluminescence imaging

To assess FLuc expression, mice injected with Ad5-FLuc, and mice injected with saline were injected intraperitoneally with ~200 µl (~10% of total body weight) luciferase substrate, D-luciferin (PerkinElmer Inc., MA, USA). After placing the mice under anesthesia using isoflurane, both groups of mice were imaged using the IVIS Kinetic Imaging system (Caliper Life Sciences Inc., MA, USA) and images were captured after 20 seconds of exposure. Bioluminescence imaging was performed at days 1, 3, 7 and 14 after injection (Appendix A – Figure 5.1).

2.9.3 Termination procedures

Before euthanasia, blood samples were taken by retro-orbital puncture and serum was harvested as described above. Mice were terminated by decapitation under anaesthesia with isoflurane at day 35 after injection. Additionally, spleens were harvested after euthanasia for further processing (Appendix A – Figure 5.1).

2.9.3.1 Splenocyte processing and stimulation

The harvested spleens were placed in individual tubes containing 500 µl Roswell Park Memorial Institute (RPMI) medium with L-glutamine (Gibco, Thermo Fischer Scientific, MA, USA). Splenocytes were isolated by gently mashing the spleen through a 100 µm strainer into a 50 ml tube and rinsing with 9.5 ml PBS (Gibco, Thermo Fischer Scientific, MA, USA) supplemented with 1% Fetal Bovine Serum (FBS). The splenocytes were then centrifuged at ~200 × g for 10 minutes and the pellet was resuspended in 3 ml 1 × red blood cell lysis buffer (Elabscience, TX, USA) and incubated at room temperature for 5 minutes. After incubation, the cells were washed with 10 ml PBS and centrifuged at ~200 × g for 5 minutes. The supernatant was discarded, and the pellet of cells was washed and resuspended in 10 ml PBS. Resuspended splenocytes were aspirated using a serological pipette and filtered through a 70 µm strainer into the same 50 ml tube. Splenocytes were then centrifuged at ~200 × g for 5 minutes and resuspended in 2-5 ml RPMI.

To determine viable cell count, 10 µl splenocyte suspensions were mixed with 10 µl trypan blue stain (Gibco, Thermo Fisher Scientific, MA, USA) and incubated for ~3 minutes at room temperature. After incubation, 10 µl of the mixtures was transferred to disposable Countless™ cell counting chamber slides (Thermo Fischer Scientific, MA, USA) and inserted into a

Countless™ 3 Automated Cell Counter (Thermo Fischer Scientific, MA, USA). Viability and live cell count was recorded and splenocytes were resuspended in RPMI for a final cell count of 10×10^6 cells/ml.

To plate cells for splenocyte stimulation, 100 µl of splenocyte resuspensions were plated in 96-well U-bottom plates for a final cell count of 1×10^6 cells/well. Cells from each spleen were divided into 5 wells for stimulation with peptide/s at 5 µg/well or 1 × Cell Stimulation Cocktails (CSC) control. Stimulation groups were as follows:

i. Unstimulated control
ii. Stimulation with HBV S peptide mix
iii. Stimulation with HBV PreS1 + PreS2 peptide mix
iv. Stimulation with HIV peptide mix as a negative control
v. Stimulation with a CSC as a positive control

Some peptides were insoluble in water and therefore, were dissolved in dimethyl sulfoxide (DMSO). To maintain uniformity throughout, cell stimulation mixes were prepared to also contain 0.2% DMSO in addition to 0.2 µg/well of CD28 co-stimulation factor, and 1912 µl RPMI and were made up to a final volume of 2 ml with PBS. Splenocytes were stimulated with 100 µl of each stimulation mix and incubated at 37°C. After 24 hours, plates were removed from the incubator and centrifuged at ~200 × g for 5 minutes (with slow acceleration and deceleration). After pelleting the splenocytes, 100 µl of supernatant was harvested and placed into clean 96-well U-bottom plates. The plates were sealed and stored at -80°C.

2.9.4 Flow cytometry analysis of cellular immune responses

To assess the concentration of a panel of 8 cytokines from stimulated splenocytes, the BioLegend LEGENDplex MU Th1/Th2 Panel (8-plex) w/ VbP V03 kit (BioLegend, CA, USA) was used according to manufacturer's instructions. The 8 cytokines quantified were IFN-γ, TNF-α, IL-5, IL-2, IL-6, IL-4, IL-10, and IL-13. Standards for the assay were prepared by 1:4 serial dilutions with concentrated standard stock. Additionally, bead mix was prepared by vigorously vortexing individual beads and mixing 230 µl of each bead with 1840 µl assay buffer. To each well, 25 µl of bead mix was added to 25 µl assay buffer and 25 µl sample/standard for a total volume of 75 µl per well. The plate was then sealed, covered in foil, and incubated at room temperature for 2 hours with shaking. Plate was centrifuged at ~250 ×

g for 5 minutes and the supernatant was discarded. All wells were washed with 200 µl 1 × wash buffer before repeating centrifugation and wash steps. After centrifuging again at ~250 × g for 5 minutes and discarding the supernatant, 25 µl of detection antibodies were added to each well. The plate was sealed and covered with foil and incubated for 1 hour at room temperature with shaking. Without washing, 25 µl SA-PE was added to each well, the plate was sealed and covered in foil, and incubated for 30 minutes at room temperature with shaking. Thereafter, centrifugation and wash steps were repeated and 150 µl wash buffer was used to resuspend beads. The samples were stored overnight at 4°C. Samples were resuspended again before running on the flow cytometer.

Samples were run on the BD Accuri™ C6 Plus flow cytometer (BD Biosciences, NJ, USA), recording 3500 events per sample. Cytokine concentrations were determined using the online BioLegened LEGENDplex software (BioLegend, CA, USA).

2.9.5 HBsAg antibody ELISA

To determine anti-HBsAg antibody levels, 200 µl SuperBlock™ Blocking Buffer (Thermo Fisher Scientific, MA, USA) was added to microwells coated with HBsAg (CTK Biotech, CA, USA) and incubated with shaking for 20 minutes. Blocking buffer was removed by washing 5 times with 300 µl 1 × wash buffer (Bio-Rad Laboratories Inc., CA, USA) using the APW-200 microplate washer (Allsheng Instruments Co., HA, CN). After washing, mouse serum samples were diluted 5 times with PBS and 50 µl was added to microwells before incubation for 1 hour at 37°C. Microwells were washed again 5 times with 300 µl 1 × wash buffer and 50 µl Goat anti-mouse IgG (H + L) HRP (EMD Millipore Corporation, MA, USA) (1/3000 dilution in SuperBlock™ Blocking Buffer supplemented with 0.05% Tween) was added to each well. The antibody was left to incubate for 30 minutes at 37°C. After incubation, wells were rinsed 5 times with 300 µl 1 × wash buffer and 50 µl 1-Step™ Ultra TMB-ELISA substrate solution (Thermo Fisher Scientific, MA, USA) was added to each well followed by incubation in the dark for 30 minutes at room temperature. Thereafter, 50 µl stopping solution (Bio-Rad Laboratories Inc., CA, USA) was added to each well, mixed and the optical density was measured at 450 nm and 655 nm.

2.10 Statistical analyses

All statistical analyses were performed on Microsoft Excel. Samples were taken as paired data and analysed using a Student's T-test with a 2-tailed distribution. Statistical analyses were conducted for *in vitro* LHBsAg, SHBsAg and FLuc transgene expression, *in vivo* bioluminescence imaging, in vivo cytokine responses and in vivo antibody levels, where the number of replicates (n) were 4, 6, 5 and 5 respectively. In all cases, $p \leq 0.05$ was considered to be statistically significant. Error bars were determined using the standard error of the mean (SEM).

Chapter 3

Results

3.1 Successful ligation of *LHBsAg*, *SHBsAg* and *FLuc* genes into pShuttle-CMV backbone

Since the *Acc*65I and *Hind*III restriction sites were flanking the *LHBsAg* in the carrier plasmid (Supplementary Data – Figure 6.1 A) and present in the pShuttle-CMV multiple cloning site (MCS) (Supplementary Data – Figure 6.2 A), the *LHBsAg* gene was isolated from its carrier plasmid by enzymatic digestion with *Acc*65I and *Hind*III and directly ligated into the pShuttle-CMV backbone linearised with *Acc*65I and *Hind*III to create pShuttle-LHBsAg (Supplementary Data – Figure 6.3 A). The carrier plasmids containing the *SHBsAg* and *FLuc* genes did not contain the *Acc*65I and *Hind*III restriction sites (Supplementary Data – Figure 6.1 B & C), therefore, the *SHBsAg* and *FLuc* genes were amplified out using PCR with primers containing the *Acc*65I and *Hind*III restriction sites (Table 2.1). Amplification of *SHBsAg* was achieved using an annealing temperature of 62.3°C (Figure 3.1 A). Amplification of *FLuc* was achieved at annealing temperatures ranging from 57.6-60.4°C (Figure 3.1 B). Agarose gel electrophoresis analysis of amplified samples showed thick bands of 681 bp and 1676 bp, corresponding to the size of *SHBsAg* and *FLuc* respectively (Figure 3.2 A & B). Bands were extracted from the agarose gel, digested with *Acc*65I and *Hind*III, and directly ligated into the pShuttle-CMV backbone linearised with *Acc*65I and *Hind*III to create pShuttle-SHBsAg and pShuttle-FLuc (Supplementary Data – Figure 6.3 B & C).

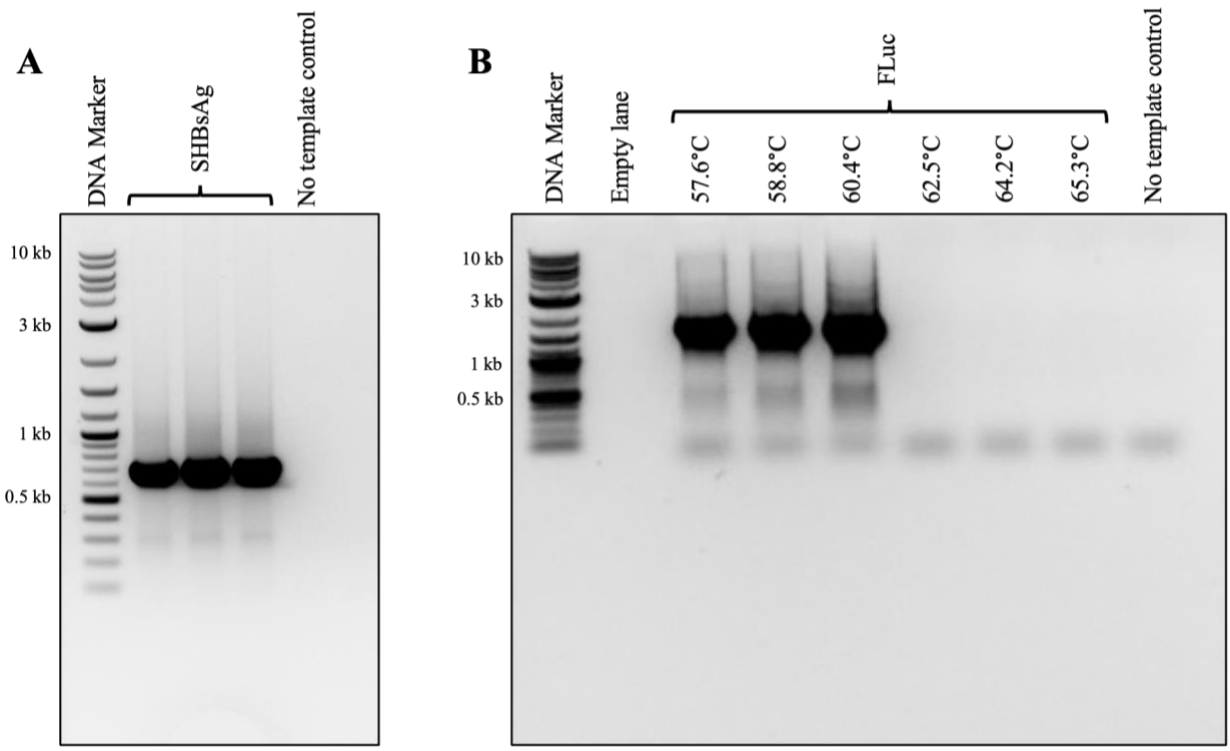

Figure 3.1: Amplification of *SHBsAg* and *FLuc* genes out of carrier plasmids.

A. Agarose gel image of PCR-amplified *SHBsAg* showing thick bands of 681 bp corresponding to the size of SHBsAg. **B.** Agarose gel of PCR-amplified *FLuc* showing thick bands of 1676 bp corresponding to the size of FLuc. Band sizes were determined using a 1 kb Plus DNA Ladder (New England Biolabs, MA, USA).

Following cloning, confirmation of positive pShuttle-LHBsAg clones by enzymatic digestion with *Apa*LI showed the expected banding pattern of 5910 bp and 2812 bp (Figure 3.2). Digestion of pShuttle-SHBsAg clone with *Eco*32I and *Bgl*II showed the expected banding pattern of 7420 bp and 709 bp (Figure 3.2). Digestion of pShuttle-FLuc with *Apa*LI and *Sca*I also showed the expected banding pattern of 3537 bp, 2812 bp and 2752 bp (Figure 3.2), with the 2812 bp and 2752 bp bands migrating together after agarose gel electrophoresis confirming successful ligation (Figure 3.2). Additional double digestion of pShuttle-LHBsAg, pShuttle-SHBsAg and pShuttle-FLuc with *Acc*65I and *Hind*III produced a larger band of 7442 bp for all shuttle plasmid clones and smaller bands of 1280 bp, 687 bp and 1659 bp for pShuttle-LHBsAg, pShuttle-SHBsAg and pShuttle-FLuc respectively (Figure 3.2). As a control, empty pShuttle-CMV DNA was digested with all enzymes and showed expected banding patterns of 4658 bp and 2812 bp after digestion with *Apa*LI, 7420 bp and 50 bp after digestion with *Eco*32I

and *Bgl*II, 4658 bp and 2812 bp after digestion with *Apa*LI and *Sca*I, and 7442 bp and 28 bp after digestion with *Acc*65I and *Hind*III (Figure 3.2).

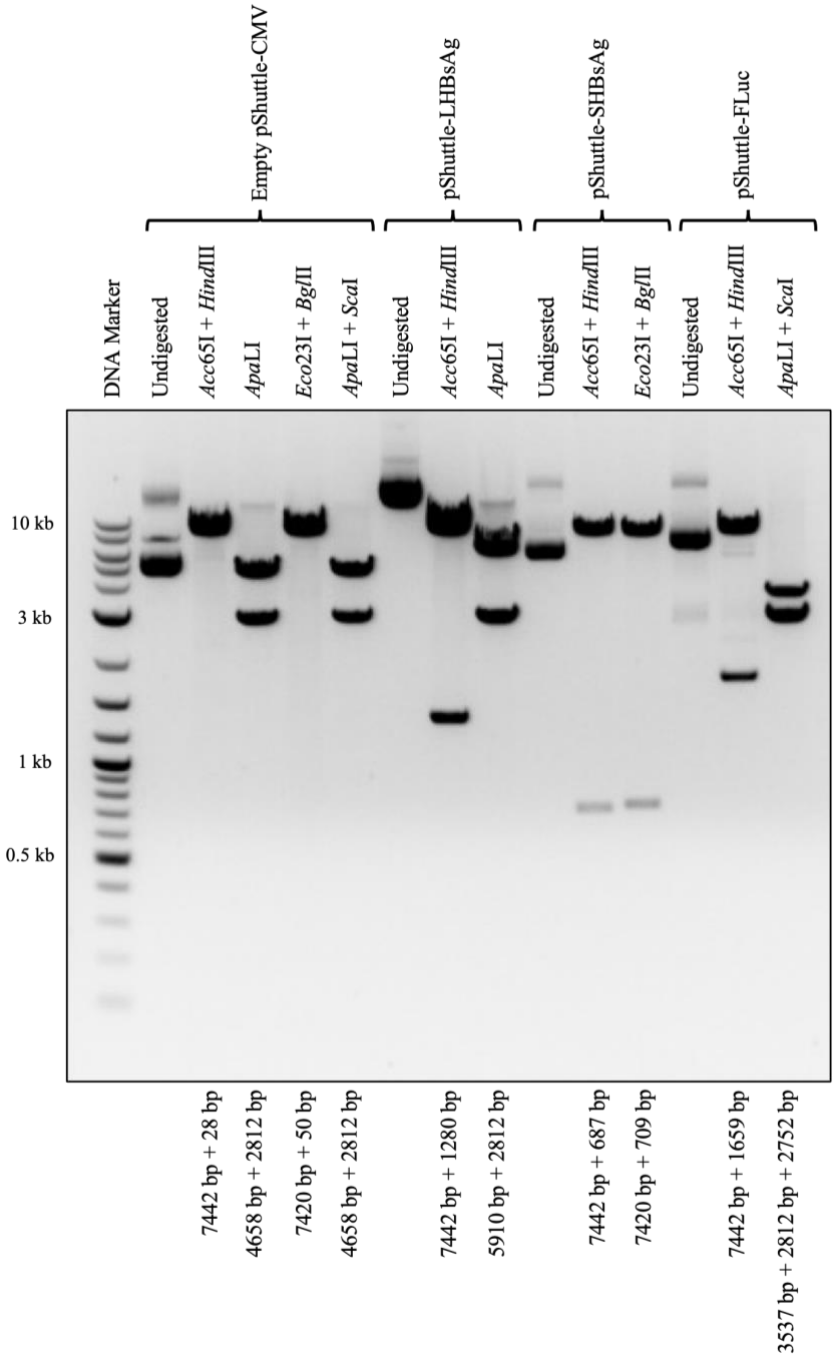

Figure 3.2: Restriction enzyme analysis of shuttle plasmid clones.

Agarose gel image of empty pShuttle-CMV, pShuttle-LHBsAg, pShuttle-SHBsAg and pShuttle-FLuc clones after enzymatic digestion with several restriction enzymes showing expected banding patterns. Expected band sizes are shown at the bottom of the gel. Band sizes were determined using a 1 kb Plus DNA Ladder (New England Biolabs, MA, USA).

3.2 Production of recombinant AdV genome plasmids carrying *LHBsAg*, *SHBsAg* and *FLuc* genes

To confirm successful recombination, samples were digested with *Pac*I and *Eco*RV. All digested recombinants showed a similar banding pattern on an agarose gel (Figure 3.3). Enzymatic digestion of recombinants with *Pac*I showed a banding pattern of ~30 kb and ~4.5 kb (Figure 3.3). For further validation of successful recombination, enzymatic digestion with *Eco*RV showed an 8-band pattern, as expected, confirming successful recombination (Figure 3.3). The pAdEasy-1 plasmid DNA was digested with *Pac*I and *Eco*RV as a control to show that the banding pattern of digested recombinant DNA was slightly different to that of pAdEasy-1. Enzymatic digestion of pAdEasy-1 with *Pac*I linearised the plasmid DNA, producing a band on the agarose gel of 33 477 bp (Figure 3.3). As opposed to the 8-band pattern produced after enzymatic digestion of recombinant DNA with *Eco*RV, the same reaction with pAdEasy-1 produced a 7-band pattern (Figure 3.3). Along with recombinants, pAd5-LHBsAg, pAd5-SHBsAg and pAd5-FLuc, a previously produced pAd5-GFP (i.e., produced using the pAdTrack-CMV shuttle plasmid) was digested in parallel with *Pac*I and *Eco*RV. Digestion showed a similar 2-band pattern and 8-band pattern after digestion with *Pac*I and *Eco*RV, respectively. Plasmid maps of recombinant pAd5-LHBsAg, pAd5-SHBsAg and pAd5-FLuc are shown in the Supplementary Data – Figure 6.4.

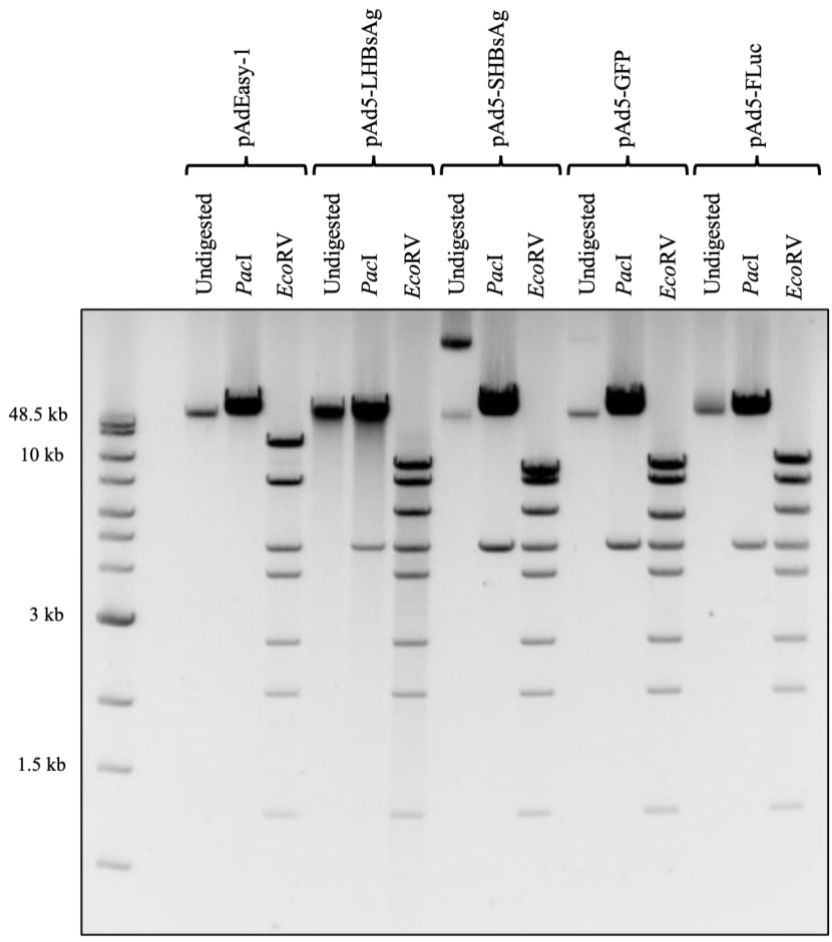

Figure 3.3: Screening of recombinant AdV DNA.

Agarose gel image of recombinant AdV DNA, pAd5-LHBsAg, pAd5-SHBsAg, pAd5-GFP, pAd5-FLuc, and pAdEasy-1 plasmid DNA after enzymatic digestion with *Pac*I and *Eco*RV to confirm successful recombination. Band sizes were determined using a Quick-Load 1 kb Extend DNA Ladder (New England Biolabs, MA, USA).

3.3 Recombinant AdV production and amplification

Recombinant AdVs were initially produced (passage 0 or P0) by transfecting HEK293T cells with ~10 µg *Pac*I-digested recombinant AdV DNA. Cells transfected with pAd5-GFP in parallel with pAd5-LHBsAg showed higher transfection efficiency under fluorescent microscopy at 24 hours/day 1 after transfection as compared to cells transfected with pAd5-GFP in parallel with cells transfected with pAd-SHBsAg and pAd5-FLuc (Figure 3.4). Note that only day 1 is shown as a representation for transfections. Additionally, Ad5-SHBsAg and Ad5-FLuc were produced at the same time, therefore, all parallel Ad5-GFP results represented are from the same batch of cells.

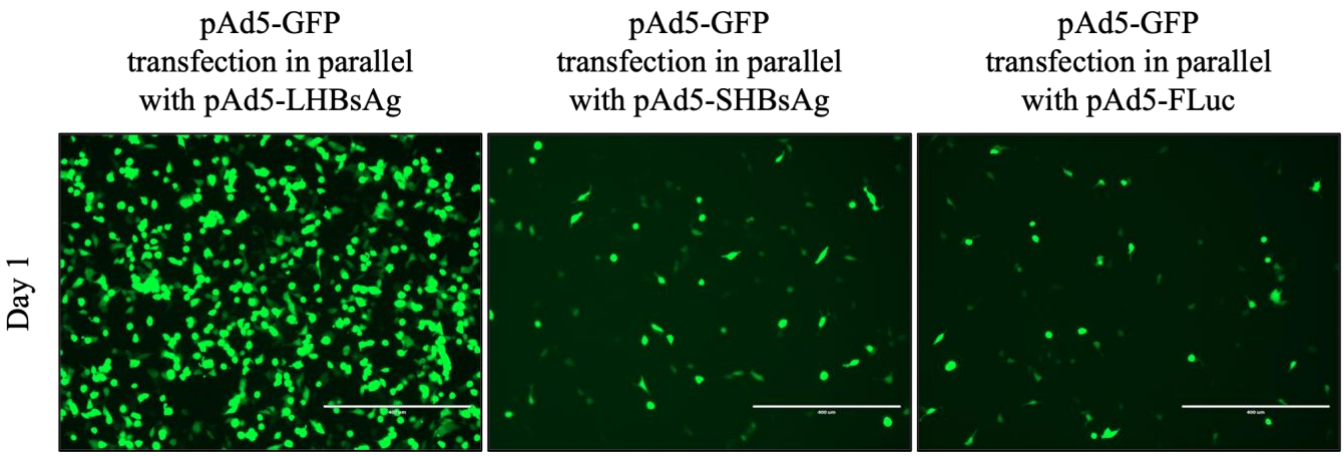

Figure 3.4: Transfection efficiency using pAd5-GFP reporter.

HEK293T cells transfected with pAd5-GFP DNA to assess transfection efficiency of recombinant AdV DNA at day 1 after transfection. Higher transfection efficiency observed in cells transfected with pAd5-GFP in parallel with cells transfected with pAd5-LHBsAg when compared to cells transfected in parallel with pAd5-SHBsAg and pAd5-FLuc (from the same flask). Fluorescent microscopy was performed using the EVOS® XL Cell Imaging System (Invitrogen, Thermo Fisher Scientific, MA, USA).

Passage 1 (P1) of AdVs was required to amplify the virus. On the day of harvest, GFP reporter AdV showed significantly greater infection of HEK293T cells when compared to days 1 and 4 (Figure 3.5). Newly infected cells were seen as dimly fluorescent cells surrounding brighter cells. Additionally, when compared to uninfected HEK293T cells, cells infected with Ad5-LHBsAg, Ad5-SHBsAg and Ad5-FLuc showed ~90 – 100% CPE at day of harvest, indicating successful viral infection and replication (Figure 3.6).

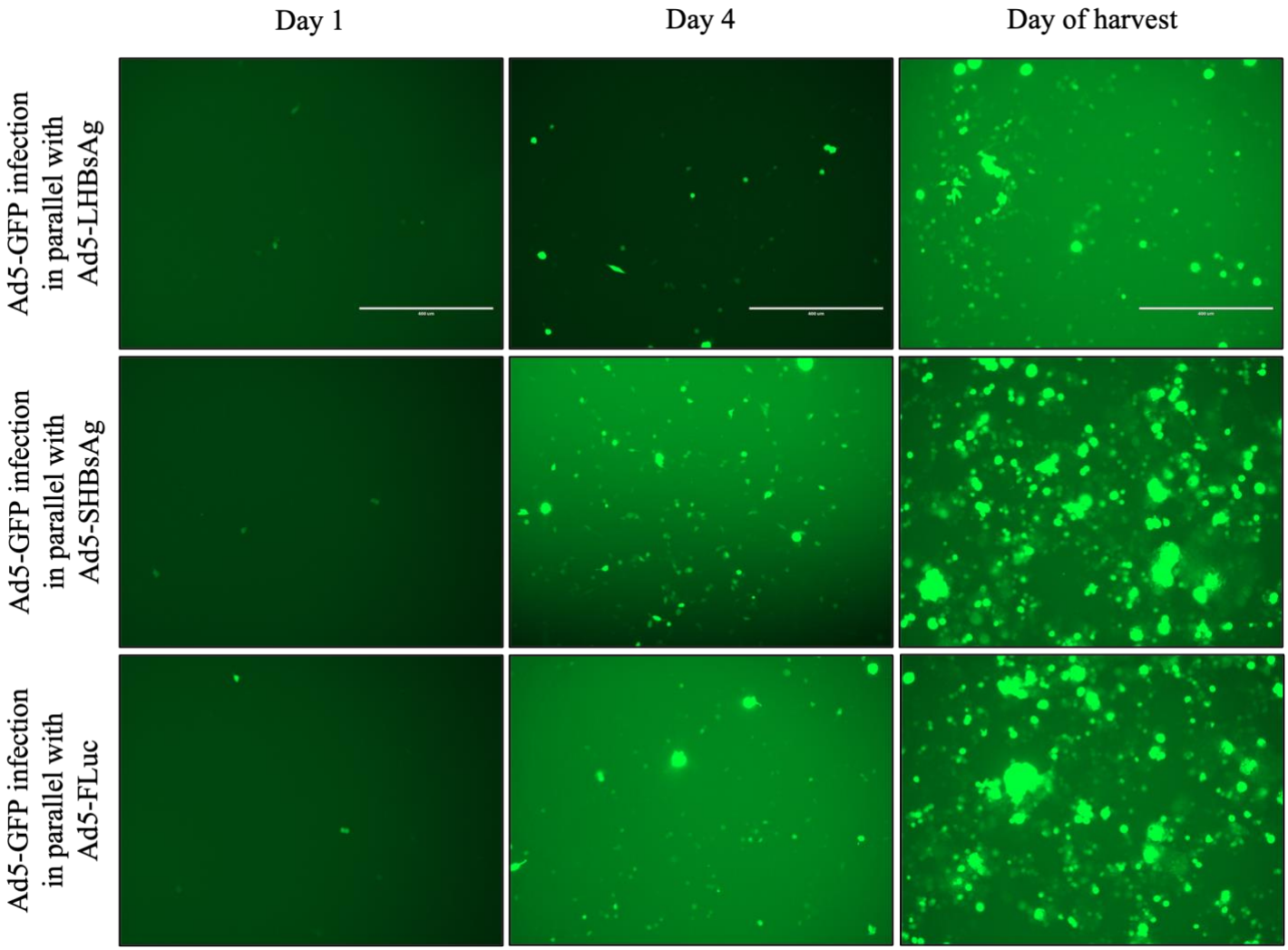

Figure 3.5: Ad5-GFP infection at P1.

HEK293T cells infected with Ad5-GFP reporter AdV at an MOI of 0.1 for AdV amplification. Viral infection and amplification shown using fluorescence microscopy at days 1 and 4 after infection and at harvest day. An increase in the number of infected cells observed as the days post-infection increase. Viral harvest for cells infected with Ad5-LHBsAg, Ad5-SHBsAg and Ad5-FLuc was performed at days 5, 7 and 7 post-infection, respectively. Fluorescent microscopy was performed using the EVOS® XL Cell Imaging System (Invitrogen, Thermo Fisher Scientific, MA, USA).

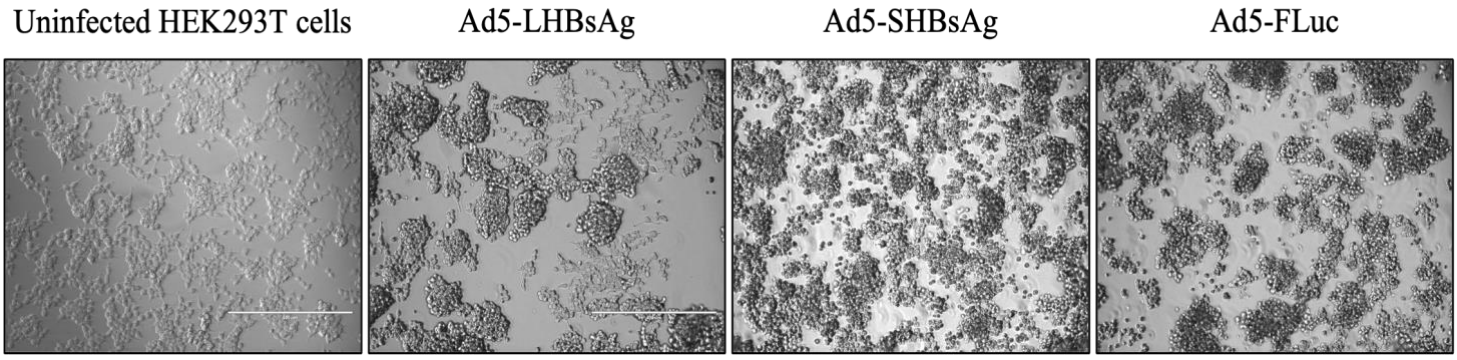

Figure 3.6: CPE at day of harvest of P1.

HEK293T cells infected with Ad5-LHBsAg, Ad5-SHBsAg and Ad5-FLuc showing CPE (i.e., cell rounding, clumping and lifting off the surface of the flask) at harvest day compared to uninfected HEK293T cells. Images taken using the EVOS® XL Cell Imaging System (Invitrogen, Thermo Fisher Scientific, MA, USA).

After P0 and P1, AdVs were quantified in ifu/ml using the Ad5-GFP reporter to estimate Ad5-LHBsAg, Ad5-SHBsAg and Ad5-FLuc quantities. Before large-scale AdV production (P2), more accurate quantification of Ad5-LHBsAg, Ad5-SHBsAg and Ad5-FLuc in ifu/ml was performed by immunostaining. Viral yields per ml increased ~10-100 fold from P0 to P1 after quantification using both GFP reporter and immunostaining (Table 3.2). It is, however, important to note that quantification using the Ad5-GFP was not used for absolute quantification but rather as an estimated indicator of transfection and subsequent infection.

Table 3.1: Viral quantification after AdV production and amplification

	AdV quantification using GFP reporter (ifu/ml)		**AdV quantification using immunostaining (ifu/ml)**	
	Production (P0)	**Amplification (P1)**	**Production (P0)**	**Amplification (P1)**
Ad5-LHBsAg	2.73E+06	8.14E+06		1.97E+07
Ad5-SHBsAg	4.84E+05	3.34E+07		5.90E+06
Ad5-FLuc	4.84E+05	3.34E+07		1.83E+07

3.3.1 Large-scale AdV production (P2) and purification

Since high quantities of recombinant AdVs were required for *in vitro* and *in vivo* analysis, AdV P2, or large-scale viral production was performed by infecting HEK293T cells at an MOI of

0.1 in several 175 cm^2 culture flasks and AdVs were harvested after 6-8 days. GFP reporter AdVs were produced in single 175cm^2 flasks alongside large-scale production of Ad5-LHBsAg, Ad5-SHBsAg and Ad5-FLuc. Infection of HEK293T cells with Ad5-FLuc (not shown) Ad5-LHBsAg and Ad5-SHBsAg showed significant CPE at day of harvest when compared to uninfected HEK293T cells (Figure 3.7).

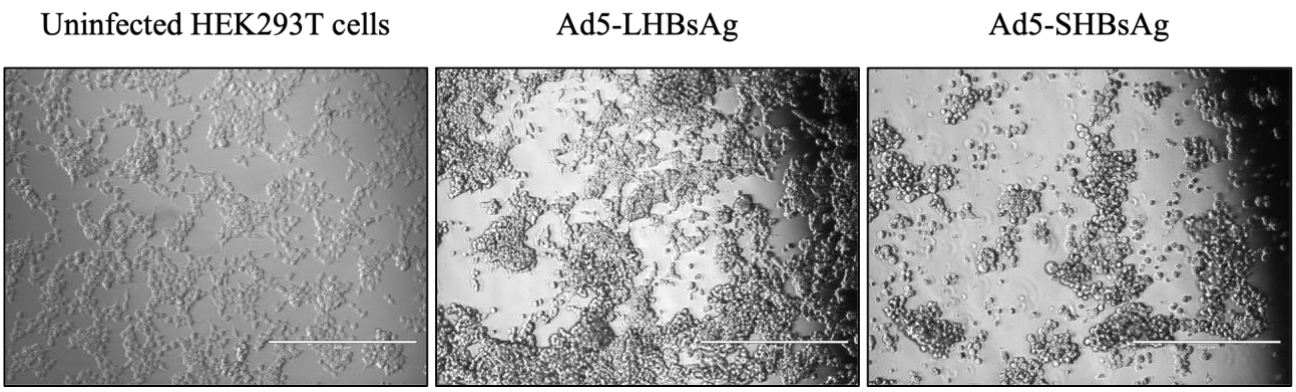

Figure 3.7: CPE at day of harvest of P2.

HEK293T cells infected with Ad5-LHBsAg and Ad5-SHBsAg showing CPE at harvest day compared to uninfected HEK293T cells. Images taken using the EVOS® XL Cell Imaging System (Invitrogen, Thermo Fisher Scientific, MA, USA). Representative images from one flask are shown.

During viral purification AdVs were concentrated in a thin layer within the bottom 1.35 g/ml CsCl layer. Subsequent ultracentrifugation at ~79 100 × g in 1.35 g/ml CsCl solution further purified and concentrated AdVs in a thin layer towards the top of the ultracentrifugation tube (Figure 3.8).

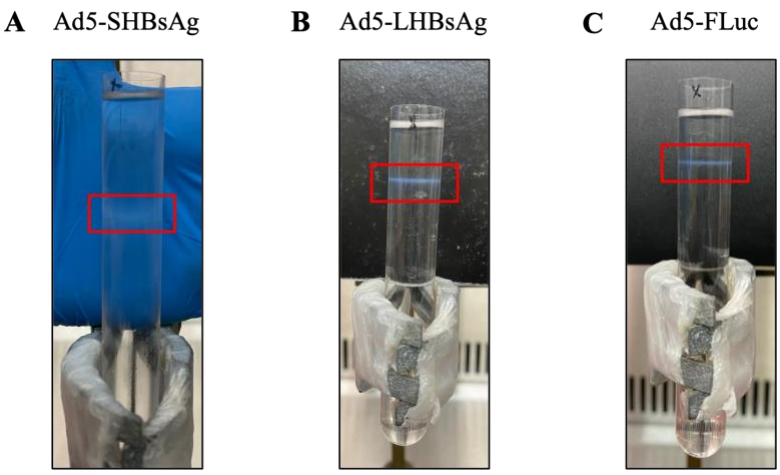

Figure 3.8: AdV purification using CsCl gradient ultracentrifugation.
Concentrated AdV bands (highlighted by the red box) in ultracentrifuge tubes after CsCl gradient ultracentrifugation at ~79 100 × g for 24 hours. **A.** Concentrated band of Ad5-SHBsAg. **B.** Concentrated band of Ad5-LHBsAg. **C.** Concentrated band of Ad5-FLuc.

After gradient ultracentrifugation and dialysis to remove CsCl from AdV solution, AdVs were quantified in vpe/µl using qPCR. P2 final yields were higher than 1.00E +11 and enough for *in vitro* and *in vivo* AdV characterisation (Table 3.3).

Table 3.2: Final average AdV yields after quantification using qPCR

	Final viral yields (vpe/µl)	Total viral yields (vpe)
Ad5-LHBsAg	3.05E+07	1.83E+11
Ad5-SHBsAg	1.04E+08	6.23E+11
Ad5-FLuc	2.78E+07	1.11E+11

3.4 Transgene expression *in vitro*

3.4.1 *In vitro LHBsAg* and *SHBsAg* expression from Ad5-LHBsAg and Ad5-SHBsAg

Infection of HEK293T cells with Ad5-LHBsAg and Ad5-SHBsAg at MOIs of 1, 10, 100 and 1000 showed dose-dependent increases in LHBsAg and SHBsAg production (Figure 3.9 A & B). Because the SHBsAg is a naturally secreted peptide, dose-dependent increases in SHBsAg production were observed in both lysate and supernatant samples (Figure 3.9 B). However, the LHBsAg is not naturally secreted and remains intracellular. Therefore, dose-dependent increases in LHBsAg production were observed only in lysate samples (Figure 3.9 A).

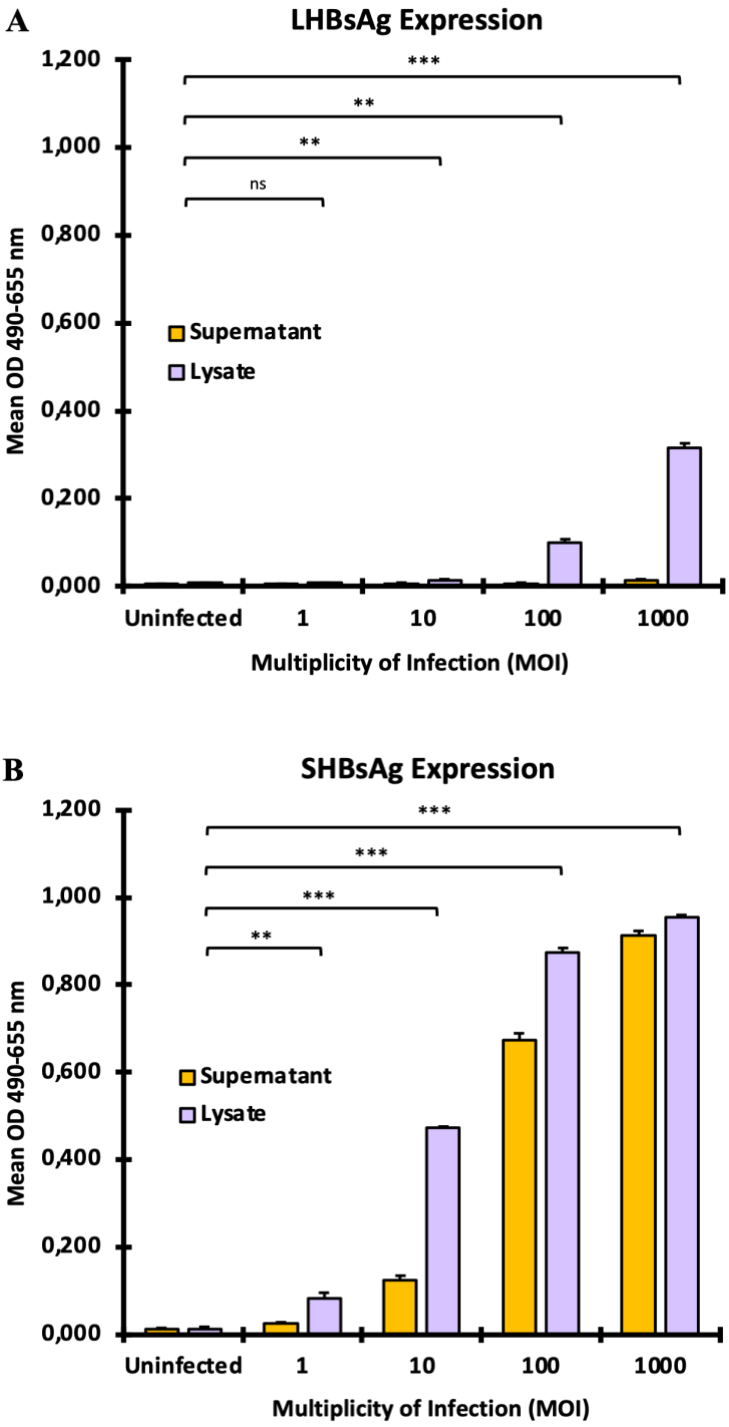

Figure 3.9: *In vitro* LHBsAg and SHBsAg expression.

Dose-dependent LHBsAg and SHBsAg levels measured after infection of HEK293T cells with Ad5-LHBsAg and Ad5-SHBsAg using the Monolisa™ HBsAg ULTRA kit (Bio-Rad Laboratories Inc., CA, USA). Antigen levels were measured at a mean optical density reading of 490 nm – 655 nm using the Multiskan SkyHigh Microplate Spectrophotometer (Thermo Fischer Scientific, MA, USA). * $p \leq 0.05$, ** $p \leq 0.01$, *** ≤ 0.001, ns (not significant) $p > 0.05$; $n = 4$ and error bars calculated using SEM.

3.4.2 *In vitro* FLuc expression from Ad5-FLuc

Infection of HEK293T cells with Ad5-FLuc at MOI's of 1, 10, 100 and 1000 showed dose-dependent increases in FLuc expression (Figure 3.10). This expression was only observed in lysate samples since FLuc remains intracellular and does not get secreted from the cell. A decrease in expression at MOI 1000 was observed, likely because of high CPE.

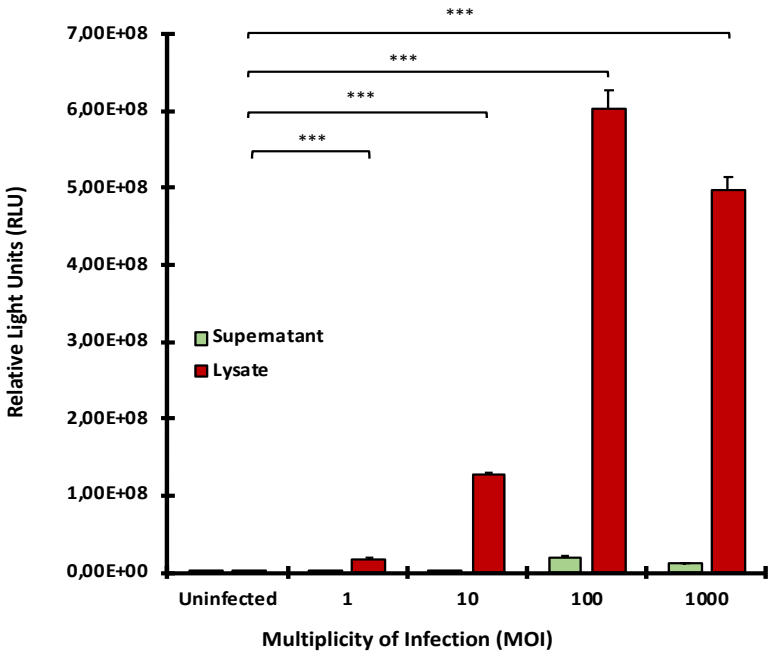

Figure 3.10: *In vitro* FLuc expression.

Dose-dependent FLuc levels measured in RLUs after infection of HEK293T cells with Ad5-FLuc. Measurements were made using the GloMax® Discover Microplate Reader (Promega Corporation, WI, USA). Dose-dependent levels of FLuc were observed in lysate samples.

* $p \leq 0.05$, ** $p \leq 0.01$, *** ≤ 0.001, ns (not significant) $p > 0.05$; $n = 4$ and error bars calculated using SEM.

3.5 Transgene expression and induction of HBV-specific immunity in mice

3.5.1 *In vivo* FLuc expression

To assess the expression of FLuc *in vivo*, two groups of 6 Balb/c mice were injected with 1×10^9 vpe per mouse of Ad5-FLuc or saline (Figure 3.11 A). Mice injected with Ad5-FLuc showed strong FLuc expression at days 1 and 3 after intramuscular injection (Figure 3.12 A & B). By day 7 after injection, FLuc expression had declined significantly, with almost total viral clearance by day 14 after injection (Figure 3.12 A & B). Additionally, at each timepoint where bioluminescence imaging was performed, it was noted that FLuc expression stayed localized

to the site of injection (i.e., the muscle), with no expression in the liver or other organs (Figure 3.12 A).

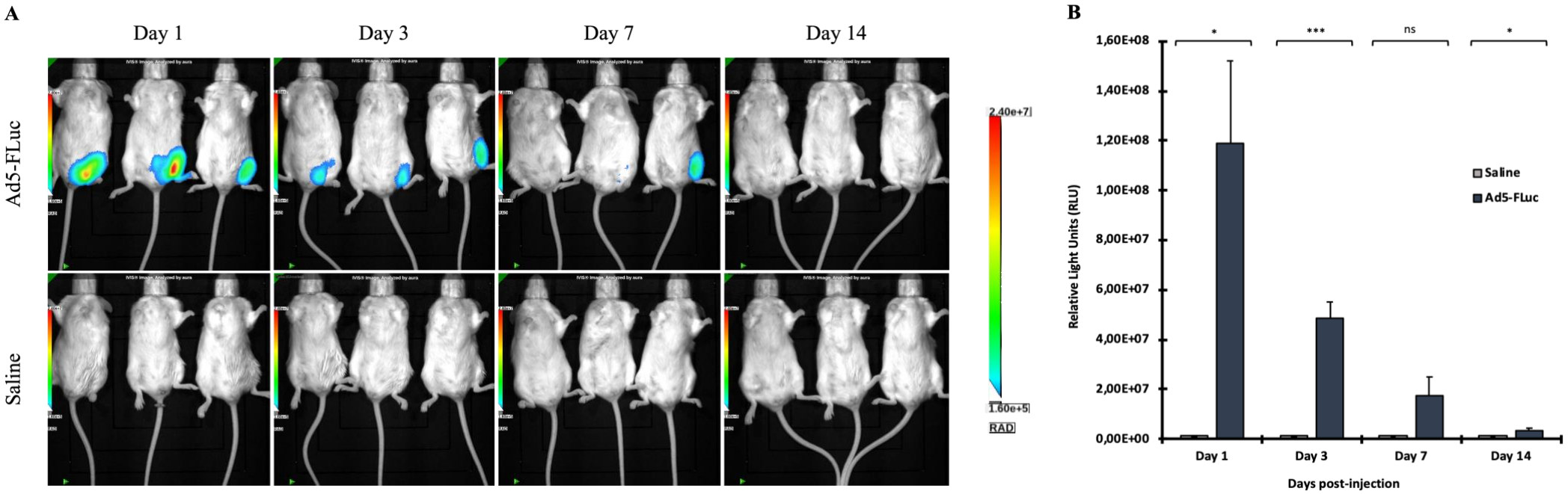

Figure 3.11: *In vivo* bioluminescence imaging.

A. *In vivo* bioluminescence imaging of Balb/c mice after intramuscular injection. Representative image from 3 mice per group is shown. Bioluminescence imaging of remaining 3 mice is shown in the Supplementary Data – Figure 6.5. **B.** Average bioluminescence quantified from 6 mice in RLUs from days 1 – 14 after injection using Aura Imaging Software. * $p \leq 0.05$, ** $p \leq 0.01$, *** ≤ 0.001, ns (not significant) $p > 0.05$, n = 6 and error bars calculated using SEM.

3.5.2 *In vivo* HBV-specific cytokine responses

To assess the induction of cell mediated immune responses, isolated splenocytes were stimulated with HBV S and PreS peptide pools. Stimulation with an HIV peptide pool and a CSC were used as controls. Testing the release of Th1/Th2 cytokines (i.e., IFN-γ, IL-5, TNF-α, IL-2, IL-6, IL-4, IL-10, and IL-13) showed an HBV-specific increase in IFN-γ and IL-6 levels after stimulation for 24 hours, particularly in mice injected with Ad5-SHBsAg and stimulated with an HBV S peptide (Figure 3.12 A & E). An increase in IFN-γ was also observed in mice injected with either Ad5-LHBsAg or EUVAX-B stimulated with the HBV S peptide (Figure 3.12 A). Additionally, increases in IFN-γ and IL-13 were observed in mice injected with Ad5-LHBsAg or Ad5-SHBsAg stimulated with the HBV PreS peptide pool (Figure 3.12 A & H). However, statistical analysis showed p-values that were higher than 0.05. As expected, stimulation with all peptide pools produced no cytokine responses in mice injected with Ad5-FLuc or saline and stimulation with CSC control resulted in elevated levels of all cytokines in all groups of mice.

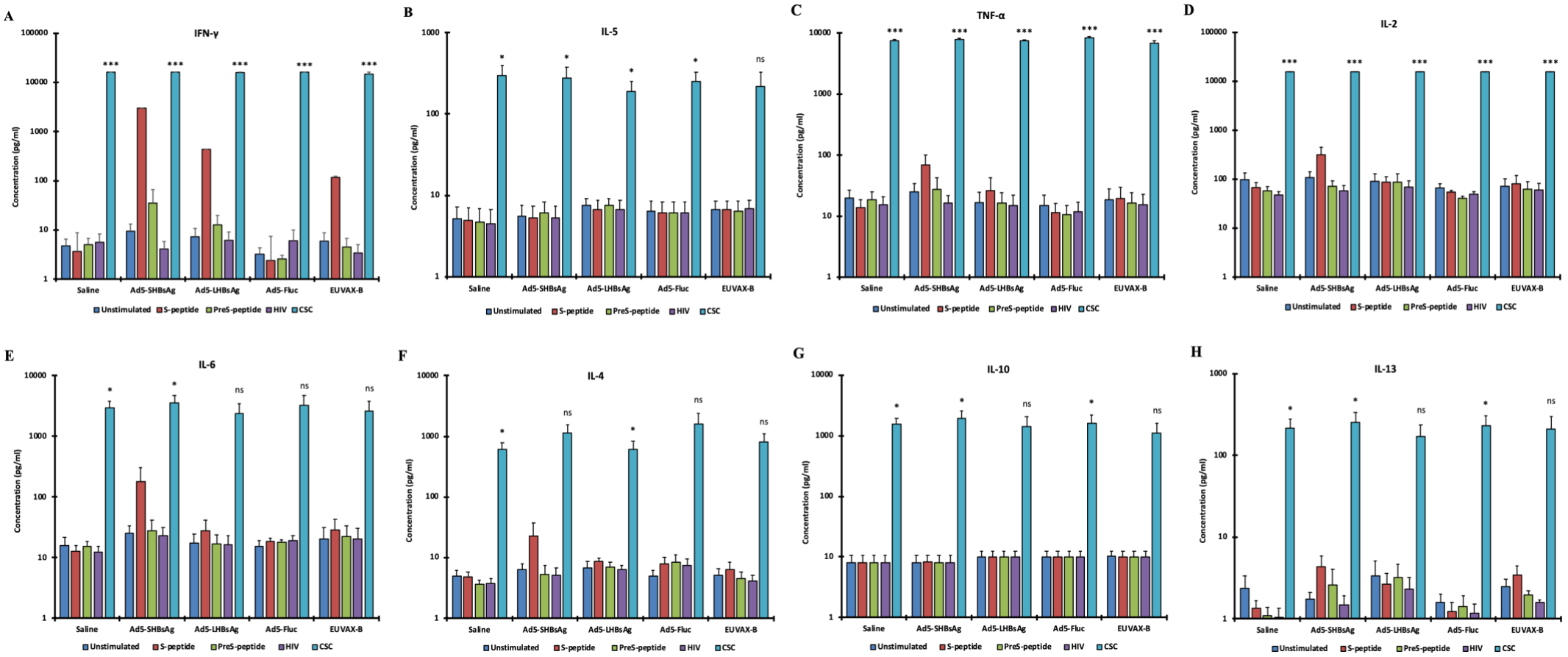

Figure 3.12: *In vivo* HBV-specific cytokine responses.

Harvested splenocytes stimulated with different peptide pools to assess HBV-specific cytokine responses. HBV-specific IFN-γ and IL-6 responses observed particularly after stimulation with the S-peptide pool. Cytokine concentration was determined using the online BioLegened LEGENDplex software (BioLegend, CA, USA). * $p \leq 0.05$, ** $p \leq 0.01$, *** ≤ 0.001, ns (not significant) $p > 0.05$ (statistical significance calculated by compared to unstimulated controls), $n = 5$ and error bars calculated using SEM.

3.5.3 *In vivo* HBsAb responses

When determining humoral immunity after vaccination with AdVs, results were considered positive for anti-HBsAg Abs if reactions exhibited an OD 450 nm – 655 nm ≥ 1.0. Average anti-HBsAg Ab levels in mice injected with Ad5-SHBsAg peaked 21 days post-vaccination and steadily reduced over the rest of the study period (Figure 3.13). Of the mice injected with EUVAX-B, Ab levels peaked 21 days post-vaccination and slight fluctuations in anti-HBsAg Ab levels were detected for the rest of the time points (Figure 3.13). As expected, mice injected with saline, Ad5-FLuc and Ad5-LHBsAg showed no significant levels of anti-HBsAg Abs at any timepoint after injection (Figure 3.13).

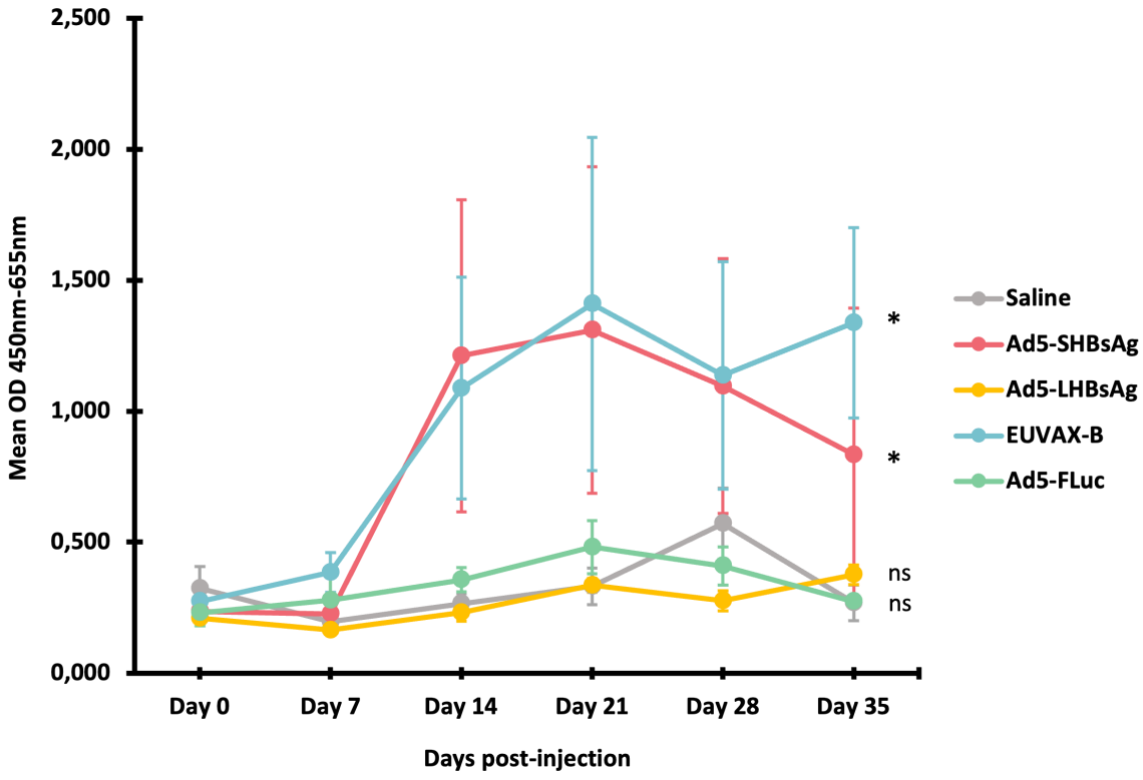

Figure 3.13: *In vivo* antibody levels after vaccination of mice.

Anti-HBsAg Ab levels detected using HRP-conjugated IgG. Average anti-HBsAg antibody levels in mice were comparable to those in mice injected with EUVAX-B control. The final colorimetric signal was recorded at an optical density of 450 nm – 655 nm using the Multiskan SkyHigh Microplate Spectrophotometer (Thermo Fischer Scientific, MA, USA).

* $p \leq 0.05$, ** $p \leq 0.01$, *** ≤ 0.001, ns (not significant) $p > 0.05$ (statistical significance calculated by comparing to saline control), n = 5 and error bars calculated using SEM.

Chapter 4

Discussion

Hepatitis B infection remains a public health concern all around the world, with a greater disease burden in endemic areas such as Sub-saharan Africa and Asia-Pacific. Vaccination against HBV remains the most effective method of disease prevention. While studies have shown that hepatitis B vaccines consisting of HBsAg purified from recombinant yeast cells and administered as a 3-dose regimen are effective against hepatitis B infection, these vaccines are often limited to humoral immunity and can be ineffective in people who are over the age of 40 years or immunocompromised. The emergence of next-generation vaccines (i.e., mRNA and viral vectors) has been an attractive approach to anti-HBV immunisation, especially in light of the COVID-19 pandemic. The use of recombinant AdVs in vaccine design have been investigated for years, and recently brought to the forefront of next-generation vaccine approaches with Ad-based vaccines against SARS-CoV-2 infection. This study investigated the use of Ads as vectors for anti-HBV vaccines.

4.1 Successful construction of recombinant pAd5 DNA

Homologous recombination of 'shuttle' and AdV 'backbone' DNA in mammalian cells has been a widely used method of recombinant AdV production. However, mammalian cells are not the most efficient for homologous recombination, making this method challenging (Luo *et al.*, 2007). Yeast and bacteria are therefore also considered for the purpose of homologous recombination (Luo *et al.*, 2007). The AdEasy system, described by He *et al.*, takes advantage of the efficiency of homologous recombination in BJ5183 *E. coli* bacterial cells for generating AdV recombinants.

The pShuttle-CMV vector is used as part of the AdEasy system for expression of transgenes under the control of a cytomegalovirus (CMV) promoter. Using the AdEasy system to produce Ad5-LHBsAg, Ad5-SHBsAg and Ad5-FLuc, transgenes encoding LHBsAg, SHBsAg and FLuc were removed from their carrier plasmids, either by restriction enzyme excision or PCR amplification (Figure 3.1). Using the restriction enzymes *Acc*65I and *Hind*III, *LHBsAg*, *SHBsAg* and *FLuc* transgenes were ligated into the pShuttle-CMV backbone. Expected banding patterns produced on an agarose gel after restriction enzyme digestion of pShuttle-LHBsAg,

pShuttle-SHBsAg and pShuttle-FLuc indicated successful ligation of *LHBsAg*, *SHBsAg* and *FLuc* transgenes into pShuttle-CMV backbone (Figure 3.2). Before co-transformation with pAdEasy-1, the shuttle plasmid clones were linearised with *Eco*RI. According to Luo *et al.*, shuttle plasmid clones can be linearised either with *Pme*I or *Eco*RI, however, due to the presence of an additional *Pme*I restriction site within the cloned region of pShuttle-LHBsAg, all clones were linearised with *Eco*RI.

Another important plasmid required for production of recombinant AdVs is the pAdEasy-1 vector plasmid. This vector is a 33.4 kb plasmid which contains the Ad5 genome, excluding the E1 and E3 genes, allowing Ads to infect but not replicate in non-permissive target cells. Co-transformation of BJ5183 bacterial cells with shuttle plasmid clones and pAdEasy-1 produced one-progeny pAd5 recombinant DNA encoding LHBsAg, SHBsAg and FLuc. Homologous recombination mechanisms may produce two recombinant DNA molecules (i.e., conservative or two-progeny) or one recombinant DNA molecule from two parental DNA molecules (i.e., non-conservative or one-progeny) (Takahashi, Yoshikura and Kobayashi, 2003). According to Takahashi *et al.*, recombination in an *E. coli* strain with a *recBC sbcBC* genotype (i.e., JC8679 cells) produced only one-progeny from two recombining DNA molecules. Because this strain lacks the RecBCD pathway of homologous recombination, the *sbcBC* mutations allow for the function of the RecF pathway, which is well suited to the task of recombinational cloning (Takahashi, Yoshikura and Kobayashi, 2003). The BJ5183 strain of *E. coli* also contains the *recBC sbcBC* genotype, meaning that, as expected, the RecF pathway produced one-progeny pAd5 recombinant DNA from the two parental DNA molecules, the shuttle plasmid clones and pAdEasy-1.

To determine the success of homologous recombination between the shuttle plasmid clones encoding LHBsAg, SHBsAg and FLuc and pAdEasy-1, recombinant DNA was digested with *Pac*I and *Eco*RV. Digestion of all selected reombinants with *Pac*I produced bands of ~30 kb and ~4.5 kb (Figure 3.3). According to Luo *et al*., enzymatic digestion of correct recombinants with *Pac*I will produce a large fragment of ~30 kb and a smaller fragment of either ~3.0 kb or ~4.5 kb. This is because, in the former case, homologous recombination between the shuttle plasmid clones and pAdEasy-1 occurs between the two homologous arms of each plasmid, whereas in the case of the latter, homologous recombination occurs between the ori regions and the one homologous arm of each plasmid (Luo *et al.*, 2007) (Appendix A – Figure 5.2). Digestion of recombinants with *Eco*RV further validated successful recombination by showing

different banding patterns on an agarose gel when compared to empty pAdEasy-1 digested with *Eco*RV (Figure 3.3).

4.2 Ad5 production and amplification

Recombinant AdVs were produced by transfecting HEK293T cells with pAd5-LHBsAg, pAd5-SHBsAg and pAd5-FLuc (P0). HEK293T cells were transfected with pAd5-GFP alongside the other Ad5 vectors as a reporter (Figure 3.4). Since Ad5-SHBsAg and Ad5-FLuc were produced and amplified at the same time, the GFP images reporting on those AdVs were from the same flask of cells. According to the GFP reporter, transfection efficiency alongside pAd5-LHBsAg was higher than that of pAd5-SHBsAg and pAd5-FLuc (Figure 3.4). However, amplification (P1) results showed increased infection in cells infected with Ad5-GFP alongside Ad5-SHBsAg and Ad5-FLuc when compared to cells infected alongside Ad5-LHBsAg (Figure 3.5). The transfection efficiency when using chemical methods (i.e., lipofectamine) depends on several factors, including the ratio of DNA to chemical agent, cell membrane conditions, pH, and cell type (Kim and Eberwine, 2010). This decrease in transfection efficiency may have been attributed to any changes in these factors. Additionally, transfection/infection of cells with Ad5-LHBsAg on a different day to transfection/infection of cells with Ad5-SHBsAg and Ad5-FLuc may have affected the efficiency. The health of the HEK293T cells is critical when producing viruses. Decreased transfection/infection efficiency may be the result of sub-optimal cell health. Ways to mitigate this include, using freshly prepared cell culture medium, avoiding prolonged exposure to TrypLE™ Express Enzyme and splitting cells to the appropriate confluency. Despite this, viral yields after large-scale production were sufficient for *in vitro* and *in vivo* analysis (Table 3.2).

4.3 Efficient *in vitro* transgene expression from recombinant AdVs

Before *in vivo* administration of recombinant AdVs, *in vitro* transgene expression was tested in HEK293T cells. Infection of HEK293T cells with AdVs produced dose-dependent levels of LHBsAg, SHBsAg and FLuc. The region of the HBV genome that encodes the surface proteins, made up of three continuous regions, namely, *pre*S1, *pre*S2 and S encodes the LHBsAg, MHBsAg and SHBsAg proteins, respectively. Expression of SHBsAg from a recombinant vaccinia virus produces both glycosylated and non-glycosylated forms of the S protein, whereafter 22 nm HBsAg particles are secreted (Cheng, Smith and Moss, 1986). Insertion of the entire *pre*S1-*pre*S2-S region into the vaccinia virus genome to express LHBsAg, also

produces glycosylated and non-glycosylated forms of LHBsAg, however, these are not secreted and remain intracellular (Cheng, Smith and Moss, 1986). In this study, dose dependent levels of SHBsAg after infection of HEK293T cells with Ad5-SHBsAg was observed in both supernatant and lysate samples due to the secretory nature of SHBsAg (Figure 3.9 B). However, dose dependent levels of LHBsAg after infection of HEK293T cells with Ad5-LHBsAg was only observed in lysate samples because LHBsAg remains intracellular (Figure 3.9 A). Additionally, LHBsAg levels were not as high compared to SHBsAg levels in lysate samples (Figure 3.9 A & B). This is because the Monolisa™ HBsAg ULTRA kit (Bio-Rad Laboratories Inc., CA, USA) used for antigen detection is more suited for SHBsAg detection. This is perhaps because the epitope that binds to the anti-HBsAg antibodies coating the Monolisa™ plate are only partially exposed in the LHBsAg structure.

FLuc is perhaps one of the best characterised bioluminescent proteins and is often used as a reporter gene/protein within living cells (Feeney *et al.*, 2016). The addition of LARII to samples produces a bioluminescent signal that can be detected using a bioluminometer. Since FLuc is also an intracellular protein, it is not secreted by the HEK293T cells. For this reason, infection of HEK293T cells with Ad5-FLuc produced dose-dependent levels of FLuc only in lysate samples (Figure 3.10). Additionally, there was a decrease in FLuc levels after infection at an MOI of 100 to an MOI of 1000 (Figure 3.10). This was not unexpected and was likely the result of the CPE of AdV infection on the HEK293T cells. At an MOI of 1000, the cells are saturated with virus, which affects their ability to efficiently support transgene expression. Therefore, the levels of proteins expressed by the virus are also decreased.

4.4 *In vivo* transgene expression and immunogenicity

Transgene expression from first-generation AdVs is very strong initially but is reduced and abolished 2-3 weeks after direct injection (Kaspar, 2009) due to viral clearance by the immune system. In this study, as expected, strong FLuc expression was observed at days 1 and 3, with decreasing expression at day 7 and almost complete clearance at day 14 after injection of Balb/c mice and bioluminescence imaging (Figure 3.11 A & B).

Cell-mediated immune responses produced after vaccination were assessed by splenocyte stimulation with HBV peptide pools. HBV-specific IFN-γ and IL-6 levels were elevated particularly in mice vaccinated with Ad5-SHBsAg and stimulated with an HBV S peptide pool

(Figure 3.12 A & E). It was concluded that the cytokine responses were HBV-specific and not directed against the AdV itself because the cytokine levels in mice injected with Ad5-FLuc were comparable to the levels in mice injected with saline. While slightly elevated cytokine levels were observed in vaccinated mice, IFN-γ levels were the most pronounced (Figure 3.12 A). Cytokines of the IFN family act as the first line of defence upon viral infection and control viral replication and dissemination (Zhong *et al.*, 2021). Upon infection with HBV, IFN-γ specifically, inhibits viral HBV replication and diminishes cccDNA in the hepatocytes.

Because AdVs can produce both cell-mediated and humoral immune responses, humoral immunity produced after vaccination was evaluated by assessing the presence of binding anti-HBsAg Abs. An Ab binding assay showed an average increase in anti-HBsAg Abs from days 7 to 14, peaking at day 21 and declining at day 28 after injection with Ad5-SHBsAg (Figure 3.13). Anti-HBsAg Ab levels also peaked at day 21 in mice injected with EUVAX-B (Figure 3.13). A study conducted by McMahon *et al* showed that after a booster dose of plasma-derived hepatitis B vaccine, anti-HBsAg Ab levels ≥10 mIU/ml were detected at 10-14 days in 77% of individuals who received the booster dose (McMahon *et al.*, 2009). To confer protection against hepatitis B infection, vaccination must produce anti-HBsAg Ab levels ≥10 mIU/ml (Di Lello, Martínez and Flichman, 2022). About one month after completing a three-dose HBV vaccine regiment, protective anti-HBsAg Ab levels can be detected in more that 90% of immunised individuals. These antibody titers tend to decline significantly during the first year after vaccination, however, immunological memory is often enough to prevent infection (Di Lello, Martínez and Flichman, 2022). The assay conducted in this study, however, was only qualitative. To assess the value of these antibodies in conferring protection, a quantitative assay will need to be optimised to quantify anti-HBsAg Ab levels after Ad5 vaccination and establish if the titers are enough to confer protection.

In comparison, there were no significant levels of anti-HBsAg Abs detected in mice vaccinated with Ad5-LHBsAg. As with the Monolisa™ HBsAg ULTRA kit used for antigen detection, it is likely that the ELISA plates used for the detection of anti-HBsAg Abs are more suited for to detect antibodies against SHBsAg specifically. However, there should be some cross-reactivity when detecting Abs against LHBsAg or SHBsAg, but with a lower sensitivity to anti-LHBsAg Abs. Since B cells mediate humoral immunity and many cytokines influence B cell development, differentiation and/or proliferation and survival (Vazquez, Catalan-Dibene and

Zlotnik, 2015), the fact that weaker cytokine responses were seen in mice vaccinated with Ad5-LHBsAg may be a contributing factor to the anti-HBsAg Ab levels in those mice.

Conclusions and Future work

The use of recombinant AdVs as vaccines has been appealing to researchers because of their ability to induce robust immune responses. Their use as vaccines against infectious diseases, including SARS-CoV-2 has made them attractive candidates for vaccines against other infectious diseases. This study investigated the use of recombinant AdVs as vectors for anti-HBV vaccines and showed that, while further study is required to improve the overall efficacy, AdVs are promising candidates for use as vaccines against HBV.

Due to time constraints, the assessment of NAb capabilities was not evaluated. Therefore, future work will focus on assessing the ability of the detected antibodies to neutralise HBV infection. Additionally, investigations into alternative Ad serotypes to Ad5 will be conducted. Vaccine regimens in mice will be altered to include a prime dose using one Ad serotype and a booster using a different serotype. Additionally, a heterologous vaccine regimen will be investigated using both AdV and RNA technologies. These strategies should contribute to more robust and stronger immune responses. Finally, challenge of vaccinated mice with HBV will assess protection against hepatitis B infection.

References

Abudoureyimu, M. *et al.* (2019) 'Oncolytic Adenovirus—A Nova for Gene-Targeted Oncolytic Viral Therapy in HCC', *Frontiers in Oncology*, 9, p. 1182.

Adugna, A. (2023) 'Antigen Recognition and Immune Response to Acute and Chronic Hepatitis B Virus Infection', *Journal of Inflammation Research*, 16, pp. 2159–2166. Available at: https://doi.org/10.2147/JIR.S411492.

Anywaine, Z. *et al.* (2022) 'Safety and immunogenicity of 2-dose heterologous Ad26.ZEBOV, MVA-BN-Filo Ebola vaccination in children and adolescents in Africa: A randomised, placebo-controlled, multicentre Phase II clinical trial', *PLOS Medicine*, 19(1), p. e1003865. Available at: https://doi.org/10.1371/journal.pmed.1003865.

Araújo, N.M. *et al.* (2022) 'The use of adenoviral vectors in gene therapy and vaccine approaches', *Genetics and Molecular Biology*, 45, p. e20220079. Available at: https://doi.org/10.1590/1678-4685-GMB-2022-0079.

Arnberg, N. *et al.* (2000) 'Adenovirus Type 37 Uses Sialic Acid as a Cellular Receptor', *Journal of Virology*, 74(1), pp. 42–48.

Atasheva, S. and Shayakhmetov, D. (2016) 'Adenovirus sensing by the immune system', *Current opinion in virology*, 21, pp. 109–113. Available at: https://doi.org/10.1016/j.coviro.2016.08.017.

Baden, L.R. *et al.* (2015) 'Induction of HIV-1–Specific Mucosal Immune Responses Following Intramuscular Recombinant Adenovirus Serotype 26 HIV-1 Vaccination of Humans', *The Journal of Infectious Diseases*, 211(4), pp. 518–528. Available at: https://doi.org/10.1093/infdis/jiu485.

Bangari, D.S. and Mittal, S.K. (2006) 'Development of nonhuman adenoviruses as vaccine vectors', *Vaccine*, 24(7), pp. 849–862. Available at: https://doi.org/10.1016/j.vaccine.2005.08.101.

Barouch, D.H. *et al.* (2018) 'Evaluation of a Mosaic HIV-1 Vaccine in a Randomized, Double-Blinded, Placebo-Controlled Phase I/IIa Clinical Trial and in Rhesus Monkeys', *Lancet*

(London, England), 392(10143), pp. 232–243. Available at: https://doi.org/10.1016/S0140-6736(18)31364-3.

Bertoletti, A. and Ferrari, C. (2016) 'Adaptive immunity in HBV infection', *Journal of Hepatology*, 64(1, Supplement), pp. S71–S83. Available at: https://doi.org/10.1016/j.jhep.2016.01.026.

Busca, A. and Kumar, A. (2014) 'Innate immune responses in hepatitis B virus (HBV) infection', *Virology Journal*, 11(1), p. 22. Available at: https://doi.org/10.1186/1743-422X-11-22.

Cai, Y. and Yin, W. (2020) 'The Multiple Functions of B Cells in Chronic HBV Infection', *Frontiers in Immunology*, 11, p. 582292.

Chang, J. (2021) 'Adenovirus Vectors: Excellent Tools for Vaccine Development', *Immune Network*, 21(1), p. e6. Available at: https://doi.org/10.4110/in.2021.21.e6.

Chen, Y. *et al.* (2005) 'Activation and function of hepatic NK cells in hepatitis B infection: an underinvestigated innate immune response', *Journal of Viral Hepatitis*, 12(1), pp. 38–45. Available at: https://doi.org/10.1111/j.1365-2893.2005.00543.x.

Cheng, K.C., Smith, G.L. and Moss, B. (1986) 'Hepatitis B virus large surface protein is not secreted but is immunogenic when selectively expressed by recombinant vaccinia virus', *Journal of Virology*, 60(2), pp. 337–344. Available at: https://doi.org/10.1128/JVI.60.2.337-344.1986.

Chengalvala, M.V. *et al.* (1994) 'Immunogenicity of high expression adenovirus-hepatitis B virus recombinant vaccines in dogs', *Journal of General Virology*, 75(1), pp. 125–131. Available at: https://doi.org/10.1099/0022-1317-75-1-125.

Chinnakannan, S.K. *et al.* (2020) 'The Design and Development of a Multi-HBV Antigen Encoded in Chimpanzee Adenoviral and Modified Vaccinia Ankara Viral Vectors; A Novel Therapeutic Vaccine Strategy against HBV', *Vaccines*, 8(2), p. 184. Available at: https://doi.org/10.3390/vaccines8020184.

Chisari, F. (1997) 'Cytotoxic T cells and viral hepatitis. - PMC', *The Journal of Clinical Investigation*, 99(7), pp. 1472–1477.

Chisari, F.V., Isogawa, M. and Wieland., S.F. (2010) 'Pathogenesis of hepatitis B virus infection', *Pathologie Biologie*, 58(4), pp. 258–266. Available at: https://doi.org/10.1016/j.patbio.2009.11.001.

Chuang, Y.-C., Tsai, K.-N. and Ou, J.-H.J. (2022) 'Pathogenicity and virulence of Hepatitis B virus', *Virulence*, 13(1), pp. 258–296. Available at: https://doi.org/10.1080/21505594.2022.2028483.

Churin, Y., Roderfeld, M. and Roeb, E. (2015) 'Hepatitis B virus large surface protein: function and fame', *Hepatobiliary Surgery and Nutrition*, 4(1), pp. 1–10. Available at: https://doi.org/10.3978/j.issn.2304-3881.2014.12.08.

Coughlan, L., Kremer, E.J. and Shayakhmetov, D.M. (2022) 'Adenovirus-based vaccines—a platform for pandemic preparedness against emerging viral pathogens', *Molecular Therapy*, 30(5), pp. 1822–1849. Available at: https://doi.org/10.1016/j.ymthe.2022.01.034.

Danthinne, X. (1999) 'New vectors for the construction of double recombinant adenoviruses', *Journal of Virological Methods*, 81(1), pp. 11–20. Available at: https://doi.org/10.1016/S0166-0934(99)00054-3.

Di Lello, F.A., Martínez, A.P. and Flichman, D.M. (2022) 'Insights into induction of the immune response by the hepatitis B vaccine', *World Journal of Gastroenterology*, 28(31), pp. 4249–4262. Available at: https://doi.org/10.3748/wjg.v28.i31.4249.

Farhad, T. *et al.* (2022) 'Adenoviral Vectors: Potential as Anti-HBV Vaccines and Therapeutics', *Genes*, 13(11), p. 1941. Available at: https://doi.org/10.3390/genes13111941.

Feeney, K.A. *et al.* (2016) 'In-depth Characterization of Firefly Luciferase as a Reporter of Circadian Gene Expression in Mammalian Cells', *Journal of Biological Rhythms*, 31(6), pp. 540–550. Available at: https://doi.org/10.1177/0748730416668898.

Fessler, S.P. and Young, C.S.H. (1998) 'Control of Adenovirus Early Gene Expression during the Late Phase of Infection', *Journal of Virology*, 72(5), pp. 4049–4056.

Folegatti, P.M. *et al.* (2020) 'Safety and immunogenicity of the ChAdOx1 nCoV-19 vaccine against SARS-CoV-2: a preliminary report of a phase 1/2, single-blind, randomised controlled

trial', *The Lancet*, 396(10249), pp. 467–478. Available at: https://doi.org/10.1016/S0140-6736(20)31604-4.

Fong, T.-L. *et al.* (1994) 'High levels of viral replication during acute hepatitis B infection predict progression to chronicity', *Journal of Medical Virology*, 43(2), pp. 155–158. Available at: https://doi.org/10.1002/jmv.1890430210.

Gaggar, A., Shayakhmetov, D.M. and Lieber, A. (2003) 'CD46 is a cellular receptor for group B adenoviruses', *Nature Medicine*, 9(11), pp. 1408–1412. Available at: https://doi.org/10.1038/nm952.

Gao, W. *et al.* (2006) 'Protection of Mice and Poultry from Lethal H5N1 Avian Influenza Virus through Adenovirus-Based Immunization', *Journal of Virology*, 80(4), pp. 1959–1964. Available at: https://doi.org/10.1128/jvi.80.4.1959-1964.2006.

Ginzberg, D., Wong, R.J. and Gish, R. (2018) 'Global HBV burden: guesstimates and facts', *Hepatology International*, 12(4), pp. 315–329. Available at: https://doi.org/10.1007/s12072-018-9884-8.

Grimm, S.K. and Ackerman, M.E. (2013) 'Vaccine Design: Emerging Concepts and Renewed Optimism', *Current Opinion in Biotechnology*, 24(6), pp. 1078–1088. Available at: https://doi.org/10.1016/j.copbio.2013.02.015.

He, T.-C. *et al.* (1998) 'A simplified system for generating recombinant adenoviruses', *Proceedings of the National Academy of Sciences of the United States of America*, 95(5), pp. 2509–2514.

Heidary, M. *et al.* (2022) 'A Comprehensive Review of the Protein Subunit Vaccines Against COVID-19', *Frontiers in Microbiology*, 13, p. 927306. Available at: https://doi.org/10.3389/fmicb.2022.927306.

Hendrickx, R. *et al.* (2014) 'Innate Immunity to Adenovirus', *Human Gene Therapy*, 25(4), pp. 265–284. Available at: https://doi.org/10.1089/hum.2014.001.

Hoeben, R.C. and Uil, T.G. (2013) 'Adenovirus DNA Replication', *Cold Spring Harbor Perspectives in Biology*, 5(3), p. a013003. Available at: https://doi.org/10.1101/cshperspect.a013003.

Hu, S. *et al.* (2019) 'Hepatitis B Virus Inhibits Neutrophil Extracellular Trap Release by Modulating Reactive Oxygen Species Production and Autophagy', *Journal of Immunology (Baltimore, Md.: 1950)*, 202(3), pp. 805–815. Available at: https://doi.org/10.4049/jimmunol.1800871.

Hutin, Y. *et al.* (2018) 'Access to treatment for hepatitis B virus infection—Worldwide, 2016', *American Journal of Transplantation*, 18(10), pp. 2595–2598. Available at: https://doi.org/10.1111/ajt.15093.

Iannacone, M. and Guidotti, L.G. (2022) 'Immunobiology and pathogenesis of hepatitis B virus infection', *Nature Reviews. Immunology*, 22(1), pp. 19–32. Available at: https://doi.org/10.1038/s41577-021-00549-4.

Jacob-Dolan, C. and Barouch, D.H. (2022) 'COVID-19 Vaccines: Adenoviral Vectors', *Annual Review of Medicine*, 73(1), pp. 41–54. Available at: https://doi.org/10.1146/annurev-med-012621-102252.

Jafari, A. *et al.* (2022) 'Current advances and challenges in COVID-19 vaccine development: from conventional vaccines to next-generation vaccine platforms', *Molecular Biology Reports*, 49(6), pp. 4943–4957. Available at: https://doi.org/10.1007/s11033-022-07132-7.

Jennings, M.R. and Parks, R.J. (2023) 'Human Adenovirus Gene Expression and Replication Is Regulated through Dynamic Changes in Nucleoprotein Structure throughout Infection', *Viruses*, 15(1), p. 161. Available at: https://doi.org/10.3390/v15010161.

Kaspar, B.K. (2009) 'Gene Therapy: Direct Viral Delivery', in L.R. Squire (ed.) *Encyclopedia of Neuroscience*. Oxford: Academic Press, pp. 633–639. Available at: https://doi.org/10.1016/B978-008045046-9.00012-7.

Kim, T.K. and Eberwine, J.H. (2010) 'Mammalian cell transfection: the present and the future', *Analytical and Bioanalytical Chemistry*, 397(8), pp. 3173–3178. Available at: https://doi.org/10.1007/s00216-010-3821-6.

Kremer, E.J. (2020) 'Pros and Cons of Adenovirus-Based SARS-CoV-2 Vaccines', *Molecular Therapy*, 28(11), pp. 2303–2304.

Larivière, Y. *et al.* (2023) 'Safety and Immunogenicity of the Heterologous 2-Dose Ad26.ZEBOV, MVA-BN-Filo Vaccine Regimen in Health Care Providers and Frontliners of the Democratic Republic of the Congo', *The Journal of Infectious Diseases*, p. jiad350. Available at: https://doi.org/10.1093/infdis/jiad350.

Lavanchy, D. (2005) 'Worldwide epidemiology of HBV infection, disease burden, and vaccine prevention', *Journal of Clinical Virology: The Official Publication of the Pan American Society for Clinical Virology*, 34 Suppl 1, pp. S1-3. Available at: https://doi.org/10.1016/s1386-6532(05)00384-7.

Leen, A.M. *et al.* (2006) 'Adenoviral Infections in Hematopoietic Stem Cell Transplantation', *Biology of Blood and Marrow Transplantation*, 12(3), pp. 243–251. Available at: https://doi.org/10.1016/j.bbmt.2005.10.024.

Logunov, D.Y. *et al.* (2020) 'Safety and immunogenicity of an rAd26 and rAd5 vector-based heterologous prime-boost COVID-19 vaccine in two formulations: two open, non-randomised phase 1/2 studies from Russia', *The Lancet*, 396(10255), pp. 887–897. Available at: https://doi.org/10.1016/S0140-6736(20)31866-3.

Logunov, D.Y. *et al.* (2021) 'Safety and efficacy of an rAd26 and rAd5 vector-based heterologous prime-boost COVID-19 vaccine: an interim analysis of a randomised controlled phase 3 trial in Russia', *The Lancet*, 397(10275), pp. 671–681. Available at: https://doi.org/10.1016/S0140-6736(21)00234-8.

Lubeck, M.D. *et al.* (1989) 'Immunogenicity and efficacy testing in chimpanzees of an oral hepatitis B vaccine based on live recombinant adenovirus.', *Proceedings of the National Academy of Sciences*, 86(17), pp. 6763–6767. Available at: https://doi.org/10.1073/pnas.86.17.6763.

Luo, J. *et al.* (2007) 'A protocol for rapid generation of recombinant adenoviruses using the AdEasy system', *Nature Protocols*, 2(5), pp. 1236–1247. Available at: https://doi.org/10.1038/nprot.2007.135.

Man-Lik Choi, E. *et al.* (2023) 'Safety and immunogenicity of an Ad26.ZEBOV booster vaccine in Human Immunodeficiency Virus positive (HIV+) adults previously vaccinated with the Ad26.ZEBOV, MVA-BN-Filo vaccine regimen against Ebola: A single-arm, open-label

Phase II clinical trial in Kenya and Uganda', *Vaccine*, 41(50), pp. 7573–7580. Available at: https://doi.org/10.1016/j.vaccine.2023.10.055.

Marshall, J.S. *et al.* (2018) 'An introduction to immunology and immunopathology', *Allergy, Asthma & Clinical Immunology*, 14(2), p. 49. Available at: https://doi.org/10.1186/s13223-018-0278-1.

Martin, P. *et al.* (2015) 'TG1050, an immunotherapeutic to treat chronic hepatitis B, induces robust T cells and exerts an antiviral effect in HBV-persistent mice', *Gut*, 64(12), pp. 1961–1971. Available at: https://doi.org/10.1136/gutjnl-2014-308041.

McMahon, B.J. *et al.* (2009) 'Antibody levels and protection after hepatitis B vaccine: results of a 22-year follow-up study and response to a booster dose', *The Journal of Infectious Diseases*, 200(9), pp. 1390–1396. Available at: https://doi.org/10.1086/606119.

McNaughton, A.L. *et al.* (2019) 'Insights From Deep Sequencing of the HBV Genome—Unique, Tiny, and Misunderstood', *Gastroenterology*, 156(2), pp. 384–399. Available at: https://doi.org/10.1053/j.gastro.2018.07.058.

Mendonça, S.A. *et al.* (2021) 'Adenoviral vector vaccine platforms in the SARS-CoV-2 pandemic', *npj Vaccines*, 6(1), pp. 1–14. Available at: https://doi.org/10.1038/s41541-021-00356-x.

Mistchenko, A.S. *et al.* (1994) 'Cytokines in adenoviral disease in children: Association of interleukin-6, interleukin-8, and tumor necrosis factor alpha levels with clinical outcome', *The Journal of Pediatrics*, 124(5, Part 1), pp. 714–720. Available at: https://doi.org/10.1016/S0022-3476(05)81360-5.

Moyle, P.M. and Toth, I. (2013) 'Modern Subunit Vaccines: Development, Components, and Research Opportunities', *ChemMedChem*, 8(3), pp. 360–376. Available at: https://doi.org/10.1002/cmdc.201200487.

Ott, J.J. *et al.* (2012) 'Global epidemiology of hepatitis B virus infection: New estimates of age-specific HBsAg seroprevalence and endemicity', *Vaccine*, 30(12), pp. 2212–2219. Available at: https://doi.org/10.1016/j.vaccine.2011.12.116.

Palmer, D. and Ng, P. (2003) 'Improved system for helper-dependent adenoviral vector production', *Molecular Therapy*, 8(5), pp. 846–852. Available at: https://doi.org/10.1016/j.ymthe.2003.08.014.

Pattyn, J. *et al.* (2021) 'Hepatitis B Vaccines', *The Journal of Infectious Diseases*, 224(Suppl 4), pp. S343–S351. Available at: https://doi.org/10.1093/infdis/jiaa668.

Peng, G. *et al.* (2008) 'Circulating CD4+ CD25+ regulatory T cells correlate with chronic hepatitis B infection', *Immunology*, 123(1), pp. 57–65. Available at: https://doi.org/10.1111/j.1365-2567.2007.02691.x.

Pollard, A.J. *et al.* (2021) 'Safety and immunogenicity of a two-dose heterologous Ad26.ZEBOV and MVA-BN-Filo Ebola vaccine regimen in adults in Europe (EBOVAC2): a randomised, observer-blind, participant-blind, placebo-controlled, phase 2 trial', *The Lancet. Infectious Diseases*, 21(4), pp. 493–506. Available at: https://doi.org/10.1016/S1473-3099(20)30476-X.

Pollicino, T. *et al.* (2012) 'Impact of hepatitis B virus (HBV) preS/S genomic variability on HBV surface antigen and HBV DNA serum levels', *Hepatology*, 56(2), pp. 434–443. Available at: https://doi.org/10.1002/hep.25592.

Pulendran, B. and Ahmed, R. (2011) 'Immunological mechanisms of vaccination', *Nature Immunology*, 12(6), pp. 509–517. Available at: https://doi.org/10.1038/ni.2039.

van Riel, D. and de Wit, E. (2020) 'Next-generation vaccine platforms for COVID-19', *Nature Materials*, 19(8), pp. 810–812. Available at: https://doi.org/10.1038/s41563-020-0746-0.

Sadoff, J., Le Gars, M., *et al.* (2021) 'Interim Results of a Phase 1-2a Trial of Ad26.COV2.S Covid-19 Vaccine', *The New England Journal of Medicine*, 384(19), pp. 1824–1835. Available at: https://doi.org/10.1056/NEJMoa2034201.

Sadoff, J., Gray, G., *et al.* (2021) 'Safety and Efficacy of Single-Dose Ad26.COV2.S Vaccine against Covid-19', *New England Journal of Medicine*, 384(23), pp. 2187–2201. Available at: https://doi.org/10.1056/NEJMoa2101544.

Sakurai, F., Tachibana, M. and Mizuguchi, H. (2022) 'Adenovirus vector-based vaccine for infectious diseases', *Drug Metabolism and Pharmacokinetics*, 42, p. 100432. Available at: https://doi.org/10.1016/j.dmpk.2021.100432.

Schreiner, S. and Nassal, M. (2017) 'A Role for the Host DNA Damage Response in Hepatitis B Virus cccDNA Formation-and Beyond?', *Viruses*, 9(5), p. 125. Available at: https://doi.org/10.3390/v9050125.

Shirley, J.L. *et al.* (2020) 'Immune Responses to Viral Gene Therapy Vectors', *Molecular Therapy*, 28(3), pp. 709–722. Available at: https://doi.org/10.1016/j.ymthe.2020.01.001.

Stoop, J.N. *et al.* (2005) 'Regulatory T cells contribute to the impaired immune response in patients with chronic hepatitis B virus infection', *Hepatology*, 41(4), pp. 771–778. Available at: https://doi.org/10.1002/hep.20649.

Takahashi, N., Yoshikura, H. and Kobayashi, I. (2003) 'An Escherichia coli strain, BJ5183, that shows highly efficient conservative (two-progeny) DNA double-strand break repair of restriction breaks', *Gene*, 303, pp. 89–97. Available at: https://doi.org/10.1016/S0378-1119(02)01107-1.

Tan, A., Koh, S. and Bertoletti, A. (2015) 'Immune Response in Hepatitis B Virus Infection', *Cold Spring Harbor Perspectives in Medicine*, 5(8), p. a021428. Available at: https://doi.org/10.1101/cshperspect.a021428.

Tatsis, N. and Ertl, H.C.J. (2004) 'Adenoviruses as vaccine vectors', *Molecular Therapy*, 10(4), pp. 616–629. Available at: https://doi.org/10.1016/j.ymthe.2004.07.013.

Travieso, T. *et al.* (2022) 'The use of viral vectors in vaccine development', *npj Vaccines*, 7(1), pp. 1–10. Available at: https://doi.org/10.1038/s41541-022-00503-y.

Tsukuda, S. and Watashi, K. (2020) 'Hepatitis B virus biology and life cycle', *Antiviral Research*, 182, p. 104925. Available at: https://doi.org/10.1016/j.antiviral.2020.104925.

Vanlandschoot, P. and Leroux-Roels, G. (2003) 'Viral apoptotic mimicry: an immune evasion strategy developed by the hepatitis B virus?', *Trends in Immunology*, 24(3), pp. 144–147. Available at: https://doi.org/10.1016/s1471-4906(03)00026-7.

Vazquez, M.I., Catalan-Dibene, J. and Zlotnik, A. (2015) 'B cells responses and cytokine production are regulated by their immune microenvironment', *Cytokine*, 74(2), pp. 318–326. Available at: https://doi.org/10.1016/j.cyto.2015.02.007.

Voysey, M. *et al.* (2021) 'Safety and efficacy of the ChAdOx1 nCoV-19 vaccine (AZD1222) against SARS-CoV-2: an interim analysis of four randomised controlled trials in Brazil, South Africa, and the UK', *Lancet (London, England)*, 397(10269), pp. 99–111. Available at: https://doi.org/10.1016/S0140-6736(20)32661-1.

Wong, G.L.-H. *et al.* (2022) 'Universal HBV vaccination dramatically reduces the prevalence of HBV infection and incidence of hepatocellular carcinoma', *Alimentary Pharmacology & Therapeutics*, 56(5), pp. 869–877. Available at: https://doi.org/10.1111/apt.17120.

Xia, Y. and Liang, T.J. (2019) 'Development of Direct-acting Antiviral and Host-targeting Agents for Treatment of Hepatitis B Virus Infection', *Gastroenterology*, 156(2), pp. 311–324. Available at: https://doi.org/10.1053/j.gastro.2018.07.057.

Xia, Y. and Protzer, U. (2017) 'Control of Hepatitis B Virus by Cytokines', *Viruses*, 9(1), p. 18. Available at: https://doi.org/10.3390/v9010018.

Xing, T., Xu, H. and Yu, W. (2013) 'Role of T follicular helper cells and their associated molecules in the pathogenesis of chronic hepatitis B virus infection', *Experimental and Therapeutic Medicine*, 5(3), pp. 885–889. Available at: https://doi.org/10.3892/etm.2012.864.

Yoo, J. *et al.* (2018) 'Update Treatment for HBV Infection and Persistent Risk for Hepatocellular Carcinoma: Prospect for an HBV Cure', *Diseases*, 6(2), p. 27. Available at: https://doi.org/10.3390/diseases6020027.

Zhong, S. *et al.* (2021) 'Cytokines and Chemokines in HBV Infection', *Frontiers in Molecular Biosciences*, 8, p. 805625. Available at: https://doi.org/10.3389/fmolb.2021.805625.

Appendix A – General protocols and recipes

5.1 Bacterial work

5.1.1 Growth media

5.1.1.1 Luria-Bertani (LB) medium

LB medium for bacterial growth was prepared by mixing 10 g tryptone, 5 g NaCl and 5 g yeast in 1L dH_2O and autoclaving for 20 minutes to completely dissolve. Antibiotic [1000 × ampicillin (100 mg/ml) or 1000 × kanamycin (50 mg/ml)] was added to 1 × when necessary.

5.1.1.2 Luria-Bertani (LB) agar

LB agar plates for bacterial growth were prepared by mixing 5 g tryptone, 2.5 g NaCl, 2.5 g yeast extract and 5 g agar in 500 ml dH_2O. After autoclaving for 20 minutes, the agar was left to cool and 250 µl of 1000 × ampicillin was added to half of the agar mix (250 ml) and 250 µl of 1000 × kanamycin was added to the other half of the agar mix (250 ml). The mixtures were poured into petri dishes and left to set. Petri dishes were stored at 4°C.

5.1.1.3 Antibiotics (Ampicillin and Kanamycin)

Ampicillin (1000 × stock) was prepared by mixing 1 g ampicillin powder with 7 ml 100% ethanol and 3 ml dH_2O. The mixture was filtered into a 15 ml tube and stored at -20°C.

Kanamycin (1000 × stock) was prepared by mixing 0.5 g kanamycin powder with 10 ml dH_2O. The mixture was filtered into a 15 ml tube and aliquoted into 1.5 ml tubes and stored at 20°C.

5.1.2 Bacterial transformation

5.1.2.1 $CaCl_2$ transformation buffer

First, 1.47 g $CaCl_2$, 0.30 g PIPES and 15 ml glycerol were added to a total volume of 80 ml dH_2O. After mixing, the pH was adjusted to ~7.15. The volume was made up to 100 ml with dH_2O and the complete buffer was autoclaved for 20 minutes.

5.1.2.2 Preparation of competent bacteria

Competent bacteria were prepared by inoculating 10 ml LB medium with 20 µl *E. coli* from a freezer stock and incubating overnight at 37°C with shaking. After overnight culture, 150-200 ml LB medium was inoculated with the 10 ml culture and incubated at 37°C with shaking for

4 hours. The culture was then centrifuged at ~3220 × g at 4°C for 25 minutes to pellet the bacteria. After discarding the supernatant, the pellet was resuspended in a total of 3 ml transformation buffer and the volume was made up to 35 ml with transformation buffer. Bacteria were incubated on ice for 30 minutes and centrifuged at ~1610 × g at 4°C for 10 minutes and the bacterial pellet was resuspended in 2 ml transformation buffer. A volume of 100 µl was aliquoted into tubes and stored at -80°C.

5.1.3 Heat shock transformation of competent *E. coli*

Chemically competent *E. coli* were transformed by adding 0.5-2 µg of plasmid DNA to 10-100 µl of competent *E.coli* and incubating on ice for 20 minutes. The reaction was then heat shocked at 42°C for 90 seconds and incubated on ice for another 5 minutes. Transformed bacteria were plated on agar supplemented with 1 × kanamycin or 1 × ampicillin and incubated overnight at 37°C.

5.2 Plasmid and DNA preparations

5.2.1 Buffer preparations

5.2.1.1 Resuspension buffer (buffer P1)

Resuspension buffer was prepared by dissolving 6.06 g Tris base and 3.72 g $Na_2EDTA.2H_2O$ in 800 ml dH_2O and adjusting the pH to 8.0 with HCl. The volume was made up to 1 L with dH_2O and the mixture was autoclaved for 20 minutes. After cooling, 100 mg RNase A was added, and the solution was stored at 4°C.

5.2.1.2 Lysis buffer (buffer P2)

Lysis buffer was prepared by dissolving 8.0 g NaOH pellets and 10 g sodium dodecyl sulphate (SDS) in 500 ml dH_2O. The volume was made up to 1 L with dH_2O and stored at room temperature.

5.2.1.3 Neutralisation buffer (buffer P3)

Neutralisation buffer was prepared by dissolving 294.5 g potassium acetate in 500 ml dH_2O and adjusting the pH to 5.5 with acetic acid. The volume was made up to 1 L with dH_2O and stored at 4°C.

5.2.1.4 Wash buffer (buffer QC)

Wash buffer was prepared by dissolving 58.44 g NaCl and 10.4 g 3-(N-morpholino) propane-1-sulfonic acid (MOPS) in 800 ml dH_2O. The pH was adjusted to 7 with NaOH and 150 ml isopropanol was added. The volume was made up to 1 L with dH_2O and stored at room temperature.

5.2.1.5 Equilibration buffer (buffer QBT)

Equilibration buffer was prepared by dissolving 43.83 g NaCl and 10.4 g MOPS in 800 ml dH_2O. The pH was adjusted to 7 with NaOH. Next, 150 ml isopropanol and 15 ml 10% Triton-X solution (v/v) was added. The volume was made up to 1 L with dH_2O and stored and room temperature.

5.2.1.6 Elution buffer (buffer QF)

Elution buffer was prepared by dissolving 73.05 g NaCl and 6.06 g Tris base in 800 ml dH_2O. The pH was adjusted to 8.5 with HCl and 150 ml isopropanol was added. The volume was made up to 1 L with dH_2O and stored at room temperature.

5.2.2 Large-scale plasmid isolation

First, bacteria containing plasmid DNA for purification was added to 150-200 ml LB medium supplemented with 1 × antibiotic (i.e., ampicillin or kanamycin). From bacteria growing on an agar plate, a single colony was added to the medium. From bacteria in liquid stocks, 10-100 µl was added to the medium. The culture was left to grow overnight at 37°C with shaking.

After overnight culture, bacterial cells were harvested by centrifugation at ~3220 × g for 40 minutes and the pellet was resuspended in 10 ml resuspension buffer (P1). Ten millilitres of lysis buffer (P2) was added, mixed vigorously, and incubated at room temperature for 5 minutes. Ten millilitres neutralization buffer (P3) was added, mixed vigorously, and incubated on ice for 20 minutes. The mixture was centrifuged at ~3220 × g at 4°C for 45 minutes, the clear layer of liquid was removed and applied to a QIAGEN-tip 500 column (Qiagen, MD, USA) equilibrated with 10 ml equilibration buffer (buffer QBT). The QIAGEN-tip column was washed twice with 30 ml wash buffer (buffer QC) and the DNA was eluted from the column with 15 ml elution buffer (buffer QF) into 10.5 ml 100% isopropanol to precipitate the DNA. The sample was then centrifuged at ~3220 × g for 45 minutes. The DNA pellet was washed

with 5 ml 70% ethanol and centrifuged at ~3220 × g for 10 minutes. The washed pellet was left to air-dry and redissolved in dH_2O. DNA concentration, A_{260}/A_{280} and A_{260}/A_{230} values were measured using the NanoPhotometer® Spectrophotometer (Implen Inc., CA, USA).

5.2.3 Small-scale plasmid isolation

Bacterial cultures were prepared by inoculating 10 ml LB medium supplemented with 1 × antibiotic (i.e., ampicillin or kanamycin) with selected colonies growing on agar plates. Cultures were incubated at 37°C with shaking.

Bacterial cultures were centrifuged at ~3220 × g for 20 minutes and the bacterial pellet was resuspended in 180 µl resuspension buffer (P1). One hundred and sixty microliters lysis buffer (P2) was added to the tube, mixed, and incubated at room temperature for 5 minutes. After incubation, 120 µl neutralization buffer (P3) was added, mixed, and incubated on ice for 5 minutes. The mixture was centrifuged at ~18 000 × g at 4°C for 10 minutes and the clear liquid layer was transferred to a clean tube. DNA was precipitated by adding 600 µl 100% isopropanol and left to stand for 2 minutes before centrifugation at ~18 000 × g for 20 minutes. The supernatant was carefully removed, and the pellet was washed with 150 µl 70% ethanol before centrifugation at ~18 000 × g at 4°C for 2 minutes. The supernatant was removed, and the pellet was left to air-dry. Once dry, the pellet was dissolved in 50 µl dH_2O. DNA concentration, A_{260}/A_{280} and A_{260}/A_{230} values were measured using the NanoPhotometer® Spectrophotometer (Implen Inc., CA, USA).

5.3 Plasmid DNA manipulations

5.3.1 PCR amplification

Reactions to amplify out *SHBsAg* and *FLuc* genes were set up using 2 × Taq polymerase master mix (Thermo Fischer Scientific, MA, USA) under the following cycling conditions:

Table 5.1: Cycling conditions for PCR amplification of *SHBsAg* and *FLuc* sequences

Step	Temperature	Duration	Cycles
Initial denaturation	95°C	3 minutes	1
Denaturation	98°C	20 seconds	30
Annealing	62.3°C (SHBsAg) 57.6°C; 58.8°C; 60.4°C; 62.5°C; 64.2°C; 65.3 °C (FLuc)	15 seconds	
Extension	72°C	60 seconds	
Final Extension	72°C	5 minutes	1

5.3.2 Plasmid linearisation

Shuttle plasmid clones were linearised with *Eco*RI. Linearisation reactions were set up with ~60 µg plasmid DNA and *Eco*RI. Reactions were incubated overnight at 37°C. To confirm linearisation, an aliquot of the digested plasmid DNA was run on a 1% agarose gel.

5.3.3 Ligation reactions

Ligation of *LHBsAg* gene into the pShuttle-CMV backbone was performed at a 1:3 backbone to insert molar ratio. Ligation of *SHBsAg* and *FLuc* into the pShuttle-CMV backbone was performed according to the same procedure, however, reactions were set up at 1:3., 1:6 and 1:9 backbone to insert molar ratios. Reactions were incubated at 16°C overnight.

5.3.4 Restriction digestion

Restriction digestion reactions were set up according to manufacturer's instructions. DNA to be digested, enzyme, appropriate enzyme buffer and dH_2O were added together to the reaction tubes. Volumes of reaction components varied depending on the amount of DNA being digested. Reactions were incubated between 1 hour-overnight at 37°C.

5.4 Plasmid DNA extraction and agarose gel analysis

5.4.1 Agarose gel electrophoresis

Agarose gels were prepared at 1% by dissolving agarose powder in Tris-acetate-EDTA (TAE) buffer. Ethidium bromide (2-5 µl) was added to the 50-100 ml agarose mixture and poured into a casting chamber. Gels were left to set, and samples were loaded into the wells after mixing with gel loading dye to 1× (New England Biolabs, MA, USA). Gels were run at 100-120 V

for 30 minutes-4 hours to separate the bands and imaged using the Omega Fluor™ Gel Documentation System (Gel Company Inc., CA, USA).

5.4.2 Gel extraction

DNA was extracted from agarose gels using the QIAGEN QIAquick Gel Extraction Kit (Qiagen, MD, USA). With a clean, sharp scalpel, DNA fragments were excised from the gel. The gel slices were weighed in tubes and 3 volumes buffer QG was added. The tubes were incubated at 50°C for 10 minutes, vortexing every 2-3 minutes until gel was completely dissolved. The samples were applied to a QIAquick spin column (Qiagen, MD, USA) that had been placed in a 2 ml collection tube and centrifuged at ~16 100 × g for 1 minute. Another 500 µl buffer QG was added to the column and centrifuged at ~16 100 × g for 1 minute. The column was centrifuged twice at ~16 100 × g for 1 minute after addition of 750 µl buffer PE. The column was placed in a clean tube and the DNA was eluted by adding 30 µl dH_2O and centrifuging at ~16 100 × g for 1 minute. DNA concentration, A_{260}/A_{280} and A_{260}/A_{230} values were measured using a NanoPhotometer® Spectrophotometer (Implen Inc., CA, USA).

5.5 Tissue culturing

5.5.1 Cell culture media and reagents

5.5.1.1 High glucose Dulbecco's modified Eagles medium (DMEM) (5L)

DMEM (Gibco, Thermo Fisher Scientific, MA, USA) solution was prepared by dissolving 67.5 g powdered Dulbecco's modified Eagles medium in 5 L SABAX pour water. After powder was dissolved, 3.7 g $NaHCO_3$ was added per 1 L of water (i.e., 18.5 g for 5 L) and mixed. The pH of the solution was equilibrated to ~6.8 and the solution was filtered using a PALL VacuCap® 90 mm PF 0.8/0.2 µm filtration device (Pall Corporation, NY, USA) into 500 ml bottles. Before cell culture, complete media was prepared by supplementing DMEM with 10% FBS (Sigma-Aldrich, MO, USA) and 1 × penicillin/streptomycin (pen/strep).

5.5.1.2 Saline-Ethylenediaminetetraacetic acid (EDTA)

A saline-EDTA solution was prepared to wash cells by adding 1ml of 1000 × EDTA to 1 L SABAX pour saline (0.9%) solution (Adcock Ingram, JHB, SA).

5.5.2 Cell culture procedures

5.5.2.1 Cell resuscitation from freezer stocks

Cryotubes containing stored cells (i.e., HEK293T cells) were removed from liquid N_2 (LN_2) storage and placed in a 37°C water bath to thaw. Once thawed, cells were transferred to a 15 ml falcon tube containing 8 ml pre-warmed medium and 1 ml medium was used to wash the cryotube and transfer the remaining cells to the same 15 ml tube. Cells were centrifuged at ~100 × g for 3 minutes and the supernatant was discarded. Cell pellet was resuspended in 1 ml pre-warmed medium and transferred to a 25 cm^2 cell culture flask containing 5 ml pre-warmed medium. Cells were incubated at 37°C and 5% CO_2.

5.5.2.2 Cell detachment and seeding

Cells were detached and prepared for transfer by decanting spent medium from the cell culture flask, washing the cells with saline-EDTA (Table 5.2), and incubating at 37°C for 10 minutes. Saline-EDTA was decanted, and cells were detached by adding TrypLE™ Express Enzyme (Gibco, Thermo Fisher Scientific, MA, USA) (Table 5.2) and incubated at 37°C for 3 minutes. Detached cells were removed from the flask by tapping and the enzyme was inactivated by adding pre-warmed complete medium and transferring to a falcon tube. Cells were centrifuged at ~100 × g for 3 minutes and supernatant was discarded. Cell pellet was resuspended in an appropriate amount of pre-warmed medium depending on the procedure to follow.

Table 5.2: Volumes for cell culture procedures

Flask area	Total Medium (ml)	Saline-EDTA (ml)	TrypLE™ Express (ml)
25 cm^2	5	3-5	0.5-1
75 cm^2	15	10	2
125 cm^2	25	10	3

5.5.2.3 Cell storage in LN_2

Cells were detached from the flask as described above and resuspended in 1 ml freezing solution [5.6 ml medium, 3.4 ml FBS, 1 ml DMSO (Sigma-Aldrich, MO, USA)]. Freezing solution was added to make up the volume for freezing (e.g., if freezing 5 ml, cell resuspension was topped up with 4 ml freezing solution). Cells were aliquoted into 1 ml cryotubes and stored at -80°C overnight. Cells were then transferred to LN_2 for long-term storage.

5.6 AdV production, amplification, and purification

5.6.1 CsCl gradient

Higher density CsCl solution was prepared at 1.35 g/ml by dissolving 70.4 g CsCl in 129.6 ml 10 mM Tris-HCl. Lower density CsCl solution was prepared at 1.25 g/ml by dissolving 54 g CsCl in 146 ml 10 mM Tris-HCl. The mixtures were filtered using a PALL Acrodisc® 25 mm PF 0.8/0.2 µm Supor Membrane syringe filter (Pall Corporation, NY, USA) and stored at ~4°C.

5.6.2 10 mM Tris-HCl

Tris-HCl solution (1 M) was prepared by dissolving 121.14 g Tris base in 800 ml dH_2O. The pH was adjusted to 7 with concentrated HCl and the final volume was made up to 1 L with dH_2O. The mixture was autoclaved and stored at room temperature. Tris-HCl (10 mM) was prepared by mixing 10 ml 1 M Tris-HCl in 990 ml dH_2O. The mixture was autoclaved and stored at 4°C.

5.6.3 40% sucrose

Sucrose solution was prepared to 40% by dissolving 40 g sucrose in 100 ml dH_2O. The mixture was autoclaved and stored at ~4°C.

5.6.4 AdV quantification

5.6.4.1 Immunostaining

Permeabilisation solution for immunostaining was prepared by mixing 0.5% bovine serum albumin (BSA) and Triton-X in 1× PBS to a concentration of 0.5% and 0.25% respectively.

5.7 ELISA

5.7.1 ELISA wash buffer

ELISA wash buffer was prepared to 1 × concentration by mixing 40 ml 20 × wash buffer (Bio-Rad Laboratories Inc., CA, USA) with 800 ml ddH_2O.

5.8 *In vivo* procedures

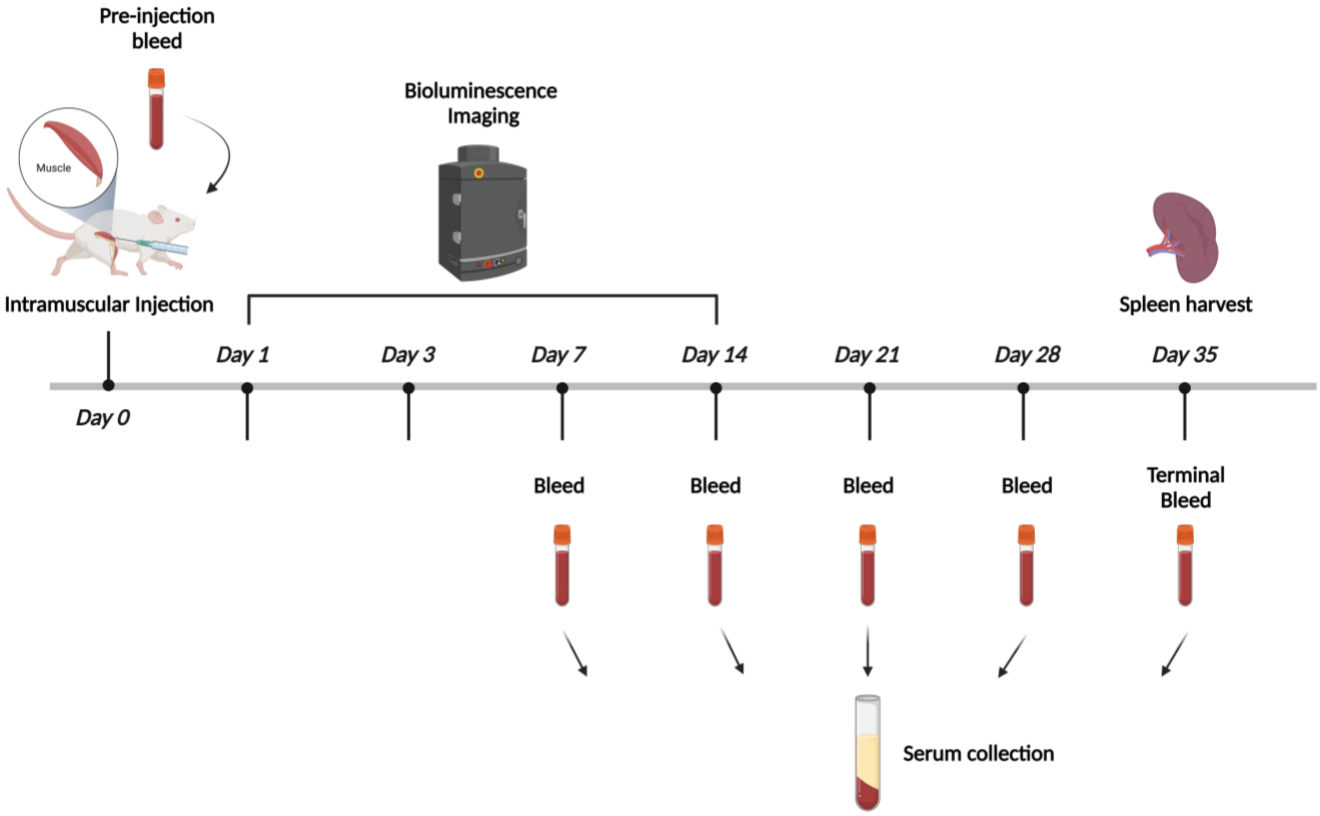

Figure 5.1: *In vivo* timeline.

Timeline showing procedures performed on female Balb/c mice from day 0 to termination at day 35. Intramuscular injection was performed at day 0 after a pre-injection bleed. Bioluminescence imaging was performed at days 1, 3, 7 and 14 and weekly bleeds were taken at days 7, 14, 21, 28 and 35. At termination on day 35, spleens were harvested for further analysis.

5.9 Complete study design

The AdEasy system, described by Luo *et al*, takes advantage of the efficiency of homologous recombination in BJ5183 *E. coli* cells, which do not contain enzymes that mediate DNA recombination in bacteria, but still allow for efficient production of recombinants.

Recombinant AdVs were produced by removing the *LHBsAg*, *SHBsAg* and *FLuc* genes from their carrier plasmids and subcloning into pShuttle-CMV. Next, competent BJ5183 *E. coli* cells we co-transformed with subcloned shuttle plasmids clones and pAdEasy-1, providing most of the Ad genome excluding those required for viral propagation in naturally occurring cells. Finally, HEK293T cells were transfected with recombinant AdV DNA for viral production. The recombinant AdVs produced and purified were ready for *in vitro* and *in vivo* administration (Figure 5.2).

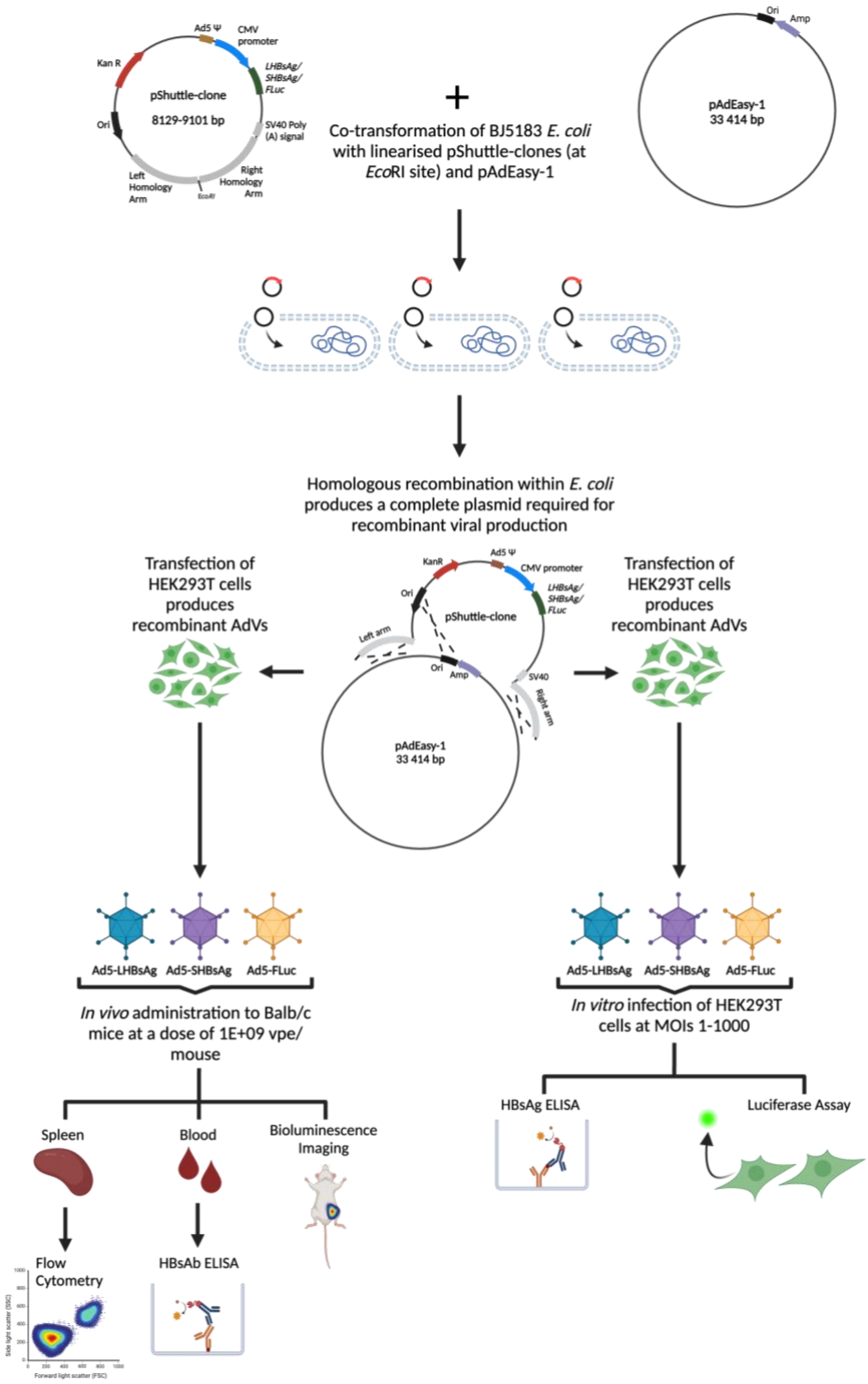

Figure 5.2: Recombinant AdV production.

Process of producing recombinant AdVs encoding HBV surface antigens and subsequent *in vitro* and *in vivo* characterisation. Recombinant AdV DNA was produced by co-transforming competent *E. coli* with shuttle plasmid clones and pAdEasy-1. Recombinant AdVs were produced by transfecting HEK293T cells with AdV DNA. Subsequent *in vitro* and *in vivo* characterisation was performed in HEK293T cells and Balb/c mice, respectively.

Supplementary Data

6.1 General DNA and plasmid information

6.1.1 Plasmids used in this study

Table 6.1: Description and source of plasmids used in this study

Plasmid	Description	Source/Reference
pUC-57-LHBs (co)	pUC-57 plasmid carrying the *LHBsAg* transgene	AGTRU
pUC-57-MCS-polyA-SHBs	pUC-57 plasmid carrying the *SHBsAg* transgene	AGTRU
PGL4.50 [Luc2/CMV/ Hygro]	Plasmid carrying the *FLuc* transgene	AGTRU
pShuttle-CMV	Plasmid backbone bearing homology arms to the AdV genome and a CMV promoter	Addgene
pAdEasy-1	Plasmid containing AdV genome	Addgene
pAdTrack-CMV	Shuttle plasmid containing GFP tracer	Addgene
pNG150D	Plasmid bearing both helper virus and HDAdV PCR target amplification sequence	Donated by Philip Ng, Houston Baylor College of Medicine

6.1.2 Maps of plasmids used in this study

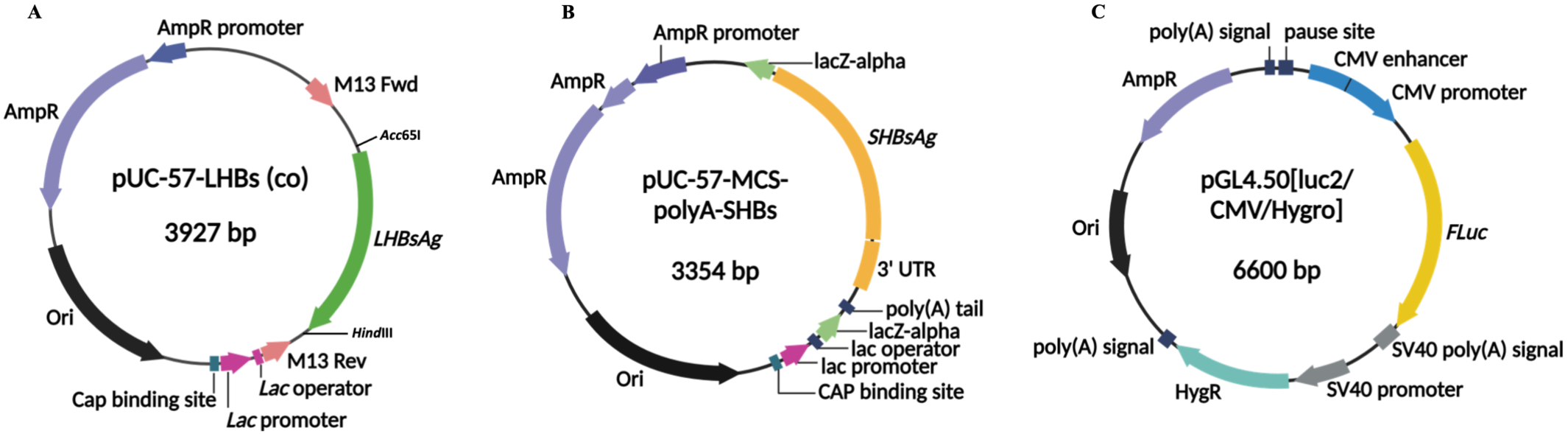

Figure 6.1: Transgene carrier plasmid maps.

A. Plasmid carrying the *LHBsAg* transgene. **B.** Plasmid carrying the *SHBsAg* transgene. **C.** Plasmid carrying the *FLuc* transgene.

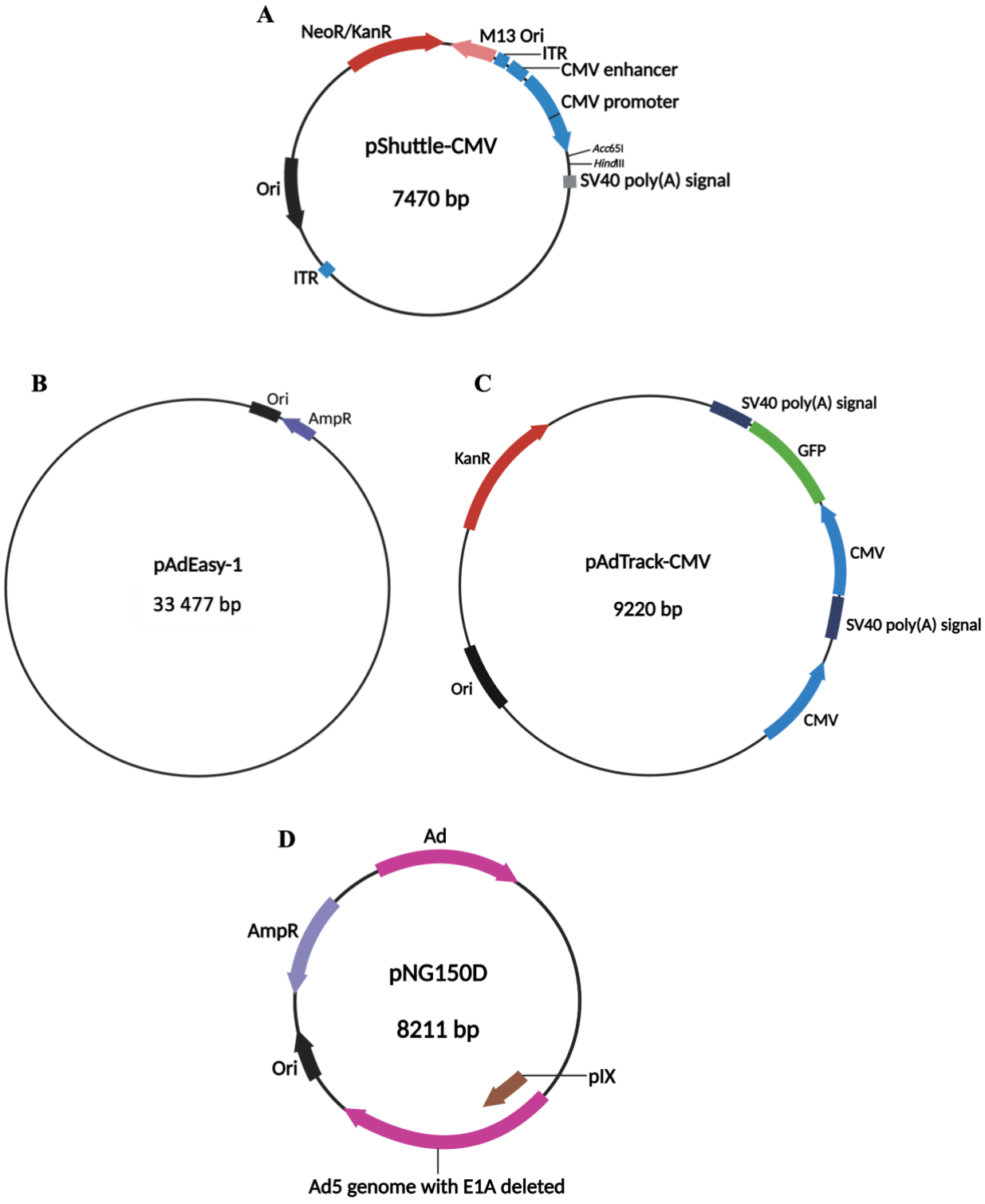

Figure 6.2: Plasmids used for viral production and quantification.

A. pShuttle-CMV plasmid into which transgenes were cloned. **B.** pAdEasy-1 plasmid encoding AdV genome. **C.** pAdTrack-CMV shuttle plasmid encoding GFP tracer. **D.** pNG150D used for AdV quantification.

6.1.3 Plasmids constructed in this study

Table 6.2: Description of plasmids constructed in this study

Plasmid	Description
pShuttle-LHBsAg	Plasmid backbone bearing homology arms to the AdV genome and a CMV promoter, carrying the *LHBsAg* transgene
pShuttle-SHBsAg	Plasmid backbone bearing homology arms to the AdV genome and a CMV promoter, carrying the *SHBsAg* transgene
pShuttle-FLuc	Plasmid backbone bearing homology arms to the AdV genome and a CMV promoter, carrying the *FLuc* transgene
pAd5-LHBsAg	AdV plasmid carrying the *LHBsAg* transgene
pAd5-SHBsAg	AdV plasmid carrying the *SHBsAg* transgene
pAd5-FLuc	AdV plasmid carrying the *FLuc* transgene

6.1.4 Maps of shuttle plasmids constructed in this study

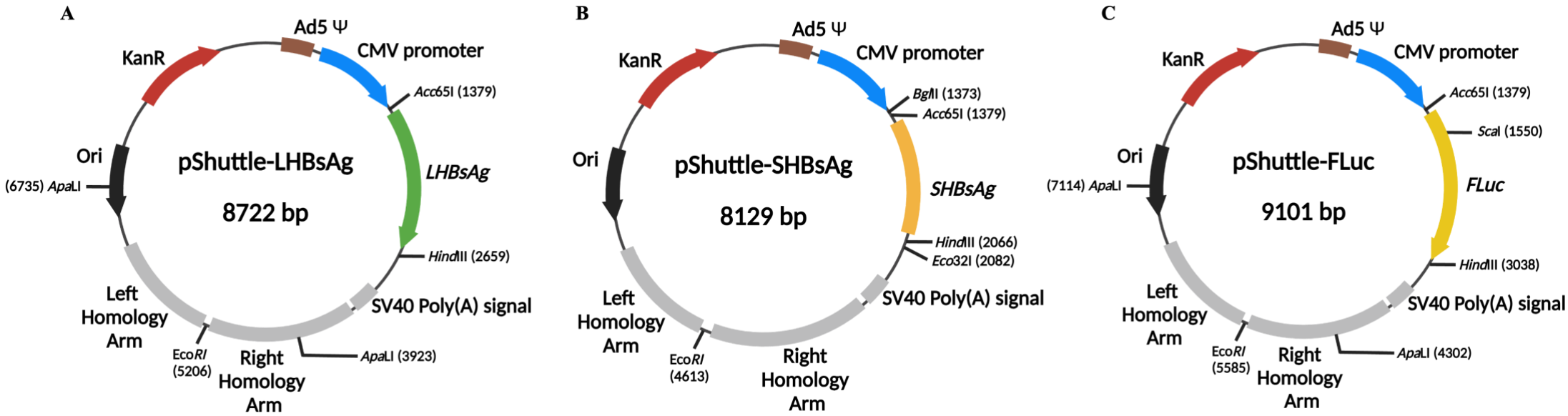

Figure 6.3: pShuttle-CMV clones constructed in this study.

A. pShuttle-CMV clone carrying *LHBsAg* transgene. **B.** pShuttle-CMV clone carrying *SHBsAg* transgene. **C.** pShuttle-CMV clone carrying *FLuc* transgene.

6.1.5 Maps of pAdEasy plasmids constructed in this study

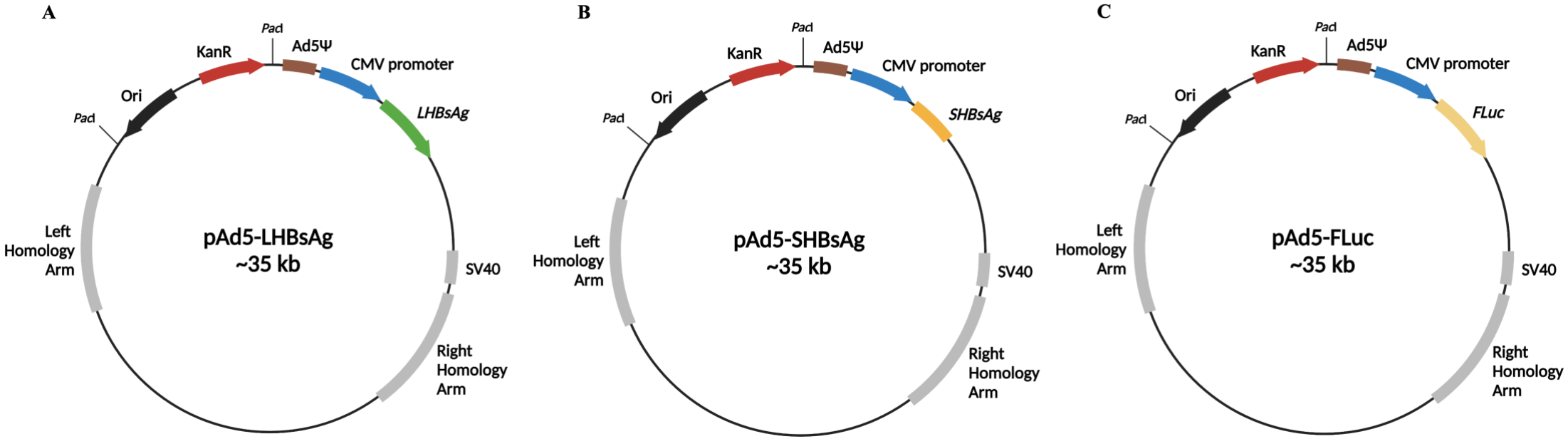

Figure 6.4: Recombinant AdV plasmids constructed in this study.

A. pAdEasy-1 carrying *LHBsAg* used to produce Ad5-LHBsAg **B.** pAdEasy-1 carrying *SHBsAg* transgene used produce Ad5-SHBsAg. **C.** pAdEasy-1 carrying *FLuc* used to produce Ad5-FLuc.

6.1.6 AdVs produced in this study

Table 6.3: Recombinant AdVs produced in this study

AdV	Description
Ad5-LHBsAg	Recombinant AdV encoding the *LHBsAg*
Ad5-SHBsAg	Recombinant AdV encoding the *SHBsAg*
Ad5-FLuc	Recombinant AdV encoding *FLuc*, used as a reporter virus for *in vivo* functionality tests in Balb/c mice
Ad5-GFP	Recombinant AdV encoding *GFP*, used as a reporter virus for AdV production, amplification, and large-scale production

6.2 *In vivo* FLuc expression

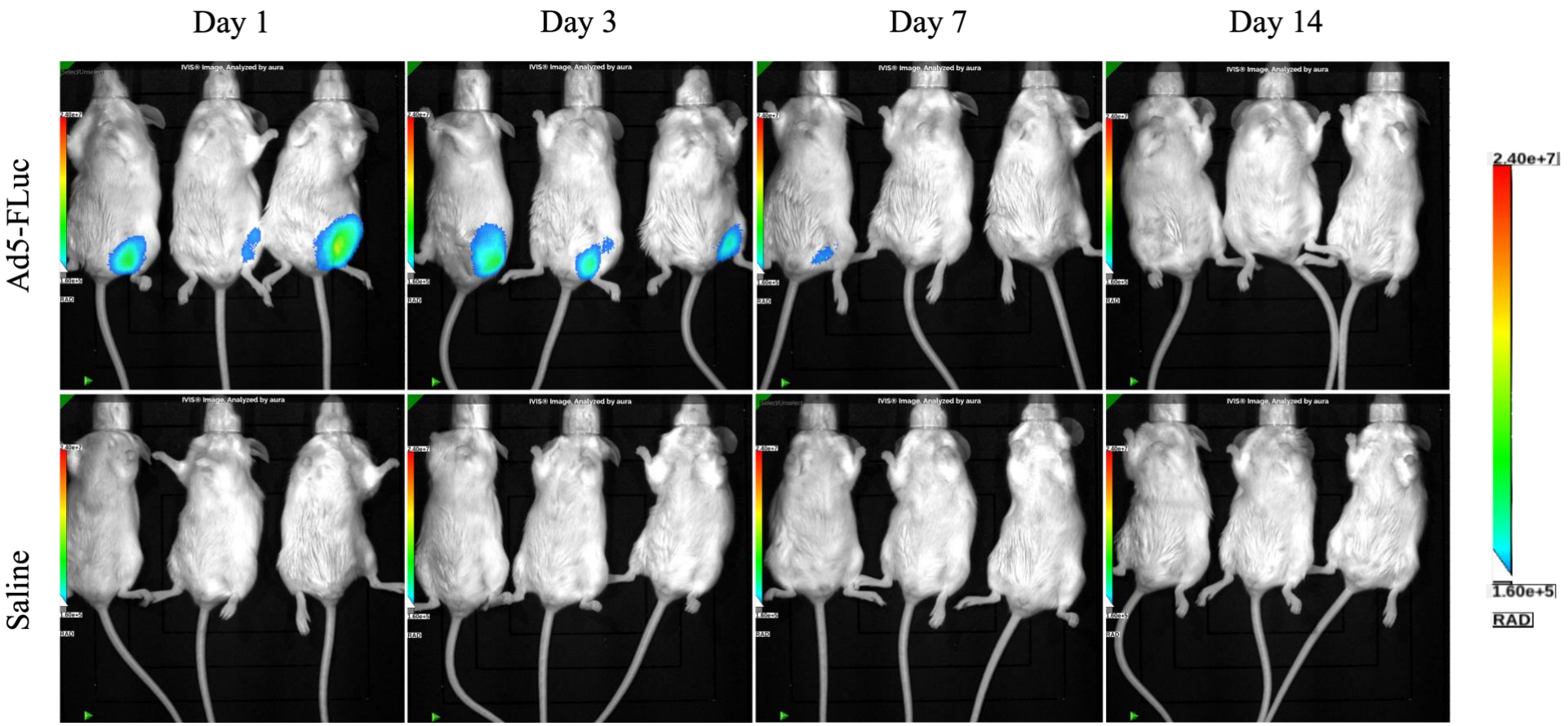

Figure 6.5: *In vivo* bioluminescence imaging.

In vivo bioluminescence imaging of Balb/c mice not shown in main text after intramuscular injection with Ad5-FLuc.

ANIMALS RESEARCH ETHICS COMMITTEE (AREC)

UNIVERSITY OF THE WITWATERSRAND JOHANNESBURG

STRICTLY CONFIDENTIAL

CLEARANCE CERTIFICATE NUMBER: 2022/09/03/C

APPLICANT: Ms K Neves
School: ; Department: Wits/SAMRC Antiviral Gene Therapy Research Unit, Infectious Diseases and Oncology Research Institute (IDORI); Location: WRAF

PROJECT TITLE: Application of adenoviral vectors to induce HBV-specific immune responses in BALB/c mice.
Category: C; Species and Numbers involved: 54X, 6-8 weeks (approximately 20-30g), Female, Balb/c Mice

Approval is hereby given for the use of animals for the research project named above and described in the application reviewed by a quorate meeting of the AREC held on 27 Sep 2022. This approval remains valid until 15 Mar 2025 and is conditional to the following (if blank there are no special conditions):

Condition 1	Condition 2	Condition 3	Condition 4

All material changes to the approved research must be reported to the AREC before they are implemented. Failure to do so will invalidate this clearance certificate.

An annual progress report must be provided to the AREC.

The use of these animals is subject to AREC guidelines on the use and care of laboratory animals, is limited to the procedures described in the application and is subject to additional conditions listed below:

I, the Chair of the AREC (or my designated representative) am satisfied that the proposed research is ethical as judged by local law, international standards and University policy.

Signed: _____ _____ Date: ____17/02/2023_____

(Chairperson of the AREC)

I am satisfied that the persons listed in this application are competent to perform the procedures described in the application, in the context of Section 23 (1) (c) of the veterinary and Para-veterinary Professions Act (19 of 1982).

Signed: __ _____ Date: _17 March 2023_____

CC: Student supervisor: «Title1» «Initials1» «Supervisor_surname»
Director Wits Research Animal Facility (WRAF): Dr Kim Jardine

ANIMALS RESEARCH ETHICS COMMITTEE (AREC)

UNIVERSITY OF THE WITWATERSRAND, JOHANNESBURG

(Registered Veterinarian)

CC: Student supervisor: «Title1» «Initials1» «Supervisor_surname»
Director Wits Research Animal Facility (WRAF): Dr Kim Jardine